Bauhaus-Universität Weimar

Quality assessment of kinematical models by means of global and goal-oriented error estimation techniques

(Anwendung globaler und zielorientierter Fehlerschätzer zur Beurteilung der Notwendigkeit einer geometrisch nicht-linearen Berechnung)

DISSERTATION

Zur Erlangung des akademischen Grades

Doktor - Ingenieur

an der Fakultät Bauingenieurwesen
der Bauhaus Universität Weimar

vorgelegt von

Susanne Nikulla

geboren am 10. April 1984 in Gera

Gutachter: Prof. Dr.-Ing. habil. Carsten Könke
Prof. Dr. rer. nat. habil. Klaus Gürlebeck
Prof. Dr.-Ing. Friedel Hartmann

Tag der Disputation: 30.01.2012

Abstract

Methods for model quality assessment are aiming to find the most appropriate model with respect to accuracy and computational effort for a structural system under investigation. Model error estimation techniques can be applied for this purpose when kinematical models are investigated. They are counted among the class of white box models, which means that the model hierarchy and therewith the best model is known. This thesis gives an overview of discretisation error estimators. Deduced from these, methods for model error estimation are presented. Their general goal is to make a prediction of the inaccuracies that are introduced using the simpler model without knowing the solution of a more complex model. This information can be used to steer an adaptive process. Techniques for linear and non-linear problems as well as global and goal-oriented errors are introduced. The estimation of the error in local quantities is realised by solving a dual problem, which serves as a weight for the primal error. So far, such techniques have mainly been applied in material modelling and for dimensional adaptivity. Within the scope of this thesis, available model error estimators are adapted for an application to kinematical models. Their applicability is tested regarding the question of whether a geometrical non-linear calculation is necessary or not. The analysis is limited to non-linear estimators due to the structure of the underlying differential equations. These methods often involve simplification, e.g linearisations. It is investigated to which extent such assumptions lead to meaningful results, when applied to kinematical models.

Keywords:
Model quality, Model error estimation, Kinematical model, Geometric non-linearity, Finite Element method

Zusammenfassung

Die verschiedenen Methoden zur Bewertung der Modellqualität haben ein Ziel: Das passende Modell in Bezug auf Genauigkeit und Berechnungsaufwand für eine konkrete Struktur zu finden. Steht dabei die Untersuchung eines Kinematik-Modells im Vordergrund, können Modellfehlerschätzer zur Modellbewertung verwendet werden. Dieser Zusammenhang gilt, solange es sich um mechanisch motivierte Modelle handelt, bei denen die Modellhierarchie und damit das beste Modell bekannt sind. Die vorliegende Arbeit beschreibt den Weg von den einfachen Fehlerschätzern für Diskretisierungsfehler bis zu den daraus abgeleiteten Modellfehlerschätzern. Das Ziel der letztgenannten besteht in der Vorhersage von Ungenauigkeit, die durch die Verwendung eines vereinfachten anstatt des komplexen Modells entstehen. Aus den gewonnenen Informationen wird eine adaptive Modellanpassung entwickelt. Die Methoden lassen sich dabei nach verschiedenen Kriterien unterscheiden. Diese diffenzieren zwischen den verschiedenen Anwendungsbereichen, zwischen linearen und nicht-linearen Modellen sowie zwischen globalen und ziel-orientierten Fehlern. Die bislang in der Literatur hauptsächlich zu findenden Anwendungsgebiete sind die Materialmodellierung und die Dimensionsadaptivität. Im Rahmen dieser Arbeit werden nun die bekannten Methoden zur Abschätzung des Modellfehlers auf kinematische Modelle erweitert. Zudem wird die Frage, ob eine geometrisch nicht-lineare Berechnung notwendig ist oder nicht, untersucht. Aufgrund der Struktur der zugrunde liegenden Differentialgleichungen beschränken sich die Analysen auf nicht-lineare Fehlerschätzer. Da diese Methoden oft auf Vereinfachungen wie z.B. die Linearisierung der Grundgleichungen zurückgreifen, wird in der vorliegenden Arbeit untersucht, inwieweit diese Annahmen zu verwertbaren Ergebnissen führen.

Schlagwörter:
Modellqualität, Modellfehlerschätzer, Geometrisch nicht-lineare Berechnung, Kinematik Modell, Finite Elemente Methode

Ehrenwörtliche Erklärung

Ich erkläre hiermit ehrenwörtlich, dass ich die vorliegende Arbeit ohne unzulässige Hilfe Dritter und ohne Benutzung anderer als der angegebenen Hilfsmittel angefertigt habe. Die aus anderen Quellen direkt oder indirekt übernommenen Daten und Konzepte sind unter Angabe der Quelle gekennzeichnet.

Weitere Personen waren an der inhaltlich-materiellen Erstellung der vorliegenden Arbeit nicht beteiligt. Insbesondere habe ich hierfür nicht die entgeltliche Hilfe von Vermittlungs- bzw. Beratungsdiensten (Promotionsberater oder anderer Personen) in Anspruch genommen. Niemand hat von mir unmittelbar oder mittelbar geldwerte Leistungen für Arbeiten erhalten, die im Zusammenhang mit dem Inhalt der vorgelegten Dissertation stehen.

Die Arbeit wurde bisher weder im In- noch im Ausland in gleicher oder ähnlicher Form einer anderen Prüfungsbehörde vorgelegt.
Ich versichere ehrenwörtlich, dass ich nach bestem Wissen die reine Wahrheit gesagt und nichts verschwiegen habe.

Weimar, 30.09.2011

Susanne Nikulla

Danksagung

Die vorliegende Arbeit entstand in meiner Zeit als wissenschaftlicher Mitarbeiter am Graduiertenkolleg 1462 „Bewertung gekoppelter numerischer Partialmodelle im Konstruktiven Ingenieurbau" der Bauhaus-Universität Weimar und wurde von der Fakultät Bauingenieurwesen der Bauhaus-Universität Weimar als Dissertation angenommen. Der Deutschen Forschungsgemeinschaft DFG danke ich an dieser Stelle ausdrücklich für die finanzielle Unterstützung.

Für die Unterstützung bei der Erstellung dieser Arbeit bedanke ich mich bei:

meinem Doktorvater *Prof. Dr.-Ing. Carsten Könke* für die Betreuung der Arbeit und die konstruktiven Diskussionen,

Prof. Dr.-Ing. Friedel Hartmann für wichtige Impulse zum Gelingen der Arbeit sowie die Übernahme des Gutachtens,

Prof. Dr. rer. nat. Klaus Gürlebeck für zahlreiche Anregungen sowie die Übernahme des Gutachtens,

meinen Betreuern *Dr. Jean-Marc Battini* und *Prof. Costin Pacoste* während des Auslandsaufenthalts an der KTH (Royal Institute of Technology) in Stockholm für aufschlussreiche Einblicke in die dortige wissenschaftliche Arbeit,

den beiden PostDocs am GRK *Dr.–Ing. Thomas Most* und *Dr. rer. nat. Tom Lahmer*, die mir in schwierigen Phasen der Arbeit mit Ihrer Erfahrung beratend zur Seite standen,

meinen Kollegen am Graduiertenkolleg für die fachlichen Diskussionen, die gegenseitige Unterstützung bei Software-Problemen und die schöne Zeit, die wir zusammen hatten,

meinen *Eltern*, die mir immer beratend zur Seite stehen

und *Hagen* ohne dessen Unterstützung ich das Projekt "Promotion" nicht in Angriff genommen hätte.

Contents

Symbols and abbreviations

General notations

$det(\cdot)$	Determinate of $(\cdot)$
$(\cdot)^{-1}$	Inverse of $(\cdot)$
$(\cdot)^{T}$	Transpose of $(\cdot)$
$div(\cdot)$	Divergence of $(\cdot)$
$tr(\cdot)$	Trace of a square matrix $(\cdot)$
∇	Nabla operator
$\mathbf{I}$	Identity matrix
δ_{ij}	Kronecher delta
$\delta(\cdot)$	Dirac delta at $(\cdot)$
$\partial(\cdot)$	Partial derivative
$(\cdot)'$	Derivative of $(\cdot)$
$(\cdot)'_u$	Derivative of $(\cdot)$ with respect to u
$\mathcal{D}(\cdot)$	Gateaux derivative of $(\cdot)$
$\mathcal{L}[\cdot]$	Linearisation of $(\cdot)$
$\mathcal{L}(\cdot,\cdot)$	Lagrange multiplier method
$\|\cdot\|_E$	Energy norm of $(\cdot)$
$\|\cdot\|_{\mathcal{H}}$	Hilbert norm of $(\cdot)$
$\|\cdot\|_{\mathcal{H}}$	Hilbert semi-norm of $(\cdot)$
$\|\cdot\|_{L_2}$	L_2-norm of $(\cdot)$
$F(\cdot)$	Linear functional
$a(\cdot,\cdot)$	Bilinear functional
$a(\cdot;\cdot)$	Semi-linear functional
$a_T(\cdot;\cdot,\cdot)$	Tangent form of semi-linear functional
$d(\cdot,\cdot)$	Difference of a simple and complex model
$\hat{(\cdot)}$	Nodal/discretised value
$\widetilde{(\cdot)}$	Approximated value
i,j	Indices $i,j=1,2,3$
$\Delta(\cdot)$	Increment of $(\cdot)$

Greek letters

α	Ellipticity constant
ϵ	Integration constant $\epsilon = 0\ldots1$
$\boldsymbol{\varepsilon}$	Linearised Green strain tensor
η	Global error estimate
$\overline{\eta}$	Standardised global error estimate
ζ	Local error estimate
λ,μ	Lamé constants
ν	Poisson ratio
$\boldsymbol{\xi}$	Local natural coordinate system
$\boldsymbol{\sigma}$	Cauchy stress tensor
Γ	Boundary
Γ_D	Dirichlet boundary
Γ_N	Neumann boundary
Γ_e	Element boundary that does not belong to Γ_N
$\boldsymbol{\Phi}$	Ansatz functions
$\boldsymbol{\Psi}$	Weighting functions
Ω	Domain
$\mathcal{V}$	Solution space
$\mathcal{V}_h$	Space of ansatz functions
$\mathcal{V}_{h+}$	Space of enhanced ansatz functions
$\mathcal{V}'$	Dual space

Latin capital letters

$\mathbf{B}$	Strain-displacement matrix
$\mathbf{B_{nl}}$	Non-linear strain-displacement matrix
$\mathbf{C}_{CG}$	Right Cauchy-Green tensor
$\mathbf{C}$	Constitutive matrix
C_i	Interpolation constant
C_s	Sensitivity constant
$\mathbf{D}$	Differential operator
$\mathbf{D}_{nl}(\mathbf{u})$	Non-linear differential operator
E	Modulus of elasticity
$\mathbf{E}$	Green's strain tensor
$\mathbf{E}_{nl}(\mathbf{u})$	Non-linear part of Green's strain tensor
$\mathbf{E}_u(\mathbf{v})$	Variation of Green's strain tensor
$\mathbf{F}$	Displacement gradient
$\mathbf{G}$	Green's function
$\mathbf{H}$	Deformation gradient
I_{eff}	Effectivity index
$\mathbf{J}$	Jacobian matrix

J_r	Interface tractions
$J(\cdot)$	Goal quantity, quantity of interest
$\mathbf{K}_e$	Elastic, global stiffness matrix
$\mathbf{K}_T(\hat{\mathbf{u}})$	Tangential, global stiffness matrix
$\mathbf{N}$	Shape functions
M	Continuity constant
$\mathcal{P}$	Prolongation operator
$\mathbf{R}$	Rotation tensor
$\mathcal{R}(\widetilde{\mathbf{u}})$	Residuum due to introduction of approximated displacements
R_e	Residuum of strong equilibrium condition
$R_h(\mathbf{u}_h, \mathbf{v})$	Residuum FE solution - primal problem
$R_h^*(\mathbf{u}_h, \mathbf{v})$	Residuum FE solution - dual problem
$R_m(\mathbf{u}, \mathbf{v})$	Residuum simplified model - primal problem
ΔR	Difference of primal and dual model residuum
$\mathbf{S}$	2nd Piola-Kirchhoff strain tensor
$\mathbf{U}$	Right stretch tensor
V	Volume
$\mathbf{V}$	Left stretch tensor
W_{int}	Internal deformational energy
$\mathbf{X}$	Postion vector in the reference coordinate system

Latin lower case letters

$\mathbf{a}$	Unknown coefficients for scaling of the ansatz functions
c	Interpolation and stability constant
$\mathbf{e}_h$	Discretisation error - primal problem
$\mathbf{e}_h^*$	Discretisation error - dual problem
$\mathbf{e}_m$	Model error - primal problem
$\mathbf{e}_m^*$	Model error - dual problem
h_e	Characteristic element size
h_Γ	Edge length of an element
$\mathbf{k}_e$	Elastic, local element stiffness matrix
$\mathbf{k}_g(\hat{\mathbf{u}})$	Geometric, local element stiffness matrix
$\mathbf{k}_m(\hat{\mathbf{u}})$	Material, local element stiffness matrix
$\mathbf{k}_T(\hat{\mathbf{u}})$	Tangential, local element stiffness matrix
n_e	No. of elements
n_r	No. of boundaries of an element
$\mathbf{n}$	Unit normal through a surface
p	Polynomial degree of ansatz functions
$\mathbf{p}$	External force vector
$\mathbf{r}_i$	Linearised internal element forces
t	Time
$\mathbf{t}^{(n)}$	Stress vector on a surface
$\mathbf{t}_e$	Local boundary tractions
$\overline{\mathbf{t}}$	Traction boundary condition
u_{goal}	Goal quantity: displacement
$\mathbf{u}$	Displacement vector
$\mathbf{u}_D$	Displacement boundary condition
$\widetilde{\mathbf{u}}$	Approximated displacement
$\hat{\mathbf{u}}$	Nodal displacement
$\mathbf{v}$	Weighting functions Galerkin method
$\mathbf{x}$	Postion vector in the actual coordinate system
$\mathbf{z}$	Generalised Green's function

Indices

$(\cdot)^*$	Averaged quantity $(\cdot)$
$(\cdot)^k$	No. of iteration cycle
$(\cdot)_{app}$	Approximated value of $(\cdot)$
$(\cdot)_c$	Complex version of $(\cdot)$
$(\cdot)_e$	Property $(\cdot)$ related to element
$(\cdot)_{fs}$	Fine-scale
$(\cdot)_h$	Finite Element solution, discretised
$(\cdot)_{hom}$	Homogenised
$(\cdot)_{low}$	Lower error bound
$(\cdot)_s$	Simple version of $(\cdot)$
$(\cdot)_{upper}$	Upper error bound

Abbreviations

FE	Finite Elements
PEM	Posteriori equilibrium method
REM	Anisotropic residual error estimation

1 Introduction

> *"The goal of reliable and efficient engineering analysis is the proof of material and structural resistance against all possible loadings (actions) with sufficient safety at minimal cost, guaranteeing full usability within lifetime."*
>
> *(*STEIN ET AL. [66] *p. 104)*

1.1 Theory of modelling

The postulate of STEIN leads to the formulation of a complex problem. For its solution, numerous simplifications have to be introduced, leading to a model of the physical problem. Models are an abstraction of reality, which are made for the purpose to describe, explain or predict the behaviour of an observed system. "To an observer B, an object A* is a model of an object A to the extent that B can use A* to answer questions that interest him about A." MINSKY [43] Three main features of a model can be named:

- Models always represent a current system, either a physical structure or an abstract object.
- Models represent only a reduced spectrum of effects, that exist in reality.
- Models are created for a specific purpose.

After a model for a theoretical problem is formulated in a conceptual way, a mathematical description needs to be found. The structure of such a mathematical model depends on the knowledge available about the system. Generally two types can be distinguished:

White box models: They are based on knowledge and insight about the system to be modelled that lead to a deductive modelling process. The mathematical model is derived analytically by making use of a series of progressively more specific concepts that may be broadly categorised as: laws, structure and parameters. In physical systems, these laws are usually expressions of the principles of conservations and continuity. Such models are often formulated in the form of partial differential equations.

Black box models: Experimental data comprised of observations of inputs and outputs are the basis for the model development. This leads to an inductive process, where the structure of the mathematical model is inferred from these observations. Such models might describe a physical phenomena with sufficient accuracy, but they do not represent the underlying mechanisms of the physical event. Before such models can be used for predictions they need to be trained by known input-output relations.

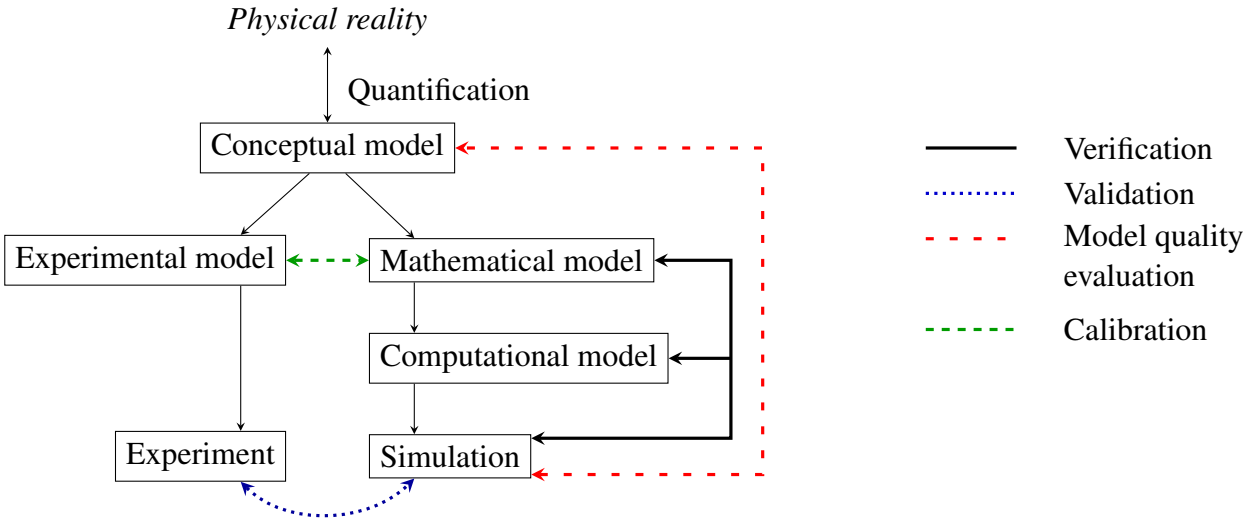

Figure 1.1.: Different kinds of models and their relation to Verification, Validation and Model Quality Assessment

Mathematical models are often far to complex to solve them by manual calculations. The transformation into a computational model becomes necessary. This includes the discretisation of the model domain, the representation of the model elements in terms of classes, inheritance hierarchies and relations, but also the choice of data structures and algorithms. The application of a computational model with a set of model parameters in order to obtain the model behaviour for this specific realisation is named simulation. The relationship between the different model types is illustrated in fig. 1.1.

A complete model of the problem under investigation would be far too complex or is simply not available, as certain mechanism are not fully understood. A model never represents a closed system, as knowledge concerning certain effects or dependencies are unknown; for more details see ORESKES ET AL. [54]. The most obvious simplification is the decomposition of the complex structure into a set of partial problems - a common method in engineering practice. To get complete information about the system behaviour, the partial models need to be coupled. This means in a conceptual way the exchange of in- and output data between partial models must be possible and meaningful. Additionally, the software coupling between the different programmes has to be realised, which is no trivial task, since it might also require the mapping of data between different programming languages and paradigms. Problems that arise concern the compatibility between different representations of the data within each application. This leads to the situation whereby interactions between partial models are approximated, and some may even be neglected.

By definition, models cannot consider all phenomena linked to a certain problem, and due to the decoupling into partial models, additional inaccuracies occur. Thus, inherent to the models is a certain amount of uncertainty. “Uncertainty is the term [...] to describe incomplete knowledge about specific factors, parameters (inputs), or models.” [19, p. 26] It is convenient to categorise the character of uncertainties as either aleatoric or epistemic. Epistemic (lat. *episteme*, knowledge)

uncertainties stem from a lack of knowledge when setting up the model. Aleatoric (lat. *alea*, dice) uncertainties are related to the intrinsic randomness of the phenomena. In this context the robustness and the sensitivity of the models with respect to the variation of the input parameters is investigated. Robustness describes the capability of a model to perform well across the full range of environmental conditions it was designed for. Additionally, the sensitivity of a system with respect to small changes of input parameters is studied. Sensitivity analysis investigates the input parameters with the largest/smallest influence on the output and the interaction between model input parameters.

It is of interest to assess and minimise the influence of these uncertainties on the quality of the simulation result. In [1], [4] or [19] the standard concepts of model quality assessment, verification and validation, are introduced. Verification is "the process of determining if a computational model [...] can be used to represent the mathematical model of the physical event with sufficient accuracy." [4, p. 4058] Two main categories can be distinguished: Code verification, which investigates the accuracy of the implementation, and solution verification, which deals with a posteriori error estimation of the discretised model. After the computational model has proven to be sufficiently correct, the validation procedure can be executed. "The fundamental strategy of validation involves identifying and quantifying the error and uncertainty in the mathematical and computational models, estimating the experimental uncertainty, and then comparing the computational results with the experimental data. This strategy does not assume that the experimental measurements are more accurate than the computational results. The strategy only asserts that experimental measurements are the most faithful reflections of reality for the purposes of validation." [44] Hence absolute validation is impossible.

1.2 Model quality assessment in structural engineering

Structural engineers are interested in the determination of serviceability and ultimate limit state of structures. For a certain problem, different options of modelling are available. All approaches have in common that the complex problem is split into several partial models. This decomposition can be done with respect to a least three different aspects:

- the physical meaning: for example material law, kinematic equations, loading, ...
- a functional differentiation: substructure, superstructure, ...
- the spatial alignment of the models: For instance, a structural model can be decomposed into columns, beams, frames. Within this context a suitable dimension (1D, 2D or 3D) needs to be choosen.

For each partial model, several options of modelling are conceivable. Considering e.g. wind loads, the alternatives of modelling range from constant static wind pressure over the height of the structure to time-dependent computational fluid dynamics.

"Structural mechanics and its models have always had an intimate relation to the computational means that were available to the engineer." [71, p. 2] Therefore, many simplified models are available for the different partial problems. During decades of application, they have proven their applicability and reliability. Following the request of designing more complex structures and supported by an increase of computational power, more sophisticated models have been developed and are now available for practical application. The question arises whether the more complex models lead to an improvement of the quality of the simulation result. When is it meaningful to use these sophisticated models as they are accompanied by an increased computational effort? According to EINSTEIN, modelling should follow the idea "As simple as possible, but not simpler."

The decision regarding the appropriate abstraction level and the associated partial models is nowadays mainly based on engineering knowledge. The possibility of errors due to incorrect decisions of the engineer is not considered in the safety concept of today's standards (EuroCode, DIN). As mentioned in PROSKE [56], it can be noticed that errors caused by incorrect human decisions contribute to a significant number of the failures of structures. An integration of human and programming errors in the current standards has not been realised yet, as a stochastic modelling of these errors is difficult. Therefore, it is desirable to develop methods that can support the decision process. In a first step, it is necessary to point up the critical steps in the modelling process with respect to the sources of uncertainties named in the previous section.

Quality of partial models: For the assessment of partial models, different strategies need to be applied to different types of models. For white box models, it is convenient to expect the most complex model to be the most reliable one. Therefore, a model hierarchy can be established. Here it seems to be meaningful to find criteria that can be used to steer an adaptive process. Starting with the most simple model, the model is upgraded if the error caused with the simple model exceeds a certain level of tolerance. Black box models demand a different approach, as the definition of the best model is not straightforward. In KEITEL [28] and KNABE [30] it was found that besides the model complexity, the uncertainty of the input parameters also need to be considered when studying model quality. Simple models with a lower number of input parameters generally behave more robustly than complex models with a high number of parameters, as their determination often suffers from a high degree of uncertainty. On the other hand, complex models have the advantage of describing more phenomena, so the degree of epistemic uncertainty is reduced.

Interaction of partial models: Two major problems occur while coupling models. First, after an appropriate abstraction level for a single models is found, it is not known, how different models affect each other and how the coupling between models of different quality affect the result of the complex model. Does a rather 'coarse' model cancel out the accuracy of a highly sophisticated model it is coupled with? The second problem results from

the uncertainty of our models. It is not known, how the inherent uncertainty of a single model propagates.

Coupling of partial models: Besides the effects that have already been mentioned in the context of verification, the coupling of partial models introduces new sources of errors, as the models are rarely implemented in the same software application. In terms of structural engineering e.g. problems are caused by mapping the results of Finite Element calculations between different meshes of several partial models or during data exchanges between models with different dimensions.

All these aspects are of importance for model choice and therewith for the quality of the simulation result. A complete view of the model quality cannot be found until all of these aspects are studied intensively and the results are combined. In this context it has to be mentioned that the quality of a model can only be investigated for a specific structure and a predefined goal quantity. Thinking of a railway bridge, a model that is suitable to determine the ultimate limit state might not be appropriate when investigating the passenger comfort for a train passing the bridge.

The inherent complexity of model quality assessment of coupled partial models makes it necessary to solve this question/problem stepwise. Therefore, in this thesis the studies are limited to the partial model "Geometric non-linear effects". The goal is to find an appropriate procedure for assessing this partial model. The underlying partial models can be assigned to the group of white box models. Models of lower quality are defined by neglecting certain effects of more complex descriptions and a hierarchy of the different models can be defined. There is no variation in the number of input parameters considered, which can, for instance, be found in the context of material modelling. From the underlying mechanical formulation, it is clear which kinematic description produces the most reliable/exact result. In a strict sense, the question of model quality can be answered easily for this partial model - the most complex one is the best. But the effort of carrying out a non-linear analysis is not necessary for structures with internal stress state insensitive to deformation. This means that the deformations are small and do not cause an increase of loading effects due to the occurrence of additional moment arms. For most applications in structural engineering, a simple model of the kinematic relationship leads to sufficiently accurate results. The decision about when to use a more complex model and which of the available options to use depends strongly on the experience of the engineer. To minimise the probability of incorrect decisions regarding the model choice, an algorithm should be found to support the choice of the most appropriate model. An ideal method used to estimate the error between simple and complex solutions should fulfil the following aspects:

- Prediction of the necessity to choose a more complex model for the kinematic formulation based on the results of a linear calculation or the simpler model, respectively.
- The error estimate should be accurate in the sense, that it is close to the actual (unknown) error.

- The effort of calculating the error estimate should be low compared to the calculation of the complex model.

- The error estimator should be used to steer an adaptive process for the choice of the kinematical formulation.

1.3 State of the art: Modelling of geometrical non-linear effects

Modelling of geometrical non-linear effects is directly linked to the description of the deformation of a structure. The core question is whether or not the deformations lead to an increase of loading effects for the structure due to additional moment arms. For deformation-insensitive structures, a kinematic linear formulation is sufficient. Here the displacements and strains are linked by a linear relationship and equilibrium for the structure can be determined in a one-step calculation.[1] For deformation-sensitive structures, like flat shells or slender columns, a more sophisticated kinematical description is necessary.

Examples where the use of simplified kinematical descriptions lead to severe damage are the roof of the gymnasium in Halstenbeck, fig. 1.2(a), the failure of a curved girder of a garage, fig. 1.2(b), and the collapse of the truss girders of a basketball arena, fig. 1.2(c). In the first example, the influence of deformation was neglected in equilibrium calculations, [31]. The failure of the curved girder of several vehicle halls in 1962/63 was caused by an underestimation of compression forces. The calculations were based on formulas deduced for straight girders, which led to a neglect of additionally destabilising forces; see [61] for details. In 1969 the roof structure of the basketball arena of Midwestern University collapsed. The failure of truss girders was caused by eccentricities in the intersection point of the top chord and the diagonals, which were neglected in the analysis of the load-bearing capacity.

For non-linear kinematic description, it is necessary to define a reference coordinate system for the description of motion. Different models of geometrical non-linearities are distinguished with respect to this property; see chapter 2.1 for details. The Lagrangian description relates the deformation of the structure to an initial global coordinate system. The non-linear displacement-strain relationship is described by Green‘s strain tensor. An alternative is the Co-rotational description. The deformation is described by linear kinematics in a local coordinate system that constantly rotates and translates with the structural elements. The rigid body movement of the structures is captured by the transformational relation between the local and the global coordinate systems. Under small strain conditions, both attempts lead to comparable results. The solution needs to be found through an iterative procedure, which can be computationally expensive. Because in this thesis non-linear material behaviour is excluded, large strain formulations and the associated logarithmic description of strain is not considered here.

[1] An additional requirement for the determination of equilibrium in a one-step calculation is the assumption of a linear material model.

(a) Damage of the gymnasium in Halstenbeck, [10]

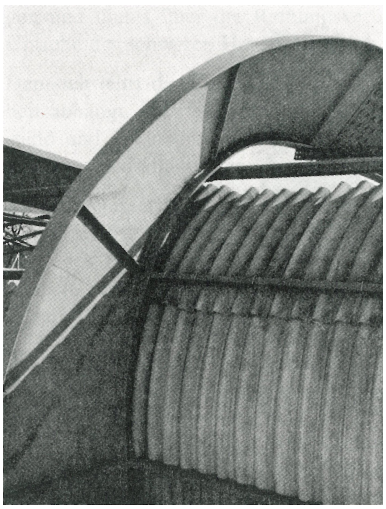

(b) Failure of curved girders, [61]

(c) Failure of truss girders, [61]

Figure 1.2.: Structural failure due to the application of insufficient kinematical models

The use of simplified approaches for the consideration of geometric non-linears effect is widespread in practical applications. The limitations of computational power, mentioned in WUNDERLICH / KIENER [71], led to the introduction of methods that are suitable for manual calculations. These approaches have proven their reliability and are still content of relevant standards in structural steelwork (DIN 18800, EC 3), timber constructions (DIN 1052, EC 5) and reinforced concrete constructions (DIN 1045, EC 2).

According to the standards, a consideration of geometrical non-linear effects is only necessary, if resulting stresses are at least 10 % larger compared to linear theory. But even then simplified methods can be applied, if certain boundary condition, e.g. slenderness ratios, are fulfilled. Equivalent member methods or nominal curvature methods can then be applied. The advantage is that the solution can be found using a one-step calculation, without any sophisticated software. A computationally more expensive iterative solution of the underlying geometrical non-linear problem is hence avoided. If the simplified methods are not applicable, a calculation considering 2nd order

theory is necessary. The mathematical model associated with this phrase is generally not specified. Obviously, a calculation of equilibrium for the deformed structural system is meant. Studying standard work in the field of structural steelwork, PETERSEN [55], it becomes clear that different methods are summarised under this labelling. Methods such as the Q_Δ-analysis [60], application of the Dischinger factor, 2nd order stress calculation or stability analyses are mentioned in this context. All of these methods are too simplified when compared to the non-linear Lagragian or Co-rotational formulation. Within the scope of this work, these simplified methods are not considered, because most of them cannot be classified as white box models. Often they are based on experiments and thus a clear hierarchy cannot be established.

1.4 Introductory studies

The goal is to establish an algorithm for the comparison of different kinematic descriptions mentioned in chapter 1.3. First a criterion needs to be found, that comprises the influence of non-linear effects. The most obvious indicator to judge the different methods might be the deformation of the structure. However, when analysing large structures, the comparison of the displacements for all degrees of freedom is ineffective. It seems to be desirable to define a scalar value that integrates the results. Thus, the deformational or internal strain energy Π_{int} is a suitable criterion. Different kinematical descriptions lead to differences in the predicted deformation of a structure. This results in different strain and stress levels and with it the system‘s energy changes. In case of deformation-sensitive structures, the modelling with or without consideration of geometrical non-linear effects leads to variations in the internal energy. The degree of deviations in the energy can be used as an indicator to steer an adaptive process.

For practical problems, it is not reasonable to investigate a problem by applying all available methods and comparing results. It is more convenient to make a prediction based on results of the simplest method. Kinematic formulations can be assigned to the group of white box models, which are in hierarchical order. It is known which effects, and therewith which parts, of the mathematical model are neglected by the linear formulation. Nevertheless, these parts of the model can be calculated based on deformations of the linear model. It is assumed that the resulting approximated non-linear energy gives a good estimate of the non-linear results and can therefore be used to steer an adaptive process. The load is applied in several steps, and for each step the following procedure is executed:

1. Calculation of the structural response using the linear kinematic description,
2. Approximation of strains and stresses based on non-linear model using linear displacement solution,
3. Calculation of the linear and approximated non-linear internal energy, and
4. Comparison of the internal energy, which indicates the necessity for a non-linear calculation.

This procedure can be applied either to a non-linear Lagrange or Co-rotational formulation as a complex model.

Several examples are investigated to test the proposed procedure. The structural systems that are chosen for this purpose are comparably small. So for comparison, a full geometrical non-linear calculation can be realised with reasonable effort. Figure 1.3 shows an example composed of truss elements. It can be seen that the approximated non-linear energy is a good estimate of the real value. In this case the proposed method seems to be reliable.

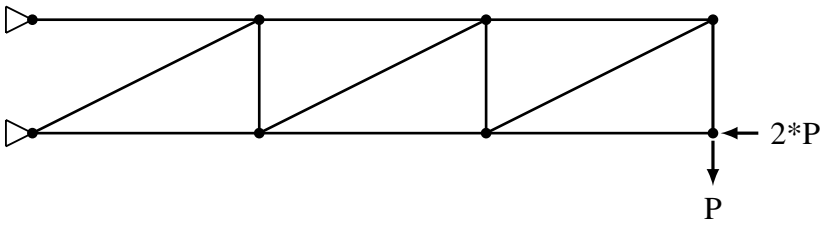

(a) Geometry

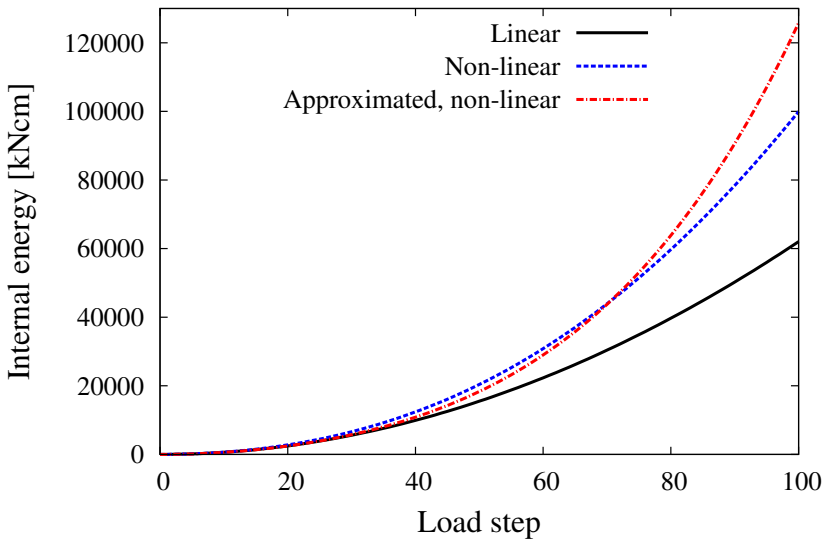

(b) Internal energy

Figure 1.3.: Prediction of internal energy for a cantilever composed of truss elements

In a second step, two beam structures, fig. 1.4, are investigated. The first one is a simple supported beam loaded in the mid-span, a deformation-insensitive structure. The second one is comparable with the 2nd Euler case. A slight imperfection is introduced so that instead of a stability problem, a geometrically non-linear stress problem can be studied. More details concerning geometry and material data for the truss and beam structures can be found in section 4.2. Both structural systems composed of beams reveal the weaknesses of the proposed method. For the bending beam, the approximation leads to an overestimation of the non-linear energy. Using this information for an adaptive process would lead to the shift in the kinematical model, which is obviously not necessary. The opposite can be observed for the Euler beam. Here the approximation of

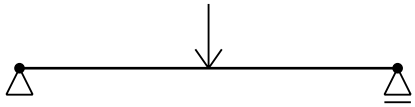

(a) Structural system: Bending beam

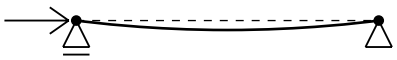

(c) Structural system: Euler beam

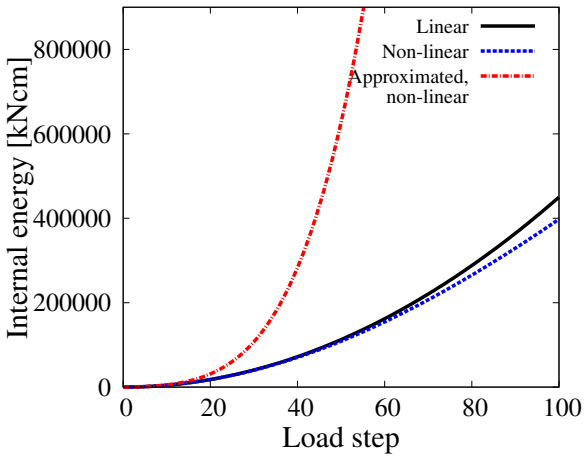

(b) Internal energy: Bending beam

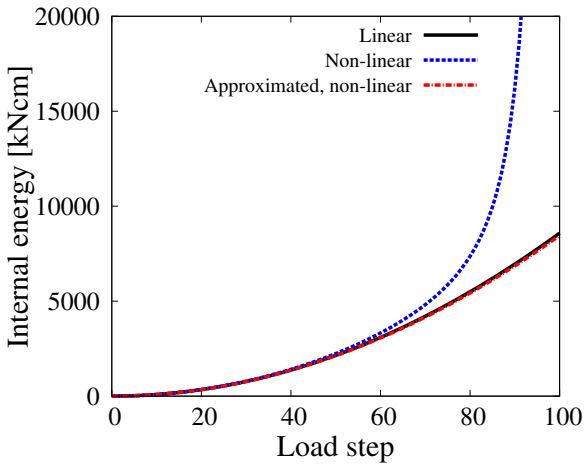

(d) Internal energy: Euler beam

Figure 1.4.: Approximated internal energy for several beam structures

the non-linear internal energy leads to a value close to the linear one. The exact value is underestimated and an adaptive process based on this information would result in an insecure design of the structure. Comparably unreliable results are achieved when investigating 2D-problems, too. It is not possible to find a general rule for the unreliable prediction. Varying parts of the internal energy that are related to normal and bending strains are totally under- or overestimated. There is no difference whether the method is applied to the non-linear Lagrangian or Co-rotational formulation. So the first idea has not proven to be a reliable/meaningful one. Additionally, it can be criticised that the comparison of internal energies only leads to overall information about the structure. For larger structures, where only parts are sensitive to deformations, geometrical non-linearities could remain undetected using a global criterion.

Simulations considering geometrical non-linear effects are generally solved in the following way. The load is applied in several steps, and for each of these steps the equilibrium state is found iteratively. Thus the question arises whether an approximation for the final displacement solution can be made based on the results of the first load steps. In the literature, comparable approaches have already been pursued. There the goal was to improve the predictor step within the solution of one load step to end up with fewer corrector iterations. Different ideas are presented and afterwards their applicability regarding the present problem is tested.

MEEK / TAN [41]: The stiffness matrix for the next load step $\mathbf{K}_{i+1}$ is defined by a 3-point Lagrange interpolation polynomial based on the stiffness matrix of the previous steps.

$$\mathbf{K}_{i+1} = 0.38\,\mathbf{K}_{i-2} - 1.25\,\mathbf{K}_{i-1} + 1.88\,\mathbf{K}_{i} \tag{1.1}$$

ERIKSSON [20]: Based on the actual equilibrium solution and the results of two to four previously solved load steps, the first- (and second-) order derivative of the stiffness matrix are determined. This is done numerically using the central difference method. Afterwards, the derivatives of the displacements $\mathbf{u}$ for the actual equilibrium point are determined. Subsequently, a prediction of the displacement increment for the new load step is made using Taylor series expansion.

$$\Delta \mathbf{u}_{i+1} = \Delta s \cdot \mathbf{u}_i' + \frac{1}{2}(\Delta s)^2 \cdot \mathbf{u}_i'' + \frac{1}{6}(\Delta s)^3 \cdot \mathbf{u}_i''' + ... \tag{1.2}$$

KIM / KIM [29]: The iteration for a new load step is not started in the previous equilibrium point. Based in the previously found displacement increments, a better starting point is determined. A neural network gives a prognosis for the direction and magnitude of the expected displacements for the new load step.

Generally speaking, the results of already solved load steps are extrapolated within a certain domain. It is tested whether this idea can be used for the prediction of displacements for the next load levels to come. Following the idea of ERIKSSON [20], a Taylor series expansion is used to predict displacements. For the Euler beam, fig. 1.4c, the load is applied in 10 increments. The attempt is made to predict the displacements based on the results of load steps one to three. In fig. 1.5 the evolution of the mid-span deflection is documented. A very poor quality of the extrapolation appears for higher load steps, when geometrical non-linear effects are more significant. A good prediction for the final load level can only be achieved if information from the eighth and ninth load steps are already known. For practical applications this is not meaningful, because the reduction of computational costs is close to zero.

At first sight both investigated procedures were promising, but when studying them in detail, severe problems occurred. An alternative needs to be found. A quite promising approach is the theory of model error estimation, which is briefly introduced in the following section and which establishes a basis for this thesis.

1.5 State of the art: Model error estimation

During the last decade, the research focus was shifted towards the determination of modelling errors, to assess the model quality with respect to complexity, robustness and efficiency. The goal is to achieve results with sufficient accuracy using the least effort. White box models with an inherent hierarchy are suitable for such an attempt. To the knowledge of the author, the focus so far has been on material and dimensional modelling.

Error estimators were first introduced to determine the discretisation error in Finite Element models; an overview can be found in GRÄTSCH / BATHE [21] or AINSWORTH / ODEN [2]. Differences can be distinguished between *a priori* and *a posteriori* estimators. The former provide

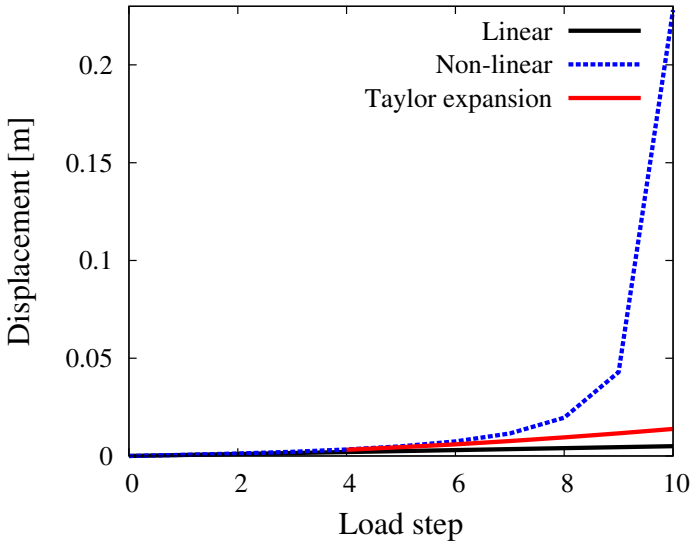

Figure 1.5.: Taylor series expansion based on results of the first load steps to predict the final displacements for the Euler beam

knowledge regarding the convergence behaviour of a solution while the mesh is refined. *A posteriori* techniques provide information concerning approximations of error bounds using the FE solution. Generally speaking, upper and lower bounds are provided by a global error estimate η and some unknown constants C_1 and C_2.

$$C_1\eta \leq \|\mathbf{u} - \mathbf{u}_h\| \leq C_2\eta \tag{1.3}$$

Here $\mathbf{u}$ describe the exact displacements and $\mathbf{u}_h$ are the approximated displacements determined by the Finite Element method. Most famous in this field are the residual-based error estimators first introduced by BABUSKA / RHEINBOLDT [5] and the gradient smoothing techniques provided by ZIENKIEWICZ / ZHU [72]. A large number of publications dealing with this topic are available, improving these methods and introducing new approaches such as hierarchical error estimators or gradient-free methods.

The methods mentioned so far can be summarised as global error estimators. In structural engineering local quantities such as stresses or displacements in certain points are of greater interest to determine the ultimate or serviceability limit state. Therefore, it would be more beneficial to improve the discretisation with respect to these quantities. Basic work in the field of goal-oriented or local error estimators was done by BECKER / RANNACHER [11], [12], who first introduced the dual-weight residual method (DWR). Here a dual problem that is deduced from the quantity of interest/goal quantity is solved. The procedure is comparable to the concept of influence functions, with the result of the dual problem serving as a weight for the primal solution. BECKER/RANNACHER introduced implicit error estimation techniques, which were extended by ODEN / PRUDHOMME [46], [47] to explicit error estimators with guaranteed upper and lower bounds

using parallelogram law. Later these methods were applied to material and geometrical non-linear problems; see CIRAK / RAMM [17] or OHNIMUS ET AL. [53].

First attempts to adopt error estimators to model problems were made by ODEN / ZOHDI [51] using global error estimation techniques. Soon it turned out that the application of goal-oriented techniques is more beneficial and the ideas of RANNACHER/BECKER and ODEN/PRUDHOMME were extended to the model problem by e.g. ODEN / VEMAGANTI [50]. After starting with linear problems, the methods have been extended to physical non-linear problems, too. For reference, see the works of BRAACK / ERN [14] or ODEN / PRUDHOMME [48]. A large variety of model problems have been investigated so far. Following these concepts, e.g. errors due to the dimensional reduction in models [64] have been investigated. A large number of publications are dedicated to questions concerning material modelling with respect to homogenisation, see ODEN ET AL., or multi-scale modelling LARSSON / RUNESSON [37]. A comprehensive overview concerning adaptive Finite Element modelling, especially goal-oriented discretisation and model error estimation, is given in STEIN ET AL. [66].

It is the goal of this thesis to investigate to which extent already introduced methods for model error estimators can by applied to geometrical non-linear problems and which adaptations are necessary when indicated.

1.6 Outline

This work is organised as follows. After this introduction, in the second chapter the basic principles of continuum mechanics are summarised, as they are essential for understanding the Finite Element Method and the problem of geometrical non-linearity. Knowledge about the interaction of kinematics, kinetics and the equilibrium equation is provided. Subsequently, the underlying equations are discretised and the finite element method is introduced. The third chapter gives a survey on error estimation techniques for discretisation and modelling problems. Global and goal-oriented error estimation strategies are introduced for linear and non-linear problems. Thereby it is shown how methods for approximating model errors are deduced from well-established discretisation error estimators. In the fourth chapter, the applicability of model error estimation techniques for geometrical non-linear problems is investigated. Therefore, some of the previously introduced approaches are adapted to the specific problem under consideration and tested regarding their applicability. Finally, the results are summarised and recommendations for practical applications are given.

2 Mechanical fundamentals

This chapter gives an introduction in continuum mechanics with the main focus being on the kinematical description. Using the basic equations - kinematics, material law and equilibrium - a system of differential equations is formed. An approximate solution is found by applying the Galerkin method, which leads, after a limitation of the ansatz function, to the weak equilibrium formulation. An enhancement for larger structures is the Finite Element method, where the ansatz functions are defined over single subdomains. The discretisation of the differential equations leads to the well-known matrix equations, which have to be solved in case of non-linearities using an iterative method.

2.1 Continuum mechanics

2.1.1 Kinematics

Description of motion The deformation of a body can be described with respect to different coordinate systems, fig. 2.1 or [39], [25]. Physical properties can be related to the initial configuration of a body or to the deformed state. The first is called material or Lagrangian formulation and is mainly used in solid mechanics. If, for instance, the variation of material density ρ is the quantity of interest, it is described with respect to the original/initial coordinate $\mathbf{X}$ with $\rho = \rho(\mathbf{X}, t)$. That means, the material density of a specific particle changes over time. If the load is applied in multiple steps, one can distinguish between two approaches. The total Lagrangian formulation refers to the initial state at $t = 0$, whereas the updated Lagrangian formulation refers to the equilibrium position of the previous load step. In fluid mechanics the so-called spatial or Eulerian description is preferred. Changes of specific properties are observed for a fixed position over time. The change of material density is formulated with respect to the position in space $\mathbf{x}$, which is currently occupied by the material particle at time t, which results in $\rho = \rho(\mathbf{x}, t)$.

An alternative procedure, the Co-rotational method, was introduced by Rankin/Brogan [57], Crisfield [18] and Crisfield/Jelenic [26]. Here, a local coordinate system is assigned to each element. It constantly moves and rotates with the element and strain and stresses are formulated with respect to this local coordinate system. Thus, the geometric non-linearity induced by the large rigid-body motion is incorporated in the transformation matrices relating local and global coordinate systems. As long as the deformations are small, a linear kinematic description is sufficient on element level to capture this behaviour. As pointed out by HAUGEN / FELIPPA [22], the main benefit of such an assumption is the possibility to reuse existing high-performance linear elements.

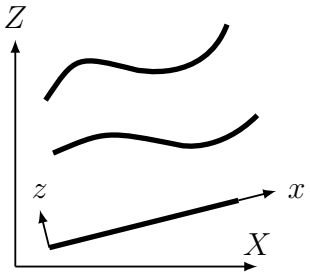

neighbouring configuration $t + \Delta t$

actual configuration t

initial configuration t_0, reference configuration

(a) Total Lagrangian

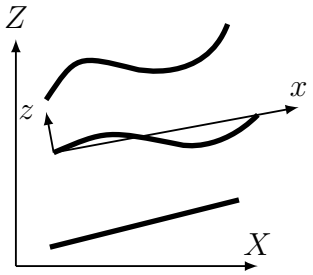

neighbouring configuration $t + \Delta t$

actual configuration t, reference configuration

initial configuration t_0

(b) Updated Lagrangian

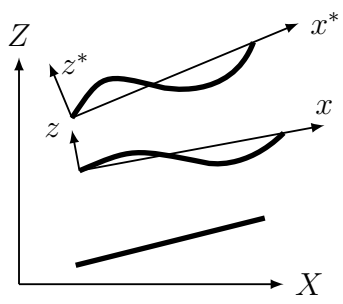

neighbouring configuration $t + \Delta t$, reference configuration at $t + \Delta t$

actual configuration t , reference configuration at t

initial configuration t_0

(c) Co-rotational

Figure 2.1.: Reference systems for description of motion

Deformation gradient Using Lagrangian formulation, the deformation of a three-dimensional continuous body is described in relation to the original configuration at $t = 0$. The initial position is described using capital letters, whereas for the state after deformation, lowercase letters are used. The displacement vector is formulated as

$$\mathbf{u}(\mathbf{X}, t) = \mathbf{x}(\mathbf{X}, t) - \mathbf{X}. \tag{2.1}$$

For the purpose of this work, only static problems are considered.

Investigating two neighbouring points located at $\mathbf{X}$ and $\mathbf{X} + d\mathbf{X}$, see figure 2.2, the position of the second point after deformation is

$$\mathbf{x} + d\mathbf{x} = \mathbf{X} + d\mathbf{X} + \mathbf{u}(\mathbf{X} + d\mathbf{X}). \tag{2.2}$$

Here $d\mathbf{X}$ and $d\mathbf{x}$ are a differentially small distance between two neighbouring points. Inserting equation (2.1) and rearranging with respect to $d\mathbf{x}$ leads to

$$d\mathbf{x} = d\mathbf{X} + \mathbf{u}(\mathbf{X} + d\mathbf{X}) - \mathbf{u}(\mathbf{X}). \tag{2.3}$$

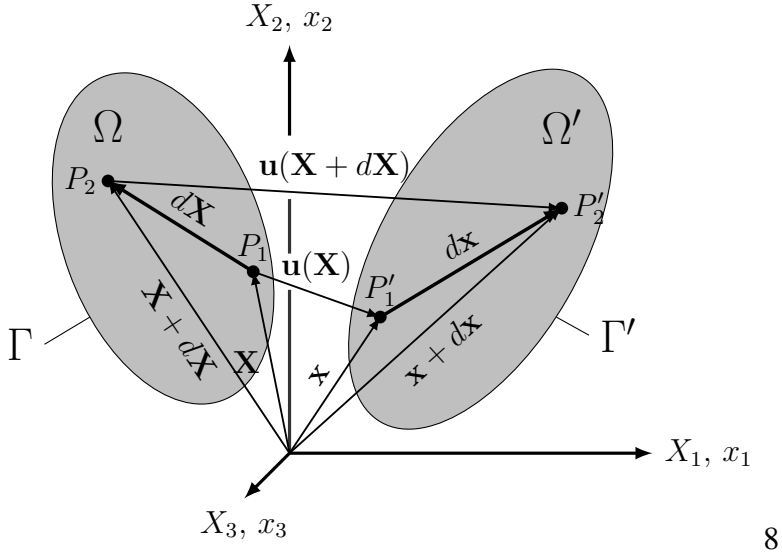

Figure 2.2.: Body in initial and reference configuration

The second term in equation (2.3) is expanded in a Taylor series. In index notation the equation becomes

$$dx_i = dX_i + \cancel{u_i(X_j)} + \frac{\partial u_i}{\partial X_j} dX_j + \frac{1}{2!}\frac{\partial^2 u_i}{\partial X_j \partial X_k} dX_j dX_k + ... - \cancel{u_i(X_j)}. \tag{2.4}$$

The series expansion is truncated after the first term, resulting in a linear approximation of the distance between two neighbouring points in the deformed configuration. This is reasonable, as the distance between the neighbouring points is assumed to be small, so highe-order terms are small compared to the linear one. Based on eq. (2.4), the deformation gradient is defined as

$$d\mathbf{x} = d\mathbf{X} + \underbrace{\frac{\partial \mathbf{u}}{\partial \mathbf{X}}}_{\mathbf{H}} d\mathbf{X} = \underbrace{(\mathbf{H}+\mathbf{I})}_{\mathbf{F} = \frac{\partial \mathbf{x}}{\partial \mathbf{X}}} d\mathbf{X}\ ; \qquad \begin{array}{ll} \mathbf{H} & \text{... displacement gradient} \\ \mathbf{F} & \text{... deformation gradient} \end{array} \tag{2.5}$$

Strain The deformation gradient $\mathbf{F}$ describes the total motion of a body. No distinction between rigid body motion, including displacement and rotation, and strain is made. For this reason a self-contained measure for strain is introduced. It is derived from the change in the quadratic distance between the two neighbouring points in initial and deformed configurations.

$$\begin{aligned} ds^2 - dS^2 &= \left(\delta_{ij} + \frac{\partial u_i}{\partial X_j}\right)\left(\delta_{ik} + \frac{\partial u_i}{\partial X_k}\right) dX_j dX_k - dX_j dX_k \\ &= \left(\frac{\partial u_i}{\partial X_j} + \frac{\partial u_j}{\partial X_i} + \frac{\partial u_k}{\partial X_i}\frac{\partial u_k}{\partial X_j}\right) dX_j dX_k \\ &= d\mathbf{X}^T \cdot 2\mathbf{E} \cdot d\mathbf{X} \end{aligned} \tag{2.6}$$

The *Green-Lagrange strain tensor* $\mathbf{E}$ is thus defined as

$$E_{ij} = \frac{1}{2}\left(u_{i,j} + u_{j,i} + u_{k,i}u_{k,j}\right). \tag{2.7}$$

Using polar decomposition of the deformation gradient $\mathbf{F}$, one can show that the strain tensor $\mathbf{E}$ is invariant with respect to rigid body movement. The decomposition of $\mathbf{F}$, eq. (2.8), results in a symmetric tensor $\mathbf{U}$ or $\mathbf{V}$ and a orthonormal[1] tensor $\mathbf{R}$ describing the rigid body rotation. $\mathbf{U}$ and $\mathbf{V}$ represent the right and left stretch tensors, respectively.

$$\mathbf{F} = \mathbf{RU} = \mathbf{VR} \tag{2.8}$$

According to equation (2.6), $\mathbf{E}$ can be expressed as $\mathbf{E} = \frac{1}{2}\left(\mathbf{F}^T\mathbf{F} - \mathbf{I}\right) = \frac{1}{2}\left(\mathbf{C}_{CG} - \mathbf{I}\right)$ with $\mathbf{C}_{CG}$ being the right Cauchy-Green tensor, eq. (2.9). Because the rotation tensor $\mathbf{R}$ is orthogonal, $\mathbf{C}_{CG}$ only depends on stretch tensor $\mathbf{U}$, which shows the independence of $\mathbf{E}$ on rigid body movement; see equation (2.9).

$$\mathbf{C}_{CG} = \mathbf{F}^T\mathbf{F} = \mathbf{U}^T\underbrace{\mathbf{R}^T\mathbf{R}}_{\mathbf{I}}\mathbf{U} = \mathbf{U}^T\mathbf{U} \tag{2.9}$$

In case of small strains,[2] the term $\frac{\partial u_i}{\partial X_j}$ becomes much smaller than one. The quadratic term of strain tensor $\mathbf{E}$ can thus be neglected, and a linearised strain tensor $\boldsymbol{\varepsilon}$ can be defined as:

$$\varepsilon_{ij} = \frac{1}{2}\left(u_{i,j} + u_{j,i}\right). \tag{2.10}$$

Symmetry condition can be applied and the linearised strain formulation can be written in matrix-vector notation as

$$\boldsymbol{\varepsilon} = \mathbf{Du} = \begin{bmatrix} \frac{\partial}{\partial X_1} & 0 & 0 \\ 0 & \frac{\partial}{\partial X_2} & 0 \\ 0 & 0 & \frac{\partial}{\partial X_3} \\ \frac{\partial}{\partial X_2} & \frac{\partial}{\partial X_1} & 0 \\ 0 & \frac{\partial}{\partial X_3} & \frac{\partial}{\partial X_2} \\ \frac{\partial}{\partial X_3} & 0 & \frac{\partial}{\partial X_1} \end{bmatrix} \begin{bmatrix} u_1 \\ u_2 \\ u_3 \end{bmatrix}. \tag{2.11}$$

Thus, the Green-Lagrange strain tensor $\mathbf{E}$ can be written as

$$\mathbf{E} = \mathbf{Du} + \mathbf{E}_{nl}(\mathbf{u}). \tag{2.12}$$

[1] orthonormal means: $\mathbf{R}^T = \mathbf{R}^{-1}$ and $det\,\mathbf{R} = 1$

[2] In literature different definition of small strain can be found: $\varepsilon_{ij} \leq 0.01$ [27], $\varepsilon_{ij} \leq 0.02 \ldots 0.05$ [38]

2.1.2 Stress formulation

In continuum mechanics, [39], [25], stress is a measure of the average force per unit area. It is important to note that the area is related to the deformed configuration. The stress tensor is decomposed in two components: one normal and one tangential to the surface. The components of the stress tensor are derived by studying a differential small volume and setting up the equilibrium equation in each direction. Based on figure 2.3, force equilibrium for y-direction can be formulated, according to equation (2.13).

$$\sum F_y = 0 = (\sigma_y - \sigma_y + d\sigma_y)dxdz + (\tau_{zy} - \tau_{zy} + d\tau_{zy})dydx + (-\tau_{xy} + \tau_{xy} + d\tau_{xy})dzdy + p_y dxdydz \quad (2.13)$$

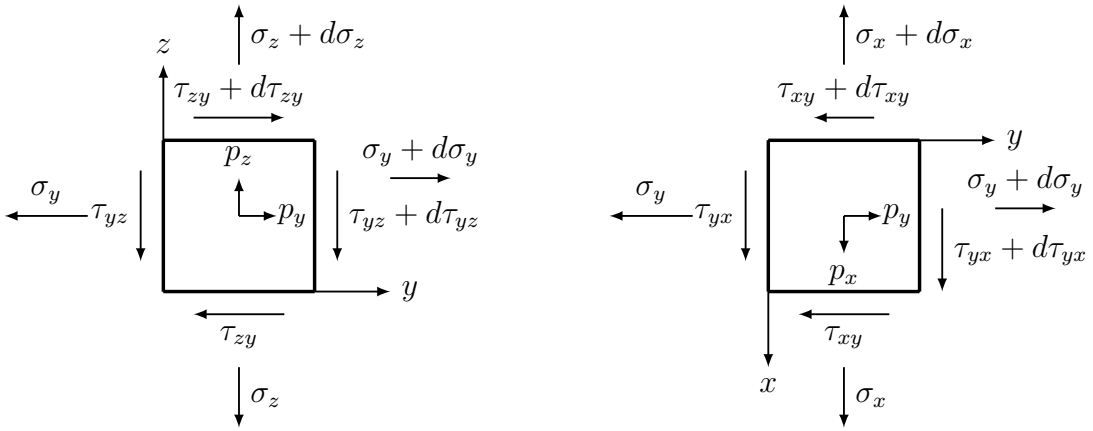

Figure 2.3.: Stresses acting on a cube

Applying the relations $d\sigma_y = \frac{\partial \sigma_y}{\partial y} dy$ and $dxdydz = dV$, the *Cauchy equations of motion* for static loading are deduced. Here eq. (2.14) shows the relationship for the y-direction; x- and z-directions are derived analogously.

$$0 = \frac{\partial \sigma_y}{\partial y} + \frac{\partial \tau_{zy}}{\partial z} + \frac{\partial \tau_{xy}}{\partial x} + p_y \quad (2.14)$$

In index notation the whole set of Cauchy equations of motion with the symmetric Cauchy stress tensor σ_{ji} can be written as

$$0 = \sigma_{ji,j} + p_i; \qquad i, j = 1, 2, 3. \quad (2.15)$$

Additionally, Cauchy's stress theorem (2.16) states, that the stress vector $\mathbf{t}^{(n)}$ on a surface is uniquely defined by the stress tensor $\boldsymbol{\sigma}$ and the unit normal $\mathbf{n}$ through the surface. The upper index n of the stress vector denotes the orientation of the surface the vector is acting on.

$$\mathbf{t}^{(n)} = \boldsymbol{\sigma}\, \mathbf{n} \quad (2.16)$$

The cauchy stress tensor is related to the deformed configuration. In contrast the Green-Lagrange strain tensor is related to the reference configuration. Hence, a new energy-conjugated stress measure needs to be derived. This stress measure is called *2. Piola-Kirchhoff stress tensor* and is defined according to equation (2.17). For a detailed derivation, see A.2.1. For small strains, the relationship $\mathbf{S} = \boldsymbol{\sigma}$ is valid.

$$\mathbf{S} = \mathbf{F}^{-1}\boldsymbol{\sigma}(\mathbf{F}^{-1})^T det\mathbf{F} \tag{2.17}$$

The equilibrium equation for non-linear problem reads

$$-div(\mathbf{S} + \nabla \mathbf{u}\, \mathbf{S}) = \mathbf{p}. \tag{2.18}$$

2.1.3 Constitutive equations

Within the scope of this work, linear elastic material behaviour is assumed. The stress-strain relationship for the 3-dimensional case is described by generalising *Hooke's law* as

$$\sigma_{ij} = E_{ijkl}\varepsilon_{kl}. \tag{2.19}$$

The material tensor E_{ijkl} has in case of anisotropic, linear -elastic material 81 components. Due to symmetry of the strain and the stress tensor, as well as permutability of indices, the number of unknowns can be reduced to 21. In matrix-vector notation the constitutive equation becomes

$$\begin{bmatrix} \sigma_{11} \\ \sigma_{22} \\ \sigma_{33} \\ \sigma_{23} \\ \sigma_{31} \\ \sigma_{12} \end{bmatrix} = \begin{bmatrix} E_{11} & E_{12} & E_{13} & E_{14} & E_{15} & E_{16} \\ & E_{22} & E_{23} & E_{24} & E_{25} & E_{26} \\ & & E_{33} & E_{34} & E_{35} & E_{36} \\ & \text{sym.} & & E_{44} & E_{45} & E_{46} \\ & & & & E_{55} & E_{56} \\ & & & & & E_{66} \end{bmatrix} \begin{bmatrix} \varepsilon_{11} \\ \varepsilon_{22} \\ \varepsilon_{33} \\ \varepsilon_{23} \\ \varepsilon_{31} \\ \varepsilon_{12} \end{bmatrix}. \tag{2.20}$$

An additional reduction of unknowns is possible if symmetry properties of the material are considered. In case of isotropic material, two material constants, the Lamé constants λ and μ, are sufficient to describe the material behaviour.

$$\sigma_{ij} = \lambda\varepsilon_{kk}\delta_{ij} + 2\mu\varepsilon_{ij} \qquad \text{with } \delta_{ij} = \begin{cases} 1 & \text{if i=j} \\ 0 & \text{if i}\neq\text{ j} \end{cases} \tag{2.21}$$

The relations between the Lamé constants and Young's modulus E and Poisson ratio ν are given as

$$E = \frac{\mu(3\lambda + 2\mu)}{\mu + \lambda} \qquad \text{and} \qquad \nu = \frac{\lambda}{2(\lambda + \mu)}. \tag{2.22}$$

The constitutive matrix $\mathbf{C}$ for linear elastic, isotropic materials can thus be defined as

$$\mathbf{C} = \frac{E}{(1+\nu)(1-2\nu)} \begin{bmatrix} 1-\nu & \nu & \nu & 0 & 0 & 0 \\ & 1-\nu & \nu & 0 & 0 & 0 \\ & & 1-\nu & 0 & 0 & 0 \\ & \text{sym.} & & 1-2\nu & 0 & 0 \\ & & & & 1-2\nu & 0 \\ & & & & & 1-2\nu \end{bmatrix} \tag{2.23}$$

and the constitutive law becomes

$$\boldsymbol{\sigma} = \mathbf{C}\boldsymbol{\varepsilon}. \tag{2.24}$$

According to this, the 2nd Piola-Kirchhoff stress tensor can be expressed as

$$\begin{aligned} \mathbf{S}(\mathbf{u}) &= \mathbf{C}\,\mathbf{E}(\mathbf{u}) = 2\mu\mathbf{E} + \lambda(tr\,\mathbf{E})\mathbf{I} \\ &= \mu(\nabla\mathbf{u} + \nabla\mathbf{u}^T) + \lambda(tr\,\nabla\mathbf{u})\mathbf{I} + \mu(\nabla\mathbf{u}^T\nabla\mathbf{u}) + \frac{1}{2}\lambda(tr\,(\nabla\mathbf{u}^T\nabla\mathbf{u}))\mathbf{I}. \end{aligned} \tag{2.25}$$

2.1.4 Strong equilibrium formulation

Based on the Cauchy equation of motion (2.15), the kinematic relationship (2.10) and the constitutive law (2.24), the linear form of *Navier differential equation* is formulated.

$$(\lambda+\mu)u_{j,ji} + \mu u_{i,jj} + p_i = 0 \tag{2.26}$$

Stresses and strains are eliminated and displacements remain as only unknowns. To solve this system of equations, appropriate boundary conditions have to be formulated. Differences can be distinguished between Dirichlet or displacement boundary conditions

$$u_i = u_{D,i} \qquad \text{on } \Gamma_D, \qquad \Gamma_D \ldots \text{Dirichlet boundary} \tag{2.27}$$

and Neumann or traction boundary conditions

$$\sigma_{ij}n_j = \bar{t}_i \qquad \text{on } \Gamma_N, \qquad \Gamma_N \ldots \text{Neumann boundary.} \tag{2.28}$$

Navier differential equation represents the strong form of the equilibrium equation, because equilibrium as well as kinematic equations and material law are fulfilled in each point of the continuum.

The differential equation describing the non-linear problem is formulated by inserting (2.25) in (2.18).

$$-div(\mathbf{S}(\mathbf{u}) + \nabla\mathbf{u}\,\mathbf{S}(\mathbf{u})) = \mathbf{p} \tag{2.29}$$

2.2 Weak equilibrium formulation

An analytical solution for the system of differential equations is only possible for a limited number of cases. Different approaches are available to find an appropriate solution. The basic idea of many methods is the replacement of the exact solution $\mathbf{u}(\mathbf{x})$ with an approximate one $\widetilde{\mathbf{u}}(\mathbf{x})$. The displacements are described by ansatz functions $\mathbf{\Phi}_j$, which are scaled by unknown coefficients $\mathbf{a}$. The ansatz functions $\mathbf{\Phi}$ must fulfil the Dirichlet boundary conditions.

$$\mathbf{u}(\mathbf{x}) \approx \widetilde{\mathbf{u}}(\mathbf{x}) = \sum_{j=1}^{n} a_j \Phi_j \tag{2.30}$$

One procedure to determine the coefficient $\mathbf{a}$ is the *Ritz's method*, which is based on energy principles. The principle of a minimum of potential energy is applied, which leads to

$$\frac{d\Pi(\mathbf{x})}{d\mathbf{x}} = 0. \tag{2.31}$$

Another approach is the *Method of weighted residual*. Here the idea is to minimise the error $R(\widetilde{\mathbf{u}}(\mathbf{x}))$ in the differential equation (2.26), which is caused by the approximation of the displacements by eq. (2.30). The error should be equal to zero in some average sense over the whole domain.

$$\int_{\Omega} \mathcal{R}(\widetilde{\mathbf{u}}(\mathbf{x}))d\mathbf{x} = 0 \tag{2.32}$$

A more general formulation requires the weighted residuum to be zero in some average sense.

$$\int_{\Omega} \mathcal{R}(\widetilde{\mathbf{u}}(\mathbf{x}))\mathbf{\Psi}d\mathbf{x} = 0 \tag{2.33}$$

Depending on the type of weighting functions $\mathbf{\Psi}$ different methods are distinguished. If continuous functions, e.g. sin or cos, are chosen, the procedure is called the *Galerkin method*. As the equilibrium is no longer fulfilled in every point of the continuum, it is generally known as a *weak equilibrium equation*. Applying this methodology to the equilibrium equation (2.15) with $\mathbf{v}$ as a weighting function yields

$$\int_{\Omega} \mathbf{v}\left(div\boldsymbol{\sigma} + \mathbf{p}\right) d\Omega = 0. \tag{2.34}$$

Applying the divergence theorem to the first summand, it becomes:

$$\int_{\Omega} \mathbf{v}\, div\boldsymbol{\sigma} d\Omega = \int_{\Omega} \boldsymbol{\sigma}\, \nabla\mathbf{v} d\Omega - \int_{\Gamma} \boldsymbol{\sigma}\, \mathbf{n}\cdot\mathbf{v} d\Gamma. \tag{2.35}$$

Due to the symmetry of $\boldsymbol{\sigma}$, it is convenient to write $\boldsymbol{\sigma} \cdot \nabla \mathbf{v} = \boldsymbol{\sigma} \cdot \boldsymbol{\varepsilon}(\mathbf{v})$. Additionally, eq. (2.16) is applied, which leads to

$$\underbrace{\int_{\Omega} \boldsymbol{\sigma} \cdot \boldsymbol{\varepsilon}(\mathbf{v}) d\Omega}_{a(\mathbf{u},\mathbf{v})} = \underbrace{\underbrace{\int_{\Omega} \mathbf{p} \cdot \mathbf{v} d\Omega}_{(\mathbf{p},\mathbf{v})} + \underbrace{\int_{\Gamma} \bar{\mathbf{t}} \cdot \mathbf{v} d\Gamma}_{(\mathbf{f},\mathbf{v})}}_{F(\mathbf{v})}. \tag{2.36}$$

This formulation is equivalent to the principle of virtual displacements formulated in Eulerian coordinates. The weighting functions $\mathbf{v}$ can be interpreted as virtual displacements $\delta\mathbf{v}$. In this spirit Equ. (2.34) states, that the work done by the forces acting on the virtual displacements and stresses on the virtual strains must equal zero. The left hand side of (2.36) corresponds to the internal virtual energy and external virtual energy can be assigned to the linear functional $F(\mathbf{v})$.

For geometrical non-linear problems, the same approach is used, and applying it to eq. (2.29) results in

$$\begin{aligned} \int_{\Omega} \mathbf{p} \cdot \mathbf{v} d\Omega &= -\int_{\Omega} div(\mathbf{S}(\mathbf{u}) + \nabla \mathbf{u}\, \mathbf{S}(\mathbf{u})) \cdot \mathbf{v} d\Omega \\ &= \int_{\Omega} (\mathbf{S}(\mathbf{u}) + \nabla \mathbf{u}\, \mathbf{S}(\mathbf{u})) \cdot \nabla \mathbf{v} d\Omega - \int_{\Gamma} \bar{\mathbf{t}} \cdot \mathbf{v} d\Gamma. \end{aligned} \tag{2.37}$$

Due to the symmetry of $\mathbf{S}(\mathbf{u})$, it is feasible to write

$$\begin{aligned} (\mathbf{S} + \nabla \mathbf{u}\, \mathbf{S}) \cdot \nabla \mathbf{v} &= (\mathbf{I} + \nabla \mathbf{u}) \mathbf{S} \cdot \nabla \mathbf{v} = \mathbf{S} \cdot (\mathbf{I} + \nabla \mathbf{u})^T \nabla \mathbf{v} \\ &= \mathbf{S} \cdot \frac{1}{2} \left[(\mathbf{I} + \nabla \mathbf{u})^T \nabla \mathbf{v} + \nabla \mathbf{v}^T (\mathbf{I} + \nabla \mathbf{u}) \right] \\ &= \mathbf{S} \cdot \underbrace{\frac{1}{2} (\nabla \mathbf{v} + \nabla \mathbf{v}^T + \nabla \mathbf{u}^T \nabla \mathbf{v} + \nabla \mathbf{v}^T \nabla \mathbf{u})}_{\mathbf{E}_{\mathbf{u}}(\mathbf{v})}. \end{aligned} \tag{2.38}$$

In matrix notation $\mathbf{E}_{\mathbf{u}}(\mathbf{v})$ becomes

$$\mathbf{E}_{\mathbf{u}}(\mathbf{v}) = (\mathbf{D} + \mathbf{D}_{nl}(\mathbf{u}))\mathbf{v} \quad \text{with}$$

$$\mathbf{D}_{nl}(\mathbf{u}) = \begin{bmatrix} u_{1,1}\frac{\partial}{\partial X_1} & u_{2,1}\frac{\partial}{\partial X_1} & u_{3,1}\frac{\partial}{\partial X_1} \\ u_{1,2}\frac{\partial}{\partial X_2} & u_{2,2}\frac{\partial}{\partial X_2} & u_{3,2}\frac{\partial}{\partial X_2} \\ u_{1,3}\frac{\partial}{\partial X_3} & u_{2,3}\frac{\partial}{\partial X_3} & u_{3,3}\frac{\partial}{\partial X_3} \\ u_{1,2}\frac{\partial}{\partial X_1} + u_{1,1}\frac{\partial}{\partial X_2} & u_{2,2}\frac{\partial}{\partial X_1} + u_{2,1}\frac{\partial}{\partial X_2} & u_{3,2}\frac{\partial}{\partial X_1} + u_{3,1}\frac{\partial}{\partial X_2} \\ u_{1,3}\frac{\partial}{\partial X_2} + u_{1,2}\frac{\partial}{\partial X_3} & u_{2,3}\frac{\partial}{\partial X_2} + u_{2,2}\frac{\partial}{\partial X_3} & u_{3,3}\frac{\partial}{\partial X_2} + u_{3,2}\frac{\partial}{\partial X_3} \\ u_{1,3}\frac{\partial}{\partial X_1} + u_{1,1}\frac{\partial}{\partial X_3} & u_{2,3}\frac{\partial}{\partial X_1} + u_{2,1}\frac{\partial}{\partial X_3} & u_{3,3}\frac{\partial}{\partial X_1} + u_{3,1}\frac{\partial}{\partial X_3} \end{bmatrix} \tag{2.39}$$

Finally this results in

$$\underbrace{-\int_{\Omega} \mathbf{S}\cdot\mathbf{E}_{\mathbf{u}}(\mathbf{v})d\Omega}_{a(\mathbf{u};\mathbf{v})} + \underbrace{\underbrace{\int_{\Omega}\mathbf{p}\cdot\mathbf{v}d\Omega}_{(\mathbf{p},\mathbf{v})} + \underbrace{\int_{\Gamma}\bar{\mathbf{t}}\cdot\mathbf{v}d\Gamma}_{(\mathbf{f},\mathbf{v})}}_{F(\mathbf{v})} = G(\mathbf{u},\mathbf{v}) = \mathbf{0}. \tag{2.40}$$

The term $a(\mathbf{u};\mathbf{v})$ is a semi-linear form that is non-linear in $\mathbf{u}$ and linear in $\mathbf{v}$. Both displacements $\mathbf{u}$ and test functions $\mathbf{v}$ are defined in the *Sobolev space* $\mathcal{H}^1(\Omega)$, see A.1.

As this equation cannot be solved directly, it needs to be linearised and solved iteratively; for more details see HOLZAPFEL [23], BONET / WOOD [13] or KUHL [32]. The linearisation $\mathcal{L}$ in a known point $\overline{\mathbf{u}}$ reads

$$\mathcal{L}[G(\mathbf{u},\mathbf{v})]_{\mathbf{u}=\overline{\mathbf{u}}} = G(\overline{\mathbf{u}},\mathbf{v}) + \mathcal{D}\,G(\overline{\mathbf{u}},\mathbf{v})\cdot\Delta\mathbf{u} + \mathcal{R}. \tag{2.41}$$

The directional or Gâteaux derivative $\mathcal{D}$ implies the differentiation with respect to $\overline{\mathbf{u}}$ in direction of $\Delta\mathbf{u}$. From eq. (2.40) it becomes clear, that only the part related to the internal energy $a(\mathbf{u};\mathbf{v})$ depends on the displacements. Thus the problem of finding the derivative of $G(\mathbf{u},\mathbf{v})$ is reduced. An obvious but tedious derivation, see KUHL [32], leads to

$$\begin{aligned}
a_T(\overline{\mathbf{u}};\Delta\mathbf{u},\mathbf{v}) &= \mathcal{D}G(\mathbf{u},\mathbf{v})\cdot\Delta\mathbf{u} \\
&= \frac{d}{d\epsilon}\left[a(\overline{\mathbf{u}}+\epsilon\Delta\mathbf{u},\mathbf{v})\right]|_{\epsilon=0} \\
&= \int_{\Omega} \mathbf{S}(\mathbf{E}(\overline{\mathbf{u}}))\cdot\mathbf{D}_{nl}(\Delta\mathbf{u})\mathbf{v} + \mathbf{E}_u(\mathbf{v})\cdot\underbrace{\mathcal{D}\mathbf{S}(\mathbf{E}(\overline{\mathbf{u}}))}_{\mathbf{C}\cdot\mathbf{E}_u(\Delta\mathbf{u})}\,d\Omega \\
&= \int_{\Omega} \mathbf{D}_{nl}(\Delta\mathbf{u})\mathbf{v}\cdot\mathbf{C}[\mathbf{D}\overline{\mathbf{u}} + \mathbf{E}_{nl}(\overline{\mathbf{u}})] \\
&\qquad + [(\mathbf{D}+\mathbf{D}_{nl}(\overline{\mathbf{u}}))\mathbf{v}]\cdot\mathbf{C}[\mathbf{D}\Delta\mathbf{u} + \Delta\mathbf{E}_{nl}(\overline{\mathbf{u}})]d\Omega.
\end{aligned} \tag{2.42}$$

Finally, the linearised weak equilibrium equation is formulated as

$$a(\overline{\mathbf{u}};\mathbf{v}) - F(\mathbf{v}) + a_T(\overline{\mathbf{u}};\Delta\mathbf{u},\mathbf{v}) = 0. \tag{2.43}$$

2.3 Finite Element Method

2.3.1 Discretisation

For complex structures it is not possible to find ansatz functions $\mathbf{\Phi}_j$ that describe the displacements in the entire domain. A solution to this problem provides the *Finite Element Method* (FEM), an enhancement of the Galerkin method. It performs a partition of the domain in subregions or elements and the definition of local ansatz functions. Within each element, the displacement field is approximated by local ansatz/shape function N, which are scaled by the nodal displacements $\hat{\mathbf{u}}$.

$$\mathbf{u}(\mathbf{x}) \approx \widetilde{\mathbf{u}}(\mathbf{x}) = \mathbf{N}(\mathbf{x})^T \hat{\mathbf{u}} \quad \text{using } \mathbf{N}(\mathbf{x}) = \begin{bmatrix} N_1 \\ N_2 \\ \vdots \\ N_n \end{bmatrix}, \ \hat{\mathbf{u}} = \begin{bmatrix} \hat{u}_1 \\ \hat{u}_2 \\ \vdots \\ \hat{u}_n \end{bmatrix} \tag{2.44}$$

As indicated in fig. 2.4, the shape functions are defined in a local natural coordinate system ξ.

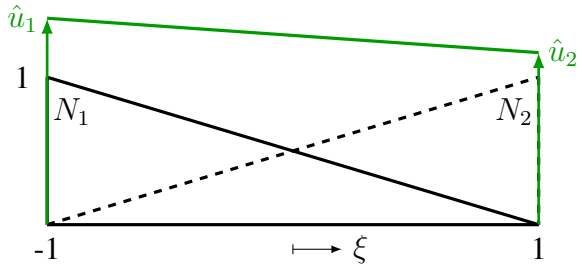

Figure 2.4.: Linear shape functions for a one-dimensional element

The iso-parametric concept uses the same shape functions $\mathbf{N}$ for the geometry mapping between the physical and the local natural coordinate systems.

$$\mathbf{x}(\boldsymbol{\xi}) = \mathbf{N}(\boldsymbol{\xi})^T \hat{\mathbf{x}} \tag{2.45}$$

The equilibrium formulation (2.36) requires the derivatives of the displacements with respect to $\mathbf{X}$. As the ansatz functions are defined in the local natural coordinate system, the chain rule has to be used, which yield

$$\frac{\partial}{\partial \mathbf{X}} = \mathbf{J}^{-1}(\boldsymbol{\xi}) \frac{\partial}{\partial \boldsymbol{\xi}} \quad \text{using } \mathbf{J} = \begin{bmatrix} \frac{\partial X_1}{\partial \xi_1} & \frac{\partial X_2}{\partial \xi_1} & \frac{\partial X_3}{\partial \xi_1} \\ \frac{\partial X_1}{\partial \xi_2} & \frac{\partial X_2}{\partial \xi_2} & \frac{\partial X_3}{\partial \xi_2} \\ \frac{\partial X_1}{\partial \xi_3} & \frac{\partial X_2}{\partial \xi_3} & \frac{\partial X_3}{\partial \xi_3} \end{bmatrix}. \tag{2.46}$$

The Jacobian matrix $\mathbf{J}$ is also used for the transformation between physical and local coordinates. The relationship $dV = dX_1 dX_2 dX_3 = det\mathbf{J}\, d\xi_1 d\xi_2 d\xi_3$ is required for the subsequent integration over the element volume.

2.3.2 Discretisation of linear equilibrium formulation

For the discretisation of eq. (2.36), first the strain tensor 2.11 needs to be expressed using shape functions. The differential operator $\mathbf{D}$, eq. (2.11) , can thus be formulated in local natural coordinates. Applying this operator to the shape functions, the $\mathbf{B}$-matrix for a volume element can be defined. The following expression is valid for the i-th node

$$\mathbf{B}_i(\boldsymbol{\xi}) = \mathbf{D}(\boldsymbol{\xi})\,\mathbf{N}_i(\boldsymbol{\xi}) = \begin{bmatrix} \frac{\partial \xi_j}{\partial X_1} N^i_{,j}(\boldsymbol{\xi}) & 0 & 0 \\ 0 & \frac{\partial \xi_j}{\partial X_2} N^i_{,j}(\boldsymbol{\xi}) & 0 \\ 0 & 0 & \frac{\partial \xi_j}{\partial X_3} N^i_{,j}(\boldsymbol{\xi}) \\ \frac{\partial \xi_j}{\partial X_2} N^i_{,j}(\boldsymbol{\xi}) & \frac{\partial \xi_j}{\partial X_1} N^i_{,j}(\boldsymbol{\xi}) & 0 \\ 0 & \frac{\partial \xi_j}{\partial X_3} N^i_{,j}(\boldsymbol{\xi}) & \frac{\partial \xi_j}{\partial X_2} N^i_{,j}(\boldsymbol{\xi}) \\ \frac{\partial \xi_j}{\partial X_3} N^i_{,j}(\boldsymbol{\xi}) & 0 & \frac{\partial \xi_j}{\partial X_1} N^i_{,j}(\boldsymbol{\xi}) \end{bmatrix} \tag{2.47}$$

The approximations of the strains become

$$\widetilde{\boldsymbol{\varepsilon}}(\boldsymbol{\xi}) = \mathbf{B}(\boldsymbol{\xi})\hat{\mathbf{u}} \qquad \text{with } \mathbf{B} = [\mathbf{B}_1\ \mathbf{B}_2\ \ldots\ \mathbf{B}_n]. \tag{2.48}$$

The stresses are defined as

$$\widetilde{\boldsymbol{\sigma}}(\boldsymbol{\xi}) = \mathbf{C}\mathbf{B}(\boldsymbol{\xi})\hat{\mathbf{u}}. \tag{2.49}$$

Inserting these approximations of strain and stress in (2.36) results in a discretised equilibrium formulation for a linear system. In local natural coordinates for one element derived by neglecting the surface forces, the expression becomes

$$\underbrace{\mathbf{v} \int_{-1}^{1}\int_{-1}^{1}\int_{-1}^{1} \mathbf{N}^T(\boldsymbol{\xi})\,\mathbf{p}(\boldsymbol{\xi})\, det\mathbf{J}\, d\xi_1 d\xi_2 d\xi_3}_{\hat{\mathbf{p}}} = \underbrace{\mathbf{v} \int_{-1}^{1}\int_{-1}^{1}\int_{-1}^{1} \mathbf{B}^T(\boldsymbol{\xi})\mathbf{C}\mathbf{B}(\boldsymbol{\xi})\, det\mathbf{J}\, d\xi_1 d\xi_2 d\xi_3}_{\mathbf{k}_e}\, \hat{\mathbf{u}}. \tag{2.50}$$

Obviously, the weighting function $\mathbf{v}$ can be cancelled. This yields the well-known matrix equation $\hat{\mathbf{p}} = \mathbf{k}_e\hat{\mathbf{u}}$, with $\mathbf{k}_e$ the elastic, local element stiffness matrix. To build up the global stiffness matrix $\mathbf{K}_e$, the local matrices must be transformed to the global coordinate system and assembled according to the relation of local and global degrees of freedom. The analytical solution of the integrals is only possible in special cases. In practice, the integrals are evaluated by numerical methods e.g. Gaussian integration.

2.3.3 Discretisation of non-linear equilibrium formulation

The discretisation of the non-linear equilibrium equation in Lagrangian coordinates eq. (2.40) is done in a comparable manner. To represent the derivation more clearly, the summands of eq. (2.43) are treated separately. The discretisation of the linear functional $\mathbf{F}(\mathbf{v})$ equals the linear formulation, see eq.(2.50). The internal energy formulated in the ξ-coordinate system becomes

$$\begin{aligned} a(\mathbf{u};\mathbf{v}) &= \int_{-1}^{1}\int_{-1}^{1}\int_{-1}^{1} \mathbf{E}_{\mathbf{u}}(\mathbf{v},\boldsymbol{\xi}) \cdot \mathbf{C}\,\mathbf{E}(\mathbf{u},\boldsymbol{\xi})\, det\mathbf{J}\, d\xi_1 d\xi_2 d\xi_3 \\ &= \int_{-1}^{1}\int_{-1}^{1}\int_{-1}^{1} [\mathbf{D}(\boldsymbol{\xi}) + \mathbf{D}_{nl}(\mathbf{u},\boldsymbol{\xi})]\,\mathbf{v}\cdot\mathbf{C}\,\mathbf{E}(\mathbf{u},\boldsymbol{\xi})\, det\mathbf{J}\, d\xi_1 d\xi_2 d\xi_3. \end{aligned} \tag{2.51}$$

The weighting functions $\mathbf{v}$ are described according to (2.44), which yields to the discretisation of $\mathbf{E}_{\mathbf{u}}(\mathbf{v},\boldsymbol{\xi})$ as follows

$$[\mathbf{D}(\boldsymbol{\xi}) + \mathbf{D}_{nl}(\mathbf{u},\boldsymbol{\xi})]\,\mathbf{N}\hat{\mathbf{v}} = (\mathbf{B}(\boldsymbol{\xi}) + \mathbf{B}_{nl}(\mathbf{u},\boldsymbol{\xi}))\hat{\mathbf{v}} = \mathbf{B}(\mathbf{u},\boldsymbol{\xi})\,\hat{\mathbf{v}}. \tag{2.52}$$

This is inserted in eq. (2.51), and the discrete values $\hat{\mathbf{v}}$ can be put in front of the integral

$$a(\mathbf{u};\mathbf{v}) \approx \hat{\mathbf{v}} \int_{-1}^{1}\int_{-1}^{1}\int_{-1}^{1} (\mathbf{B}(\boldsymbol{\xi}) + \mathbf{B}_{nl}(\mathbf{u},\boldsymbol{\xi}))\cdot\mathbf{S}(\mathbf{u},\boldsymbol{\xi})\, det\mathbf{J}\, d\xi_1 d\xi_2 d\xi_3 = \hat{\mathbf{v}}\,\mathbf{r}_i(\mathbf{u}) \tag{2.53}$$

with $\mathbf{r}_i(\mathbf{u})$ the internal force vector. The linearised internal energy (2.42) as a function of $\boldsymbol{\xi}$ becomes

$$\begin{aligned} \mathcal{D}\,W_{int} = &\int_{-1}^{1}\int_{-1}^{1}\int_{-1}^{1} \mathbf{S}(\mathbf{u},\boldsymbol{\xi})\cdot\mathbf{D}_{nl}(\Delta\mathbf{u},\boldsymbol{\xi})\mathbf{v}\, det\mathbf{J}\, d\xi_1 d\xi_2 d\xi_3 \\ &+ \int_{-1}^{1}\int_{-1}^{1}\int_{-1}^{1} [\mathbf{D}(\boldsymbol{\xi}) + \mathbf{D}_{nl}(\mathbf{u},\boldsymbol{\xi})]\mathbf{v}\cdot\mathbf{C}\,\underbrace{[\mathbf{D}(\boldsymbol{\xi})\Delta\mathbf{u} + \Delta\mathbf{E}(\mathbf{u},\boldsymbol{\xi})]}_{[\mathbf{D}(\boldsymbol{\xi}) + \mathbf{D}_{nl}(\mathbf{u},\boldsymbol{\xi})]\Delta\mathbf{u}}\, det\mathbf{J}\, d\xi_1 d\xi_2 d\xi_3. \end{aligned} \tag{2.54}$$

According to CRISFIELD [18] the term in the first integral can be substituted by

$$\mathbf{S}(\mathbf{u})\cdot\mathbf{D}_{nl}(\Delta\mathbf{u})\mathbf{v} = \hat{\mathbf{v}}\,\hat{\mathbf{S}}\,\Delta\hat{\mathbf{u}} \qquad \text{with } \hat{\mathbf{S}} = \begin{bmatrix} \mathbf{S} & & 0 \\ & \mathbf{S} & \\ 0 & & \mathbf{S} \end{bmatrix}. \tag{2.55}$$

Expressing this formulation in terms of $\boldsymbol{\xi}$ and introducing the shape functions in the second term of (2.54) leads to

$$\begin{aligned}\mathcal{D}\,W_{int} \approx \hat{\mathbf{v}} \underbrace{\int_{-1}^{1}\int_{-1}^{1}\int_{-1}^{1} \mathbf{B}_G^T(\boldsymbol{\xi})\,\hat{\mathbf{S}}(\mathbf{u},\boldsymbol{\xi})\mathbf{B}_G(\boldsymbol{\xi})\,det\mathbf{J}\,d\xi_1 d\xi_2 d\xi_3}_{\mathbf{k}_g(\hat{\mathbf{u}})}\,\Delta\hat{\mathbf{u}} \\ + \hat{\mathbf{v}} \underbrace{\int_{-1}^{1}\int_{-1}^{1}\int_{-1}^{1} [\mathbf{B}^T(\boldsymbol{\xi}) + \mathbf{B}_{nl}^T(\mathbf{u},\boldsymbol{\xi})]\cdot\mathbf{C}\,[\mathbf{B}(\boldsymbol{\xi}) + \mathbf{B}_{nl}(\mathbf{u},\boldsymbol{\xi})]\,det\mathbf{J}\,d\xi_1 d\xi_2 d\xi_3}_{\mathbf{k}_m(\hat{\mathbf{u}})}\,\Delta\hat{\mathbf{u}}.\end{aligned} \tag{2.56}$$

The geometric stiffness matrix $\mathbf{k}_g(\hat{\mathbf{u}})$ and the material stiffness matrix $\mathbf{k}_m(\hat{\mathbf{u}})$ are both dependent on the deformations. Expanding the expression in the second integral shows that the elastic stiffness matrix $\mathbf{k}_e$, eq. (2.50), can be extracted. In a compact way, the discretised, linearised internal energy for a single element can be written as

$$\mathcal{D}\,W_{int} \approx \hat{\mathbf{v}}(\mathbf{k}_g(\hat{\mathbf{u}}) + \mathbf{k}_m(\hat{\mathbf{u}}))\Delta\hat{\mathbf{u}} = \hat{\mathbf{v}}\,\mathbf{k}_T(\hat{\mathbf{u}})\,\Delta\hat{\mathbf{u}} = \hat{\mathbf{v}}\,\Delta\mathbf{r}_i(\hat{\mathbf{u}}^k). \tag{2.57}$$

All parts of tangential stiffness matrix $\mathbf{k}_T(\hat{\mathbf{u}})$ are symmetric. The product $\mathbf{k}_T(\hat{\mathbf{u}})\,\Delta\hat{\mathbf{u}}$ represents the linearised internal forces $\Delta\mathbf{r}_i(\mathbf{u})$ of an element. The global stiffness matrix $\mathbf{K}_T(\hat{\mathbf{u}})$ of the structure is composed of the local element matrices $\mathbf{k}_T(\hat{\mathbf{u}})$, which have, when indicated, be transformed to the global coordinate system.

2.3.4 Iterative solution of non-linear equilibrium formulation

Finally, the discrete equation describing the equilibrium of non-linear static systems becomes

$$\mathbf{r}_i(\hat{\mathbf{u}}) = \hat{\mathbf{p}}. \tag{2.58}$$

A solution is found by introducing an iterative procedure, e.g. the *Newton-Raphson algorithm*. Equ. (2.58) is expanded in a Taylor series, which is truncated after the first series term.

$$\mathbf{r}_i(\hat{\mathbf{u}}^{k+1}) = \mathbf{r}_i(\hat{\mathbf{u}}^k) + \frac{\partial\mathbf{r}_i(\hat{\mathbf{u}}^k)}{\partial\hat{\mathbf{u}}^k}\,\Delta\hat{\mathbf{u}} = \mathbf{r}_i(\hat{\mathbf{u}}^k) + \Delta\mathbf{r}_i(\hat{\mathbf{u}}^k) = \hat{\mathbf{p}} \tag{2.59}$$

Index k represents the number of the iteration cycle. The quotient in the second summand is known as stiffness matrix $\mathbf{k}_T(\hat{\mathbf{u}})$, so the term equals the linearised internal force vector; see (2.57). The transformation of (2.59) leads to characteristic equation

$$\Delta\hat{\mathbf{u}} = \mathbf{K}_T(\hat{\mathbf{u}})^{-1}\,\left[\hat{\mathbf{p}} - \mathbf{r}_i(\hat{\mathbf{u}}^k)\right]. \tag{2.60}$$

The total deformation becomes $\hat{\mathbf{u}}^{k+1} = \hat{\mathbf{u}}^k + \Delta\hat{\mathbf{u}}$. Equ. 2.60 has to be solved several times until the solution satisfies a predefined convergence criteria.

3 Error estimation

In this chapter the principles of error estimation are presented. First, discretisation error estimates are introduced with a focus on a posteriori methods for linear and non-linear problems. This includes approaches for the determination of the error in goal quantities, too. In the second part of this chapter, model error estimation techniques are described and a discussion of the results achieved so far is included. Again techniques for linear and non-linear problems as well as global and goal-oriented errors are distinguished.

3.1 Discretisation error

3.1.1 Overview

Applying the Finite Element method, the solution space is shifted from $\mathcal{V}$ to the test space $\mathcal{V}_h$ and equation 2.36 becomes

$$a(\mathbf{u}_h, \mathbf{v}_h) = F(\mathbf{v}_h). \tag{3.1}$$

The discretisation error is defined as

$$\mathbf{e}_h := \mathbf{u} - \mathbf{u}_h. \tag{3.2}$$

The Finite Element solution is characterisied by three properties, [9]:

1. Galerkin orthogonality, see A.1: $a(\mathbf{e}_h, \mathbf{v}_h) = 0$,

2. The strain energy of the Finite Element solution is smaller or equal compared to the one of the exact solution: $a(\mathbf{u}_h, \mathbf{u}_h) \leq a(\mathbf{u}, \mathbf{u})$,

3. The Finite Element solution $\mathbf{u}_h$ leads to the smallest strain energy compared to the other possible solutions $\mathbf{v}_h$ in $\mathcal{V}_h$: $a(\mathbf{e}_h, \mathbf{e}_h) \leq a(\mathbf{u} - \mathbf{v}_h, \mathbf{u} - \mathbf{v}_h)$.

The residual R_h of the Finite Element solution is

$$R_h(\mathbf{u}_h, \mathbf{v}) := a(\mathbf{e}_h, \mathbf{v}) = a(\mathbf{u}, \mathbf{v}) - a(\mathbf{u}_h, \mathbf{v}) = F(\mathbf{v}) - a(\mathbf{u}_h, \mathbf{v}). \tag{3.3}$$

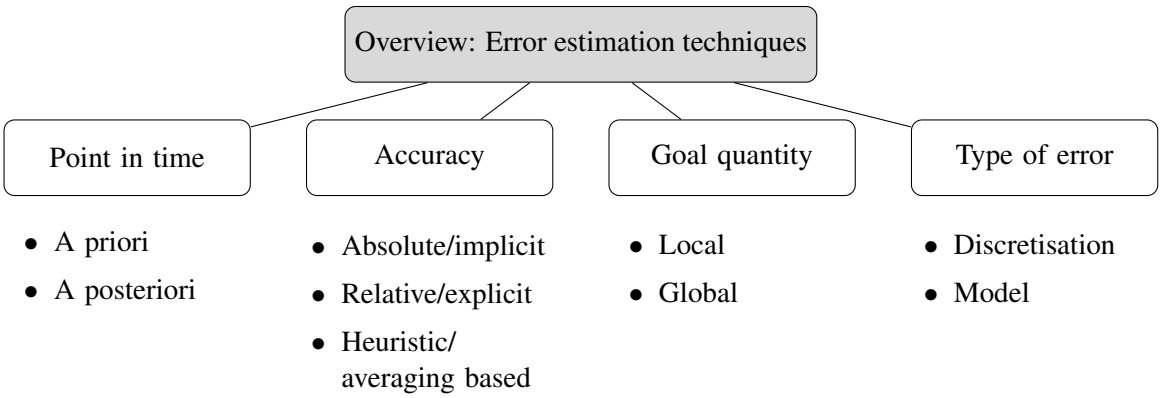

Figure 3.1.: Categorisation of error estimation techniques

Replacing $\mathbf{v}$ with the discretisation error $\mathbf{e}_h$ shows that the residum can be replaced by the energy norm of the error.

$$R_h(\mathbf{u}_h, \mathbf{e}_h) = a(\mathbf{e}_h, \mathbf{e}_h) = \|\mathbf{e}_h\|_E. \tag{3.4}$$

The reasons for the application of error estimation techniques are twofold. On the one hand, the error is assessed quantitatively by calculating lower and upper error bounds, which only yields sufficient results if these bounds are close to each other. Most of the error estimators that provide such theoretical bounds do not yield to guaranteed bounds in case of practical problems. On the other hand, error estimation techniques are used to steer an adaptive process. In this case, it is not important to get the correct value. Here, the main focus is on the error distribution and to detect the areas of the domain where mesh refinement is necessary.

The field of error estimation is wide, and uncountable contributions can be found in literature to determine $\|\mathbf{e}_h\|_E$; as summary see e.g. [2], [66] or [21]. Available methods can be distinguished with respect to four main categories, figure 3.1. First of all, it is determined, whether the estimators are applied before or after the calculation is started. A priori estimates provide knowledge regarding the convergence properties, but no information regarding error bounds. A posteriori techniques make information available concerning approximations of error bounds based on the FE solution.

A posteriori techniques can be distinguished in relative (explicit), absolute (implicit) and heuristic/ averaging-based error estimators. Relative estimators do not provide guaranteed bounds, because the error is scaled with a mostly unknown constant. Implicit error estimators tackle this problem by using information from auxiliary problems to bound the error. Averaging-based estimators make use of the fact that the gradient of the discretised solution is discontinuous across the inter-element boundaries. It is assumed that a smoothed gradient gives a better estimate of the real solution and the error is defined as the difference between the discretised and the smoothed solutions. Another distinctive feature deals with the question of whether the global error of the Finite Element solution should be found or whether the error in a certain local or goal quantity, e.g. stress

in a point $\mathbf{x}_i$, is of interest. Additionally, the error estimation techniques can not only be applied regarding the discretisation, but also the model error can be determined with such methods.

3.1.2 A priori error estimates

A priori estimates provide information concerning the convergence behaviour of the Finite Element solution before the calculation is carried out, see [21]. The main goal is to show that the error converges to zero if the element size is reduced to zero. No information regarding error bounds can be achieved using this approach. *Céa's Lemma* provides a first estimation of the error in the energy norm and it states, that the solution $\mathbf{u}_h$ is the best solution in the space $\mathcal{V}_h$.

$$\|\mathbf{e}_h\|_E = \inf_{v_h \in \mathcal{V}_h} \|\mathbf{u} - \mathbf{v}_h\|_E \tag{3.5}$$

In addition, the *Lax-Milgram theorem* states that if the bi-linear form $a(.,.)$ is continuous

$$|a(\mathbf{v}, \mathbf{w})| \leq M\|\mathbf{v}\|_{\mathcal{H}}\|\mathbf{w}\|_{\mathcal{H}}, \qquad M > 0, \text{ continuity constant} \tag{3.6}$$

and elliptic

$$a(\mathbf{v}, \mathbf{v}) \geq \alpha\|\mathbf{v}\|^2_{\mathcal{H}}, \qquad \alpha > 0, \text{ ellipticity constant,} \tag{3.7}$$

then there is a unique solution. Here the bilinear form $a(.,.)$ is defined in a Hilbert space $\mathcal{H}$ with the norm $\|.\|_{\mathcal{H}}$ (see A.1). Finally, the previously introduced relations can be summarised by the estimate

$$\|\mathbf{e}_h\|_{\mathcal{H}} \leq \frac{M}{\alpha} \inf_{v_h \in \mathcal{V}_h} \|\mathbf{u} - \mathbf{v}_h\|_{\mathcal{H}} \tag{3.8}$$

for details see e.g. MERDON [42]. Except the mesh size h_e, the quality of the solution also depends on the polynomial order p of the ansatz function, BATHE [9]. From interpolation theory, the estimate

$$\|\mathbf{e}_h\|_{\mathcal{H}^1} \leq c h_e^p \|\mathbf{u}\|_{\mathcal{H}^{p+1}} \tag{3.9}$$

can be achieved. From the definition of the norm $\|.\|_{\mathcal{H}^{p+1}}$, it becomes clear, that this formulation leads rather to an estimate for the gradients (stresses and strains) than the displacements. So the convergence of the error in the displacements is of one order higher

$$\|\mathbf{e}_h\|_{\mathcal{H}^0} \leq c h_e^{p+1} \|\mathbf{u}\|_{\mathcal{H}^{p+1}}. \tag{3.10}$$

In many publications, a simplification of (3.9) can be found

$$\|\mathbf{e}_h\| \leq c h_e^p. \tag{3.11}$$

The interpolation and stability constant c depends on the material properties and the element type, but not on the ansatz space. Only for a few cases can c be determined.

3.1.3 A posteriori error estimators

Introduction

A posteriori error estimators provide information concerning approximations of error bound based on the Finite Element solution. Generally speaking, upper and lower bounds are described by a global error estimate η and some unknown constants C_1 and C_2.

$$C_1 \eta \leq \|\mathbf{e}_h\|_E \leq C_2 \eta \tag{3.12}$$

The error is often measured in the energy norm $\|\mathbf{e}_h\|_E$, see A.1, because of the inherent physical meaning.

Residual-based estimates

The residual-based approach is a prominent representative of the class of relative / explicit error estimators. Equation (3.3) is formulated element-wise, and written in a more detailed manner based on (2.36)

$$a(\mathbf{e}_h, \mathbf{v}) = \sum_{e=1}^{n_e} \int_{\Omega_e} \mathbf{f} \cdot \mathbf{v} \, d\Omega_e + \sum_{r=1}^{n_r} \int_{\Gamma_N} \bar{\mathbf{t}} \cdot \mathbf{v} \, d\Gamma_N - \sum_{e=1}^{n_e} \int_{\Omega_e} \boldsymbol{\sigma}(\mathbf{u}_h) \cdot \boldsymbol{\varepsilon}(\mathbf{v}) \, d\Omega_e. \tag{3.13}$$

Here Γ_Ω is the inter-element boundary, and the summation is done regarding the number of elements n_e or the number of element boundaries n_r. Partial integration and the divergence theorem, see 2.35, are applied to the last term of equation (3.13), which leads after some rearrangement to

$$\begin{aligned} a(\mathbf{e}_h, \mathbf{v}) = \sum_{e=1}^{n_e} \int_{\Omega_e} (\mathbf{f} + div\, \boldsymbol{\sigma}(\mathbf{u}_h)) \cdot \mathbf{v} \, d\Omega_e \\ + \sum_{r=1}^{n_r} \int_{\Gamma_N} (\bar{\mathbf{t}} - \boldsymbol{\sigma}(\mathbf{u}_h)\mathbf{n}) \cdot \mathbf{v} \, d\Gamma_N - \sum_{r=1}^{n_r} \int_{\Gamma_e} \boldsymbol{\sigma}(\mathbf{u}_h)\mathbf{n} \cdot \mathbf{v} \, d\Gamma_e. \end{aligned} \tag{3.14}$$

In a compact way, the equation can be written as

$$a(\mathbf{e}_h, \mathbf{v}) = \sum_{e=1}^{n_e} \int_{\Omega_e} \mathbf{R}_e(\mathbf{u}_h) \cdot \mathbf{v} \, d\Omega_e + \sum_{r=1}^{n_r} \int_{\Gamma_e} \mathbf{J}_r(\mathbf{u}_h) \cdot \mathbf{v} \, d\Gamma_e \tag{3.15}$$

where $\mathbf{R}_e$, the residuum of the strong equilibrium condition, is defined as

$$\mathbf{R}_e = div\,\boldsymbol{\sigma}(\mathbf{u}_h) + \mathbf{f} \qquad \forall\, \Omega_e \tag{3.16}$$

and the jumps $\mathbf{J}_r$ on interface tractions become

$$\mathbf{J}_r = \begin{cases} \frac{1}{2}(\boldsymbol{\sigma}(\mathbf{u}_h)^{+}\mathbf{n}^{+} + \boldsymbol{\sigma}(\mathbf{u}_h)^{-}\mathbf{n}^{-}) & \text{at } \Gamma_e \\ \overline{\mathbf{t}} - \boldsymbol{\sigma}(\mathbf{u}_h)\mathbf{n} & \text{at } \Gamma_N \\ \mathbf{0} & \text{at } \Gamma_D. \end{cases} \tag{3.17}$$

In (3.15) all variables, except $\mathbf{v}$, are known from the finite element solution. Theoretically, it is possible to solve the equation using discretisation. This would be computationally expensive, as it is necessary to expand the space of the ansatz functions to prevent the solution from reaching zero. An alternative is to determine $a(\mathbf{e}_h, \mathbf{v})$ approximately. This idea was first formulated by BABUSKA / RHEINBOLDT [5] and extended to elasticity theory by BABUSKA / MILLER [3]. A summary can be found in STEEB [62] or GRÄTSCH / BATHE [21]. First, equation (3.15) is extended by subtracting $a(\mathbf{e}_h, \mathbf{v}_h)$, which is feasible due to the Galerkin orthogonality. The term $\mathbf{v}_h$ can be described by the *Clément operator*, $\mathbf{v}_h = \mathit{\Pi}_h\mathbf{v}$, which maps all continuous ansatz functions to the space $\mathcal{V}_h$. Applying the *Cauchy-Schwarz inequality* for integrals, eq. (A.9) , and describing the associated integrals by the L_2-norm, results in an upper bound of the error.

$$a(\mathbf{e}_h, \mathbf{v}) \leq \sum_{e=1}^{n_e} \|\mathbf{R}_e(\mathbf{u}_h)\|_{L_2}\, \|\mathbf{v} - \mathit{\Pi}_h\mathbf{v}\|_{L_2} + \sum_{r=1}^{n_r} \|\mathbf{J}_r(\mathbf{u}_h)\|_{L_2}\, \|\mathbf{v} - \mathit{\Pi}_h\mathbf{v}\|_{L_2} \tag{3.18}$$

The norm $\|\mathbf{v} - \mathit{\Pi}_h\mathbf{v}\|_{L^2}$ is bounded from above by a local approximation of the interpolation.

$$\begin{aligned} \|\mathbf{v} - \mathit{\Pi}_h\mathbf{v}\|_{L^2(\Omega_e)} &\leq C_{i,1} h_e |\mathbf{v}|_{\mathcal{H}^1(\Omega_e)} \\ \|\mathbf{v} - \mathit{\Pi}_h\mathbf{v}\|_{L^2(\Gamma_e)} &\leq C_{i,1} \sqrt{h_r} |\mathbf{v}|_{\mathcal{H}^1(\Gamma_e)} \end{aligned} \tag{3.19}$$

Therewith, the interpolation constant C_i is introduced, which depends on the element size, the polynomial degree and the inter-element angle. Inserting this approximation in (3.18) and re-arrangement, a second constant C_r, depending on the number of elements of the local domain, emerges. In a last step, the previously introduced $\mathcal{H}_1$-semi-norm is replaced by the energy norm. By *V-ellipticity/coercivity* the equivalence of both norms is shown, which are linked by a stability constant C_s.

$$|\mathbf{v}|_{\mathcal{H}^1} \leq C_s \|\mathbf{v}\|_E \tag{3.20}$$

The constant C_s describes the sensitivity of the differential equation regarding disturbances and equals 1.0 for elliptic partial differential equations. Subsequently, the discretisation error $\mathbf{e}_h$ is chosen as test function for (3.18), which finally leads to

$$\|\mathbf{e}_h\|_E \leq C_i C_s C_r \sqrt{\sum_{e=1}^{n_e} h_e^2 (\|\mathbf{R}_e(\mathbf{u}_h)\|_{L_2})^2 + \sum_{r=1}^{n_r} h_r (\|\mathbf{J}_r(\mathbf{u}_h)\|_{L_2})^2}. \tag{3.21}$$

Here h_e and h_Γ are the characteristic element size and the edge length, respectively. Due to the difficulties in calculating these constants, the error can hardly be quantified correctly. Therefore, this error estimation technique is often used as an indicator for mesh adaptivity. The mesh size is sufficient if the error in all elements is approximately equal.

Averaging-type estimates/Recovery-based estimates

This heuristic approach was first introduced by ZIENKIEWICZ / ZHU [72]. It is based upon the circumstance whereby the gradient of the Finite Element solution is in general discontinuous across inter-element boundaries. Based on the discrete solution $\mathbf{u}_h$, an averaged gradient is determined, and for its corresponding displacements $\mathbf{u}^*$, it is assumed that the inequality

$$\|\mathbf{u} - \mathbf{u}^*\|_E \leq C \|\mathbf{u}^* - \mathbf{u}_h\|_E \qquad \text{with } 0 < C < 1 \tag{3.22}$$

holds. An extension of the energy norm of the error $\|\mathbf{e}_h\|_E$ by $(\mathbf{u}^* - \mathbf{u}^*)$ and the application of the *triangle inequality* leads to the estimate

$$\|\mathbf{e}_h\|_E \leq \|\mathbf{u} - \mathbf{u}_h + \mathbf{u}^* - \mathbf{u}^*\|_E \leq (1 + C) \|\mathbf{u}^* - \mathbf{u}_h\|_E. \tag{3.23}$$

An alternative is the formulation of the error directly in terms of the averaged gradients, e.g. the stresses $\boldsymbol{\sigma}^*$. Following the procedure that was previously introduced for $\|\mathbf{e}_h\|_E$, leads to an error definition in the L_2-norm.

$$\begin{aligned} \|\mathbf{e}_\sigma\|_{L_2} &:= \|\boldsymbol{\sigma} - \boldsymbol{\sigma}_h\|_{L_2} \\ &= \|\boldsymbol{\sigma} - \boldsymbol{\sigma}_h + \boldsymbol{\sigma}^* - \boldsymbol{\sigma}^*\|_{L_2} \\ &\leq (1 + C) \|\boldsymbol{\sigma}^* - \boldsymbol{\sigma}_h\|_{L_2} \end{aligned} \tag{3.24}$$

To determine the averaged stresses, post-processing methods are used after the discretised solution is found. One quite inexpensive computational approach is based on local averaging. Using the same ansatz function as already introduced for the displacements, the stress values are extrapolated to the element nodes, and the average of the adjacent elements is determined. The method can be improved if instead of the nodal values, values of super-convergent points are used. Details concerning the so-called *super-convergent patch recovery technique* can be found in ZIENKIEWICZ / ZHU [73].

Applying this approach, one needs to be aware of the following drawbacks/problems:

- Under certain conditions, the averaged gradient can be qualified as super-convergent[1] because the Finite Element solution is often closer to the averaged solution than the exact one. This means that the true error might be underestimated.

- The question of whether the averaged values are better than the Finite Element solution cannot be answered generally.

- GRÄTSCH / BATHE [21] point out that for special problems with oscillating solutions, the engineer needs to pay special attention. The basic assumption, that smoothed values are better than oscillating ones is not valid in such a context.

Absolute/implicit error bounds

Improved information concerning the error inherent in the Finite Element solution can be obtained by solving auxiliary problems. These auxiliary problems are local boundary value problems formulated on a small element patch - *sub-domain residual method* - or on a single element - *element residual method*. The first approach has the drawback that it might be computationally more expensive, as each element is considered several times. E.g. if a domain with *n* nodes is divided in *n* patches, each patch consists of a central node and the adjoint elements. Higher computational costs, compared to explicit error estimates, are excepted, as tighter upper error bounds can be achieved. In the following, only local Neumann problems are considered. Fundamental work in this field was done by LADEVEZE / LEGUILLON [34] and BANK / WEISER [8].

The idea is to solve the weak error equation (3.3) element-wise. For the term $(\mathbf{f}, \mathbf{v})$, see (2.36), an adequate expression on element level needs to be found. These so-called boundary tractions, describe the equilibrium on the common edge of two neighbouring elements $\Gamma_{e,i}$ and $\Gamma_{e,j}$. Approximated local boundary tractions

$$\mathbf{t}_e \approx \boldsymbol{\sigma}(\mathbf{u}_h)_e \mathbf{n}_e \qquad \text{on } \Gamma_e \tag{3.25}$$

are defined and have to fulfil the conditions

$$\mathbf{t}_e = \bar{\mathbf{t}} \qquad \text{on } \Gamma_N \tag{3.26a}$$

$$\mathbf{t}_e^+ + \mathbf{t}_e^- = 0 \qquad \text{on } \Gamma_{e,i} \cap \Gamma_{e,j} \tag{3.26b}$$

$$\int_{\Gamma_e} \mathbf{t}_e \, d\Gamma_e = \underbrace{-\int_{\Omega_e} (\mathbf{p} - div\boldsymbol{\sigma}(\mathbf{u}_h)) \, d\Omega_e}_{\text{inner element residuals}}. \tag{3.26c}$$

[1] super-convergent means that the solution converges faster than expected

Based on the previous equation, the boundary traction can be written as

$$\int_{\Gamma_N} \overline{\mathbf{t}} \cdot \mathbf{v} \, d\Gamma_N = \sum_{e=1}^{n_e} \int_{\Gamma_e} \mathbf{t}_e \cdot \mathbf{v} \, d\Gamma_e. \tag{3.27}$$

The weak equation defining the error (3.3) can thus be rewritten in an element-wise form.

$$a(\mathbf{e}_h, \mathbf{v}) = \sum_{e=1}^{n_e} \left((\mathbf{p}, \mathbf{v})_e + \int_{\Gamma_e} \mathbf{t}_e \cdot \mathbf{v} - a_e(\mathbf{u}_h, \mathbf{v}) \, d\Gamma_e \right). \tag{3.28}$$

Applying Cauchy-Schwarz inequality and using $\mathbf{e}_h$ as a test function, results in

$$\|\mathbf{e}_h\|_E \leq \sum_{e=1}^{n_e} \|\mathbf{e}_{h,e}\|_E, \tag{3.29}$$

where $\mathbf{e}_{h,e}$ is the discretisation error of one element. It becomes clear, that the quality of the error estimate strongly depends on the quality of the approximated local tractions. The requirement that the tractions have to be in equilibrium with the inner element residuals (3.26c) can be used for their determination. From the Finite Element analysis, fictive nodal forces $\hat{\mathbf{p}}_e$ are known and can be related to the discrete inner element residuals

$$\begin{aligned} \sum_{n=1}^{n_{nodes}} \hat{\mathbf{p}}_e^i \hat{\mathbf{v}}^i &= a_e(\mathbf{u}_h, \mathbf{v}_h) - \int_{\Omega_e} \mathbf{p} \, \mathbf{v}_h \, d\Omega_e \\ &= \int_{\Gamma_e} \mathbf{t}_{e,h} \cdot \mathbf{v}_h \, d\Gamma_e \end{aligned} \tag{3.30}$$

The continuous variables $\mathbf{t}_{e,h}$ and $\mathbf{v}_h$ are discretised using bi-orthonormal[2] ansatz functions $\bar{N}^j$ and N_i. Shape functions for $\mathbf{t}_{e,h}$ have to be orthonormal with respect to the shape functions used for $\mathbf{v}_h$ ([64], p. 340). E.g. for a patch of five elements, see fig. 3.2. Inserting these ansatz functions in (3.30), results in a system of equations such as

$$\begin{bmatrix} 1 & 0 & 0 & 0 & -1 \\ -1 & 1 & 0 & 0 & 0 \\ 0 & -1 & 1 & 0 & 0 \\ 0 & 0 & -1 & 1 & 0 \\ 0 & 0 & 0 & -1 & 1 \end{bmatrix} \begin{bmatrix} \hat{\mathbf{t}}_{\Gamma_{e,1} \cap \Gamma_{e,2}} \\ \hat{\mathbf{t}}_{\Gamma_{e,2} \cap \Gamma_{e,3}} \\ \hat{\mathbf{t}}_{\Gamma_{e,3} \cap \Gamma_{e,4}} \\ \hat{\mathbf{t}}_{\Gamma_{e,4} \cap \Gamma_{e,5}} \\ \hat{\mathbf{t}}_{\Gamma_{e,5} \cap \Gamma_{e,1}} \end{bmatrix} = \begin{bmatrix} \hat{\mathbf{p}}_{e,1} \\ \hat{\mathbf{p}}_{e,2} \\ \hat{\mathbf{p}}_{e,3} \\ \hat{\mathbf{p}}_{e,4} \\ \hat{\mathbf{p}}_{e,5} \end{bmatrix}. \tag{3.31}$$

Two important things need to be considered. First eq. (3.31) is not regular and additional equations are necessary to solve it, see e.g. [53]. As mentioned in the beginning of this paragraph, this system of equations needs to be formulated for an element patch around each node to determine

[2] bi-orthonormal means that the condition $\int_{\Omega_e} \bar{N}^j N_i d\Omega_e = \delta_j^i$ is fulfilled.

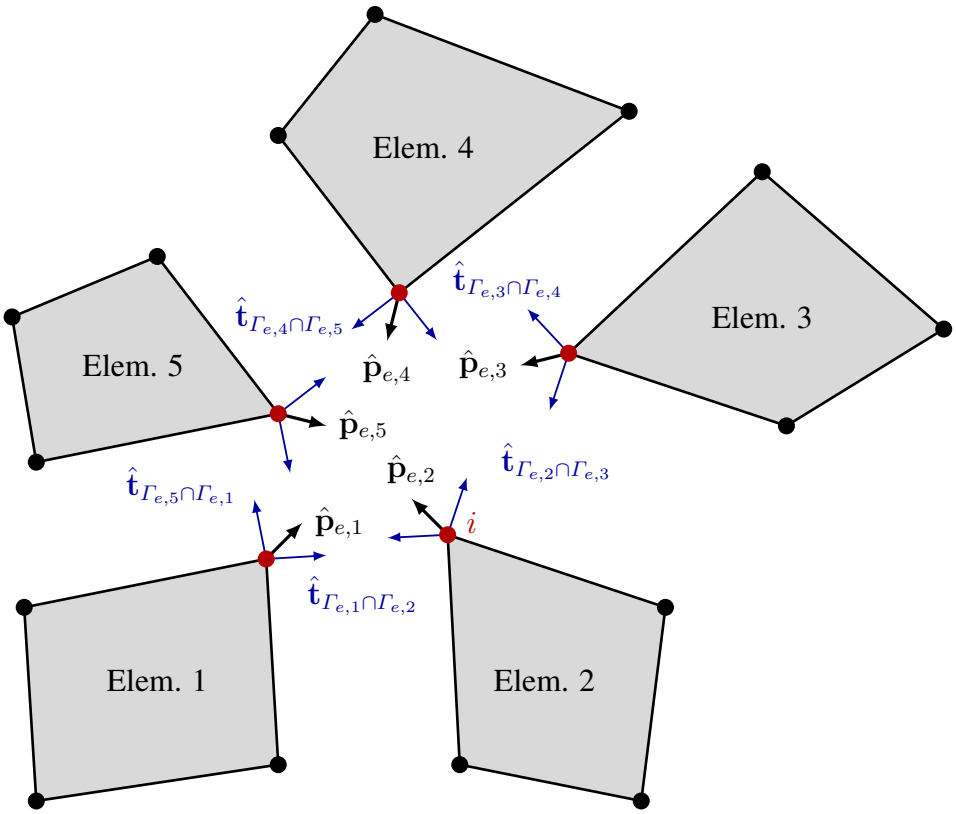

Figure 3.2.: Element patch surrounding node i for the determination of nodal forces $\hat{\mathbf{p}}$, according to [62]

the vector of local, discretised boundary tractions $\hat{\mathbf{t}}_e$. Applying the ansatz function, $\mathbf{t}_e$ is found. Using eq. (3.28) the upper bound for the discretisation error (3.29) can be calculated.

An alternative approach for calculating the error is given by STEIN / OHNIMUS [64], STEIN / OHNIMUS [65]. They call the method the posteriori equilibrium method (PEM). First, the improved equilibrated tractions are determined as described above. Afterwards, local variational problems are defined element-wise for an extended test space $\mathcal{V}_{h+}$, by using the tractions as Neumann boundary conditions. The local nodal boundary tractions are interpreted as nodal loads on the elements. Using locally expanded test spaces for each element, improved displacements $\mathbf{u}_{h+}$ are determined by solving element-wise variational problems

$$a(\mathbf{u}_{h+}, \mathbf{v}_{h+})_{\Omega_e} = F(\mathbf{v}_{h+})_{\Gamma_e} \qquad \text{with } F(\mathbf{v}_{h+})_{\Gamma_e} = \int_{\Gamma_e} \mathbf{t}_{e,h} \cdot \mathbf{v}_{h+}\, d\Gamma_e. \tag{3.32}$$

The discretisation error can thus be formulated in the energy norm as

$$\|\mathbf{e}_h\|_E^2 = \|\mathbf{u}_{h+} - \mathbf{u}_h\|_E^2 \leq a((\mathbf{u}_{h+} - \mathbf{u}_h), (\mathbf{u}_{h+} - \mathbf{u}_h)). \tag{3.33}$$

3.1.4 Goal-oriented/local error estimators

In general the structural engineer is more interested in predicting quantities of engineering significance that are relevant to determine the serviceability or the ultimate limit state of a structure. These quantities of interest or goal quantities $J(\mathbf{u})$ are functionals of the displacements $g(\mathbf{u})$, e.g. stresses in specific points or integral values like moments in beams or displacements itself.

$$J(\mathbf{u}) = \frac{1}{\Omega_{patch}} \int_{\Omega_{patch}} g(\mathbf{u})\, d\Omega_{patch} \tag{3.34}$$

Therefore the focus is shifted from global error estimation towards the error in the goal quantity due to the discretisation, see e.g. [11], [35].

$$J(\mathbf{e}_h) = J(\mathbf{u}) - J(\mathbf{u}_h) \tag{3.35}$$

The local error $J(\mathbf{e}_h)$ cannot be calculated by eq. (3.35), because $\mathbf{u}$ and with it $J(\mathbf{u})$ are unknown. So the most obvious approach, the calculation based on the displacement solution $\mathbf{u}$ of the primal problem, eq. (3.34), is not possible. An alternative way applies *Betti's theorem*, which is also known as *Reciprocal theorem*, *Green's identity* or *Concept of influence functions*. In linear elasticity theory, when the superposition principle can be applied, it holds

$$(\mathbf{p}_{primal}, \mathbf{u}_{dual}) + (\mathbf{f}_{primal}, \mathbf{u}_{dual}) = (\mathbf{p}_{dual}, \mathbf{u}_{primal}) + (\mathbf{f}_{dual}, \mathbf{u}_{primal}). \tag{3.36}$$

The work done by the primal loading on the dual displacement equals the work done by the dual loading on the primal displacements. In the case, that a nodal displacement $u(x_i)$ represents the goal quantity, the equivalent dual force is the Dirac-Delta function in this point x_i. In Finite Element calculations, this point load needs to be regularised, which means distributed over an local element patch, to prevent singularities. Anyway, for this kind of goal quantity, it follows that

$$\begin{aligned} J(\mathbf{u}_h) = u_h(x_i) = (\underbrace{u_h(x_i)}_{\text{primal displ.}}, \underbrace{\delta(x_i)}_{\text{dual load}}) &= (\mathbf{p}, \mathbf{G}_h) + (\bar{\mathbf{t}}, \mathbf{G}_h) \\ &= a(\mathbf{u}_h, \mathbf{G}_h) = a(\mathbf{G}_h, \mathbf{u}_h). \end{aligned} \tag{3.37}$$

The goal quantity can be determined by the semi-linear function $a(.,.)$. The same result can be achieved through a generalised examination. Both terms $F(.)$, (2.36), and $J(.)$ are linear functionals of a certain displacement. Therefore, $J(\mathbf{v})$ can be interpreted as the right-hand side of an equation comparable to (2.36).

$$a(\mathbf{z}, \mathbf{v}) = J(\mathbf{v}) \tag{3.38}$$

The solution $\mathbf{z}$ is named generalised Green's function. Due to symmetry of the semi-linear form $a(.,.)$ it holds

$$J(\mathbf{u}) = a(\mathbf{z}, \mathbf{u}) = a(\mathbf{u}, \mathbf{z}) = F(\mathbf{z}) \tag{3.39}$$

This relation can be used to determine $J(\mathbf{u}_h)$, if the same discretisation is used for the primal and the dual problem. After choosing the notation $\mathbf{G}$ also for the generalised Green's function, for the dual problem

$$a(\mathbf{G}, \mathbf{v}) = J(\mathbf{v}) \tag{3.40}$$

can be formulated according to (2.36). In test space $\mathcal{V}_h$ the variational formulation becomes

$$a(\mathbf{G}_h, \mathbf{v}_h) = J(\mathbf{v}_h) \tag{3.41}$$

with the dual error defined as

$$\mathbf{e}_h^* := \mathbf{G} - \mathbf{G}_h. \tag{3.42}$$

The residual R_h^* is defined as

$$R_h^*(\mathbf{G}_h, \mathbf{v}) := a(\mathbf{e}_h^*, \mathbf{v}) = J(\mathbf{v}) - a(\mathbf{G}_h, \mathbf{v}) \tag{3.43}$$

Finally, the error in the quantity of interest (3.35) can be defined as

$$J(\mathbf{e}_h) = J(\mathbf{u}) - J(\mathbf{u}_h) = a(\mathbf{G}, \mathbf{u}) - a(\mathbf{G}, \mathbf{u}_h) = a(\mathbf{G}, \mathbf{e}_h) \tag{3.44}$$

Expanding the previous description using Galerkin orthogonality by $a(\mathbf{G}_h, \mathbf{e}_h) = 0$, results in the basic equation for goal-oriented error estimates

$$J(\mathbf{e}_h) = a(\mathbf{e}_h^*, \mathbf{e}_h). \tag{3.45}$$

To determine the error in the functional $J(\mathbf{e}_h)$ different options are given below.

Energy-norm-based estimates/Duality techniques

According to CIRAK [16] the Cauchy-Schwarz inequality is applied on (3.45), which yields to

$$|J(\mathbf{e}_h)| \leq \|\mathbf{G} - \mathbf{G}_h\|_E \|\mathbf{u} - \mathbf{u}_h\|_E. \tag{3.46}$$

The energy norms for the primal and dual errors can be determined using error estimation techniques introduced in section 3.1.3. Generally, this leads to an element-wise determination of the

discretisation error, which can be summed up to acquire a global measure for the local error. From (3.46) it can be seen, that the global error is scaled by the discretisation error in Green's function. Numerical experiments show that "..., goal-oriented error estimators based on energy norm estimates [...] eliminate the cancellation of errors over the domain, and therefore produce significant error overestimation in general" [21, p. 246]. Tighter error bounds can be achieved using the parallelogram identity. This technique was introduced by BABUSKA ET AL. [6] and applied to material modelling by e.g. ODEN / PRUDHOMME [46] and ODEN / PRUDHOMME [47]

$$J(\mathbf{e}_h) = a(\mathbf{e}_h, \mathbf{e}_h^*) = \frac{1}{4}\|s\mathbf{e}_h + \frac{\mathbf{e}_h^*}{s}\|_E - \frac{1}{4}\|s\mathbf{e}_h - \frac{\mathbf{e}_h^*}{s}\|_E, \qquad \text{with } s = \sqrt{\frac{\|\mathbf{e}_h^*\|_E}{\|\mathbf{e}_h\|_E}}. \tag{3.47}$$

Upper and lower error bounds are defined

$$\frac{1}{4}(\zeta_{low}^+)^2 - \frac{1}{4}(\zeta_{upp}^-)^2 \leq J(\mathbf{e}_h) \leq \frac{1}{4}(\zeta_{upp}^+)^2 - \frac{1}{4}(\zeta_{low}^-)^2 \tag{3.48}$$

with

$$\begin{aligned} \zeta_{low}^+ &\leq \|s\mathbf{e}_h + \frac{\mathbf{e}_h^*}{s}\|_E \leq \zeta_{upp}^+, \\ \zeta_{low}^- &\leq \|s\mathbf{e}_h - \frac{\mathbf{e}_h^*}{s}\|_E \leq \zeta_{upp}^-. \end{aligned} \tag{3.49}$$

To determine $\zeta_{low/upp}^{+/-}$, in ODEN / PRUDHOMME [47] implicit error estimators are used.

Dual-weight residual method (DWR)

This technique was first introduced by BECKER / RANNACHER [11] and extended to linear elasticity by RANNACHER / SUTTMEIER [58]. The concept is based on *residual-based estimates*, which were previously introduced. Equ. (3.15) is expanded by applying the Galerkin orthogonality $a(\mathbf{e}_h, \mathbf{v}_h) = 0$. As test functions $\mathbf{v}$ can be chosen arbitrarily, here the solution of the dual problem $\mathbf{G}/\mathbf{G}_h$ is used. The same result can be achieved by applying symmetry conditions of $a(.,.)$ and the Galerkin orthogonality $a(\mathbf{e}_h, \mathbf{G}_h) = 0$ on eq. (3.44)

$$J(\mathbf{e}_h) = a(\mathbf{e}_h, \mathbf{G}) = a(\mathbf{e}_h, \mathbf{G} - \mathbf{G}_h). \tag{3.50}$$

Written in terms of the residual-based approach, eq. (3.15) becomes

$$\begin{aligned} J(\mathbf{e}_h) &= a(\mathbf{e}_h, \mathbf{G} - \mathbf{G}_h) \\ &= \sum_{e=1}^{n_e} \int_{\Omega_e} \mathbf{R}_e(\mathbf{u}_h) \cdot (\mathbf{G} - \mathbf{G}_h)\, d\Omega_e + \sum_{r=1}^{n_r} \int_{\Gamma_e} \mathbf{J}_r(\mathbf{u}_h) \cdot (\mathbf{G} - \mathbf{G}_h)\, d\Gamma_e. \end{aligned} \tag{3.51}$$

The terms $\mathbf{R}_e$ and $\mathbf{J}_r$ are the residual and jump terms of the primal problem defined in eqs. (3.16) and (3.17). The error in the dual solution $\mathbf{e}_h^* = \mathbf{G} - \mathbf{G}_h$ serves as a weight ω_e for the residual term.

A local interpolation estimate, cf. eq. (3.19), is used to determine the weight. As $\mathbf{G}$ is unknown, it needs to be replaced with an extended discretised solution $\mathbf{G}_{h+}$. This yields an estimation of the weight ω_e

$$\omega_{e,app} = C_{i,e} h_e |\nabla_h^2 \mathbf{G}_{h+}|_{\mathcal{H}^1(\Omega_e)}, \tag{3.52}$$

and the error in the goal quantity can be approximated with

$$J(\mathbf{e}_h)_{app} = \sum_{e=1}^{n_e} \int_{\Omega_e} \mathbf{R}_e(\mathbf{u}_h) \cdot \omega_{e,app} \, d\Omega_e + \sum_{r=1}^{n_r} \int_{\Gamma_e} \mathbf{J}_r(\mathbf{u}_h) \cdot \omega_{e,app} \, d\Gamma_e. \tag{3.53}$$

The local interpolation constant $C_{i,e}$ depends on the element geometry. As its determination is not straightforward, it "may be set $C_{i,e} = 1$" [58, p. 438]. It cannot be guaranteed that no underestimation of the error occurs due to this simplification. To determine the unknown $\mathbf{G}_{h+}$, several options are given in [11]. The dual problem can be solved using higher-order ansatz functions, as done previously for the determination of $\mathbf{G}_h$, or the discretisation could be refined.

3.1.5 Estimators for non-linear problems

Global estimates

An adaptation of global discretisation error estimators for non-linear problems can e.g. be found in HUERTA ET AL. [24] or CIRAK [16]. The decomposition of the functional $a(.,.)$, according to $\mathbf{u} = \mathbf{u}_h + \mathbf{e}_h$, (3.3), is not valid in the non-linear case, since

$$a(\mathbf{u}; \mathbf{v}) = a(\mathbf{u}_h + \mathbf{e}_h; \mathbf{v}) \neq a(\mathbf{u}_h; \mathbf{v}) + a(\mathbf{e}_h; \mathbf{v}). \tag{3.54}$$

It would be beneficial if error estimation techniques introduced for linear problems could be adapted to the non-linear case. The basic idea is to reduce the solution of the non-linear problem to the solution of the linearised problem. Therefore, a series expansion is performed to find a formulation for the error

$$a(\mathbf{u}_h + \mathbf{e}_h; \mathbf{v}) = a(\mathbf{u}_h; \mathbf{v}) + a_T(\mathbf{u}_h; \mathbf{e}_h, \mathbf{v}) + \mathrm{h.o.t.}. \tag{3.55}$$

The higher-order terms $\mathrm{h.o.t.}$ are neglected, as error is assumed to be small compared to the displacement solution. This leads to a definition of the residual

$$R(\mathbf{u}_h, \mathbf{v}) = F(\mathbf{v}) - a(\mathbf{u}_h; \mathbf{v}) \approx a_T(\mathbf{u}_h; \mathbf{e}_h, \mathbf{v}). \tag{3.56}$$

This equates to the error estimation in equilibrium points of certain load steps. Additionally, a non-linear energy norm must be defined. If the tangent form $a_T(\mathbf{u}_h; ., .)$ is symmetric and positive definite, the norm induced by $a_T(\mathbf{u}_h; ., .)$ can be used for this purpose.

Techniques previously introduced for linear problems can be applied to determine the error, e.g. MATERNA [40] uses *residual-based estimates*

$$a_T(\mathbf{u}_h; \mathbf{e}_h, \mathbf{v}) = \sum_{e=1}^{n_e} \int_{\Omega_e} \mathbf{R}_e(\mathbf{u}_h) \cdot \mathbf{v} \, d\Omega + \sum_{r=1}^{n_r} \int_{\Gamma_e} \mathbf{J}_r(\mathbf{u}_h) \cdot \mathbf{v} \, d\Gamma_e. \tag{3.57}$$

They differ from the linear version (3.15) in the definition of the residuum $\mathbf{R}_e(\mathbf{u}_h)$, which is defined as

$$\mathbf{R}_e(\mathbf{u}_h) = \mathbf{f} + div(\mathbf{S}_h - \nabla \mathbf{u}_h \mathbf{S}_h). \tag{3.58}$$

Goal-oriented estimates

The theory of goal-oriented error estimates for non-linear problems was introduced by BECKER / RANNACHER [12] and BANGERTH / RANNACHER [7]. To determine the error in the goal quantity, eq. (3.35) , a possibility needs to be found to express $J(\mathbf{u})$ using known quantities. In the linear case, Green's identity was used for this purpose, which is no longer valid in the non-linear case. Therefore, the derivation is based on the formulation of a constraint optimisation problem:

$$\begin{aligned} &J(\mathbf{u}) \rightarrow \min, \\ &a(\mathbf{u}; \mathbf{v}) = F(\mathbf{v}) \end{aligned} \tag{3.59}$$

The formulation using the Lagrange multiplier method reads

$$\mathcal{L}(\mathbf{u}, \mathbf{z}) = J(\mathbf{u}) - \underbrace{[a(\mathbf{u}; \mathbf{z}) - F(\mathbf{z})]}_{G(\mathbf{u}; \mathbf{z})} \tag{3.60}$$

where $\mathbf{z}$, the generalised Green's function, represents the Lagrange multiplier. The optimisation problem is solved by setting $d\mathcal{L} = 0$, which results in the formulation of the primal and the dual problem. The derivative of (3.60) with respect to $\mathbf{z}$ leads to the primal problem, which equals the fundamental variational equation

$$G'_z(\mathbf{u}; \mathbf{z}, \mathbf{v}) = \lim_{\epsilon \rightarrow 0} \epsilon^{-1} \left[G(\mathbf{u}; \mathbf{z} + \epsilon \mathbf{v}) - G(\mathbf{u}; \mathbf{z}) \right] = G(\mathbf{u}; \mathbf{v}) \tag{3.61}$$

The dual problem corresponds to the derivatives

$$J'_u(\mathbf{u}; \boldsymbol{\rho}) - G'_u(\mathbf{u}; \boldsymbol{\rho}, \mathbf{z}) = 0. \tag{3.62}$$

After introducing the Finite Element method with its inherent discretisation of the domain, eq. (3.60) becomes

$$\mathcal{L}(\mathbf{u}_h, \mathbf{z}_h) = J(\mathbf{u}_h) - [a(\mathbf{u}_h, \mathbf{z}_h) - F(\mathbf{z}_h)] \tag{3.63}$$

with the corresponding definition of the primal and the dual problem. The residual R_h is defined according to the linear case, see eq. (3.3) , as

$$R_h(\mathbf{u}_h; \mathbf{v}) := F(\mathbf{v}) - a(\mathbf{u}_h; \mathbf{v}) \tag{3.64}$$

and the adjoint or dual residual R_h^* becomes

$$R_h^*(\mathbf{u}_h; \boldsymbol{\rho}) := J'_u(\mathbf{u}_h; \boldsymbol{\rho}) - G'_u(\mathbf{u}_h; \boldsymbol{\rho}, \mathbf{z}_h). \tag{3.65}$$

The error in the goal quantity equals

$$J(\mathbf{e}_h) = J(\mathbf{u}) - J(\mathbf{u}_h) = \mathcal{L}(\mathbf{u}, \mathbf{z}) - \mathcal{L}(\mathbf{u}_h, \mathbf{z}_h) \tag{3.66}$$

The goal is to define the error in terms of the residual's R_h and R_h^*. To achieve this goal, $\mathcal{L}(\mathbf{u}, \mathbf{z})$ is expanded in a Taylor series, and after some transformation we end up with

$$\begin{aligned} J(\mathbf{u}) - J(\mathbf{u}_h) = &\frac{1}{2}\mathcal{L}'(\mathbf{u}_h, \mathbf{z}_h)(\mathbf{e}_h, \mathbf{e}_h^*) \\ &+ \frac{1}{2}\int_0^1 \mathcal{L}'''(\mathbf{u}_h + s\mathbf{e}_h, \mathbf{z}_h + s\mathbf{e}_h^*)(\mathbf{e}_h, \mathbf{e}_h^*)(\mathbf{e}_h, \mathbf{e}_h^*)(\mathbf{e}_h, \mathbf{e}_h^*)\epsilon(\epsilon - 1)\, d\epsilon. \end{aligned} \tag{3.67}$$

The first summand can be expressed using the previously defined residuals.

$$\begin{aligned} \mathcal{L}'(\mathbf{u}_h, \mathbf{z}_h)(\mathbf{e}_h, \mathbf{e}_h^*) &= \mathcal{L}'_u(\mathbf{u}_h, \mathbf{z}_h)(\mathbf{e}_h) &&+\mathcal{L}'_z(\mathbf{u}_h, \mathbf{z}_h)(\mathbf{e}_h^*) \\ &= J'_u(\mathbf{u}_h; \mathbf{e}_h) - G'_u(\mathbf{u}_h; \mathbf{e}_h, \mathbf{z}_h) &&-G(\mathbf{u}_h; \mathbf{e}_h^*) \\ &= R_h^*(\mathbf{z}_h; \mathbf{e}_h) &&+R_h(\mathbf{u}_h; \mathbf{e}_h^*) \end{aligned} \tag{3.68}$$

Additionally, a relation between the primal and dual residual, for details see [12], can be given in the form

$$R_h^*(\mathbf{z}_h; \mathbf{e}_h) = R_h(\mathbf{u}_h; \mathbf{e}_h^*) + \Delta R \tag{3.69}$$

The second summand in eq. (3.67) is cubic in the errors $\mathbf{e}_h$ and $\mathbf{e}_h^*$ and "may usually be neglected" [12, p. 10]. This finally leads to an error representation of the form

$$J(\mathbf{e}_h) = R_h(\mathbf{u}_h; \mathbf{e}_h^*) + \frac{1}{2}\Delta R. \tag{3.70}$$

This approach is e.g. applied to perfect plasticity, see [59] and [12]. The term ΔR "is not further considered" [12, p. 79], which leads to an estimate of the error

$$J(\mathbf{e}_h) \approx R_h(\mathbf{u}_h; \mathbf{e}_h^*) = F(\mathbf{e}_h^*) - a(\mathbf{u}_h; \mathbf{e}_h^*). \tag{3.71}$$

At this point the well-known residual-based error estimate, or more precisely the dual-weight residual method, introduced on p. 40, can be applied. The error is approximated with

$$J(\mathbf{e}_h) \approx \sum_{e=1}^{n_e} \int_{\Omega_e} \mathbf{R}_e(\mathbf{u}_h)\, \mathbf{e}_h^*\, d\Omega_e + \sum_{r=1}^{n_r} \int_{\Gamma_e} \mathbf{J}_r(\mathbf{u}_h)\, \mathbf{e}_h^*\, d\Gamma_e \tag{3.72}$$

$\mathbf{R}_e(\mathbf{u}_h)$ and $\mathbf{J}_r(\mathbf{u}_h)$ are determined according to eqs. (3.58) and (3.17) , respectively. The weights ω_e introduced by the difference of the dual solution are approximated by local interpolation estimates. The same result can be achieved following the approach of CIRAK / RAMM [17]. They follow the idea that was previously introduced for global discretisation errors for non-linear problems, see p. 41, and incorporate the linearisation of the underlying non-linear formulation.

3.2 Model error estimates

3.2.1 Overview

Since the mid-1990s the research in the field of error estimators has been broadened to include model error estimates. The fundamental idea was to establish methods, that allow the estimation of the modelling error based on the solution of a simplified model. The magnitude of the error is used as an indicator to steer an adaptive process, where more sophisticated models are introduced if necessary. ODEN ET AL. [74], [51] started to work on global model error estimates for heterogenous materials. They extended the theory to local error estimates [45], [50]. In this context the parallelogram identity, which has proven to be useful to find tighter error bounds for discretisation errors [46], is applied. In ODEN ET AL. [49] the theory is extended to non-linear problems and applied to global problems when modelling non-linear viscoelastic material. Based on the ideas of BECKER / RANNACHER [12] local model error estimators are introduced in ODEN / PRUDHOMME [48]. LARSSON / RUNESSON [37] also work on non-linear global and local error estimators for material model problems. In their derivations of error estimators, they choose an alternative way compared to ODEN ET AL. They linearise the underlying equation and are then able to apply techniques already introduced for linear problems. A comprehensive overview of linear and non-linear model error estimates, based on BECKER / RANNACHER [12], is also given in BRAACK / ERN [14]. Here the applications of interest are diffusion problems and Poisson's equation.

In contrast to the previously introduced research, which is mainly dedicated to material modelling, STEIN ET. AL introduced model error estimators that deal with the problem of dimension and model adaptivity. Using dimensional reduced models involves approximations of kinematic and/or physical hypotheses, e.g the Bernoulli hypothesis. In large domains of the structure, 1D- or 2D- models lead to considerably good results, whereas disturbances near supports or appearance of concentrated loads requires higher quality models. The goal is to estimate these errors and steer an adaptive process of dimensional and model change based on these results. First attempts of dealing with modelling errors caused by dimensional reduction were done on the basis of heuristic strategies, OHNIMUS [52]. Additionally, the anisotropic residual error estimation (REM) was introduced, where the dimension adaptivity was linked with p-adaptivity, see also STEIN / OHNIMUS [63]. In STEIN / OHNIMUS [64] the posteriori equilibrium method (PEM), which is based on local variational Neumann problems, is adjusted to deal with modelling errors. STEIN ET AL. [67] and [68] extend this theory to non-linear problems and goal-oriented error estimates, still with the focus on dimensional adaptivity.

In model error estimation it is assumed, that a problem can be described using a simple model a_s and a complex, more sophisticated one a_c. The complex model can be split in two parts

$$a_c(\mathbf{u};\mathbf{v}) = a_s(\mathbf{u};\mathbf{v}) + d(\mathbf{u};\mathbf{v}). \tag{3.73}$$

The application of both models to a certain structural problem leads to different displacement solutions $\mathbf{u}_s$ and $\mathbf{u}_c$, for the simplified and the complex model, respectively.

$$\begin{aligned} a_s(\mathbf{u}_s;\mathbf{v}) &= (\mathbf{p},\mathbf{v}) \\ a_c(\mathbf{u}_c;\mathbf{v}) = a_s(\mathbf{u}_c;\mathbf{v}) + d(\mathbf{u}_c;\mathbf{v}) &= (\mathbf{p},\mathbf{v}) \end{aligned} \tag{3.74}$$

Because the right-hand sides are equal, the difference term can be calculated using

$$\begin{aligned} a_s(\mathbf{u}_c;\mathbf{v}) + d(\mathbf{u}_c;\mathbf{v}) &= a_s(\mathbf{u}_s;\mathbf{v}) \\ a_s(\mathbf{u}_c;\mathbf{v}) - a_s(\mathbf{u}_s;\mathbf{v}) &= -d(\mathbf{u}_c;\mathbf{v}). \end{aligned} \tag{3.75}$$

For linear models, see e.g. BRAACK / ERN [14], it is possible to write

$$a_s(\mathbf{e}_m,\mathbf{v}) = -d(\mathbf{u}_c,\mathbf{v}) \tag{3.76}$$

with the model error defined as

$$\mathbf{e}_m = \mathbf{u}_c - \mathbf{u}_s \tag{3.77}$$

the difference of the displacement solution of the simplified and the complex model. The error in the energy norm can be found by replacing $\mathbf{v}$ with $\mathbf{e}_m$, see e.g. ODEN / ZOHDI [51],

$$a_s(\mathbf{e}_m,\mathbf{e}_m) = \|\mathbf{e}_m\|_E^2 = -d(\mathbf{u}_c,\mathbf{e}_m). \tag{3.78}$$

For linear models, the dual problem can be formulated according to (3.40) and the theory of Green's function given in sec. 3.1.4,

$$\begin{aligned} a_s(\mathbf{G_s},\mathbf{v}) &= J(\mathbf{v}) \\ a_c(\mathbf{G_c},\mathbf{v}) = a_s(\mathbf{G}_c,\mathbf{v}) + d(\mathbf{G}_c,\mathbf{v}) &= J(\mathbf{v}). \end{aligned} \tag{3.79}$$

In the second equation, $\mathbf{v}$ is substituted by $\mathbf{e}_m$ and in the a- and d-term, the order of the coefficients is changed

$$a_s(\mathbf{e}_m,\mathbf{G}_c) + d(\mathbf{e}_m,\mathbf{G}_c) = J(\mathbf{e}_m). \tag{3.80}$$

Using the relationship given in (3.76) and split $d(\mathbf{e}_m,\mathbf{G}_c)$ in $d(\mathbf{u}_c-\mathbf{u}_s,\mathbf{G}_c)$ results in

$$-d(\mathbf{u}_s,\mathbf{G}_c) = J(\mathbf{e}_m). \tag{3.81}$$

Generally, one needs to make sure, that the discretisation error is sufficiently small before the model error estimation strategies are applied and the model is adapted.

3.2.2 Global model error estimates for linear problems

Application to material modelling

Research in the field of error estimation in the field of material modelling has been carried out by Oden and coworkers since the mid-1990s. Their goal has been the computation of an "estimate of the modelling error introduced by replacing the actual fine-scale material tensor with that of a homogenised material [...]." [74, p. 273] This information is used to steer an adaptive process that introduces the fine-scale material tensor in areas with high errors. In ZOHDI ET AL. [74] a global error estimator is derived for elastostatic problems. The derivation differs in some details from the general approach given in eqs.(3.73) to (3.76) , as the difference term d should be calculated using the result of the simple model. Two models are distinguished: a complex model incorporating the fine-scale elasticity tensor $\mathbf{C}_{fs}$ and a simple model, with the homogenised material tensor $\mathbf{C}_{hom}$

$$a_c(\mathbf{u}_c, \mathbf{v}) = \int_\Omega \nabla\mathbf{v} : \mathbf{C}_{fs}\nabla\mathbf{u}_c d\Omega = F(\mathbf{v}), \tag{3.82a}$$

$$a_s(\mathbf{u}_s, \mathbf{v}) = \int_\Omega \nabla\mathbf{v} : \mathbf{C}_{hom}\nabla\mathbf{u}_s d\Omega = F(\mathbf{v}). \tag{3.82b}$$

The difference between both models can be formulated as

$$d(\mathbf{u}_s, \mathbf{v}) = a_c(\mathbf{u}_s, \mathbf{v}) - a_s(\mathbf{u}_s, \mathbf{v}) = \int_\Omega \nabla\mathbf{v} : (\mathbf{C}_{fs} - \mathbf{C}_{hom})\nabla\mathbf{u}_s d\Omega. \tag{3.83}$$

As the right-hand sides of eqs. (3.82a) and (3.82b) are equal, by using (3.83) it can be written

$$\begin{aligned} a_c(\mathbf{u}_c, \mathbf{v}) - a_c(\mathbf{u}_s, \mathbf{v}) &= a_c(\mathbf{u}_c - \mathbf{u}_s, \mathbf{v}) \\ &= a_c(\mathbf{e}_m, \mathbf{v}) = -d(\mathbf{u}_s, \mathbf{v}) \\ &=: R_m(\mathbf{u}_s, \mathbf{v}). \end{aligned} \tag{3.84}$$

Setting $\mathbf{v} = \mathbf{u}_c - \mathbf{u}_s$ and applying Cauchy-Schwarz inequality, gives

$$\begin{aligned} \|\mathbf{e}_m\|_E^2 &= \|\mathbf{u}_c - \mathbf{u}_s\|_E^2 \\ &= -\int_\Omega \nabla(\mathbf{u}_c - \mathbf{u}_s) : (\mathbf{C}_{fs} - \mathbf{C}_{hom})\nabla\mathbf{u}_s d\Omega \\ &\le \|\mathbf{u}_c - \mathbf{u}_s\|_E \|\mathcal{I}_0\nabla\mathbf{u}_s\|_E, \qquad \mathcal{I}_0 = \mathbf{I} - \mathbf{C}_{fs}^{-1}\mathbf{C}_{hom}. \end{aligned} \tag{3.85}$$

Finally, the displacement error in the energy norm can be bounded from above by

$$\|\mathbf{u}_c - \mathbf{u}_s\|_E \le \|\mathcal{I}_0\nabla\mathbf{u}_s\|_E = \eta_{upp}. \tag{3.86}$$

A lower error bound can be found using the residual $R_m(\mathbf{u}_0, \mathbf{v})$, eq. (3.84) . The energy norm of the error equals the norm of the residual in the dual space $\|R_m\|_{\mathcal{V}'}$. For this norm, a lower error bound is defined as

$$\|\mathbf{e}_m\|_E = \|R_m\|_{\mathcal{V}'} := \sup_{v \in \mathcal{V}} \frac{|R_m(\mathbf{u}_s, \mathbf{v})|}{\|\mathbf{v}\|_E} \geq \frac{|R_m(\mathbf{u}_s, \mathbf{u}_s)|}{\|\mathbf{u}_s\|_E} = \eta_{low}. \tag{3.87}$$

To control the quality of the estimate, the effectivity index is defined. It relates the error estimate to the real error and leads e.g. the upper error bound to

$$I_{eff} = \frac{\eta_{upp}}{\|\mathbf{u}_c - \mathbf{u}_s\|_E}. \tag{3.88}$$

Table 3.1 shows the effectivity indices for the upper and lower bounds of the global error. For the presented examples, the exact model could be evaluated. For these examples, the derived bounds lead to good estimates for the error. An exception is the cantilever modelled with a checkerboard microstructure. It could be shown using [51] that this is due to disadvantageous model of the inclusions. Investigations of the same structure using ellipsoidal and spherical inclusions leads to much better efficiency indices.

Table 3.1.: Effectivity indices: Global model error estimates - Examples by ZOHDI, VEMAGANTI

Structural system	Effectivity index	
	η_{low}	η_{upp}
Heterogeneous bar, [74], [45]	0.7 ... 0.98	1.00
3D analysis of a cube in shear		
checkerboard microstructure, [74]	-	1.4 ... 2.7
ellipsoidal/spherical inclusions, [51]	-	1.0 ... 1.05
Wall structure with spherical inclusions, [50]	0.494	1.085

Application to dimensional adaptivity

Modelling in structural engineering is affected by simplifications. Very common are dimensional reductions of the structure using beam (1D elements), plate or shell elements (2D) instead of a full 3-dimensional modelling. Such dimensional reductions involve model simplification, like the introduction of kinematical and/or physical hypotheses, e.g the Bernoulli hypothesis. In undisturbed domains such approaches are sufficient, but they can lead to inaccuracies when e.g. supports or point loads occur. STEIN ET AL. provide different methods to determine the model error due to dimensional reduction and provide therewith the basis for dimensional adaptivity. Their first publications dealing with this topic, [52], [63] and [64], are dedicated to linear model problems, where the global model error is determined.

The first attempt made by OHNIMUS [52] is a heuristic error estimator. Based on St. Venant's principle, the dimension is increased, if the element length is 2.5 times smaller than its height. Residual-based estimates, see p. 32, are the basis for the anisotropic residual-based error estimator (REM), [52]. The model/dimension error is not determined directly but in a roundabout way by calculating the discretisation error. If the error estimator leads to the result, that for certain direction p- or h-adaptivity is necessary, this is interpreted as an indicator for dimensional expansion. The dimensional reduction is equated with hierarchical reduction of the ansatz space. In contrast to the classical procedure introduced by BABUSKA / RHEINBOLDT [5], the variational problem, eq. (3.15) , is solved directly. As it would be quite time-consuming to solve the problem for the entire system, an element-wise approach is preferred. Based on the current model, the element residuals are determined according to eqs. (3.16) , (3.17) . These results are projected on a patch $\mathcal{P}_e$ surrounding the element. The error at the boundaries of the patch is assumed to be zero, which is valid due to St. Venant's principle of decaying local disturbances. To solve the variational problem on the patch, higher-order test spaces have to be used either with respect to mesh refinement or polynomial expansion. This provides the opportunity to use different ansatz spaces for different directions. The whole procedure is sped up by mapping the information from $\mathcal{P}_e$ onto a parametric patch $\mathcal{I}_e$ using Jacobian transformation. The underlying equation system, including e.g stiffness matrixes, only needs to be set up once for all elements. The resulting equation system, and therewith the element-wise error, for each element can then be evaluated by either solving a general eigenvalue problem or by inverting the local stiffness matrix of the element patch.

An alternative procedure to determine the dimensional error directly is proposed in STEIN / OHNIMUS [64]. The posteriori equilibrium method (PEM) yields an error estimator with an upper bound, and an adaptive split of discretisation and model error is possible. The procedure equals the implicit error estimates introduced on p. 35 ff. Equilibrated tractions are determined and the error is calculated in a comparable manner to eqs. (3.32) , (3.33) . In contrast to discretisation error estimation, here the ansatz space as well as the dimensional model are expanded for the local Neumann problems. The hierarchical expanded model is named a_{s+} and yields to improved displacements on element level $\mathbf{u}_{h+,s}$. To solve the equations on the element level, it is necessary to eliminate rigid body modes. Finally eq. (3.32) becomes

$$a_{s+}(\mathbf{u}_{h+,s}, \mathbf{v}_{h+})_{\Omega_e} = F(\mathbf{v}_{h+})_{\Gamma_e}. \tag{3.89}$$

Improved displacements of the simpler model $\mathbf{u}_{h+}$ are found using locally expanded test spaces. The definition of the error η^2_{E,σ_e} in the energy norm using the stresses of the current and improved model, has proven to be the most meaningful one.

$$\eta^2_{E,\sigma_e} = \|\boldsymbol{\sigma}_{h+,s} - \boldsymbol{\sigma}_{h+}\|^2_E \tag{3.90}$$

To determine the difference of $\boldsymbol{\sigma}_{h+,s}$ and $\boldsymbol{\sigma}_{h+}$ a prolongation $\mathcal{P}\mathbf{u}_s$ between the solution spaces needs to be guaranteed. It can be observed, that PEM leads to better efficiency indices than REM.

3.2.3 Global model error estimates for non-linear problems

Estimates based on the difference of the complex and the simplified model

Similar to discretisation error theory, the strategy for the definition of the model error for linear problems, introduced in sec. 3.2.2, cannot be applied to non-linear problems. The reason is that the relation used in eq. (3.84) to derive the estimate is not valid for non-linear variational problems. For applications where both models are linear, it can be shown that this spilt is feasible.

$$\int_\Omega \varepsilon(\mathbf{v})\mathbf{C}_{fs}\varepsilon(\mathbf{u}_c)d\Omega - \int_\Omega \varepsilon(\mathbf{v})\mathbf{C}_{fs}\varepsilon(\mathbf{u}_s)d\Omega = \int_\Omega \varepsilon(\mathbf{v})\mathbf{C}_{fs}(\varepsilon(\mathbf{u}_c) - \varepsilon(\mathbf{u}_s))d\Omega \tag{3.91}$$

Considering non-linearities, e.g. in the kinematical description, leads to the appearance of quadratic or even higher-order terms with respect to the displacement, which makes a split like eq. (3.91) incorrect. Therefore, another approach needs to be found for non-linear problems.

ODEN ET AL. [49] derive a global error bound for non-linear material models, that can be used to steer an adaptive process. The method was tested on a class of visco-elastic material models of hierarchical order. The derivation for the global modelling residual is comparable to the approach that was used for linear models as well, see sec. 3.2.2. A residuum is defined based on the differences between the simplified and complex models.

The model in the variational form also considers inertia terms and the time t dependence reads as follows

$$\int_\Omega \rho_0 \ddot{\mathbf{u}}(t)\cdot\mathbf{v}d\Omega + \int_\Omega \mathbf{F}(\mathbf{u},t)\mathcal{P}(\nabla\mathbf{u}^t(s),t) : \nabla\mathbf{v}d\Omega = F(\mathbf{u}(t);\mathbf{v},t). \tag{3.92}$$

Here $\mathcal{P}(\nabla\mathbf{u}^t(s),t)$ is the constitutive functional, which depends amongst others on internal variables s, like the temperature or entropy. A simplified and a complex model vary in the formulation of the constitutive functional, where the simplified version is labelled $\mathcal{P}_s(\nabla\mathbf{u}_s^t(s),t)$ and $\mathbf{u}_s$ the associated displacement solution. It is not difficult but time-consuming to show that the difference between both models becomes

$$\underbrace{\int_\Omega \left[\rho_0\ddot{\mathbf{e}}_u(t)\cdot\mathbf{v} + \nabla\mathbf{e}_u(t)\mathcal{P}_c(\nabla\mathbf{u}_s^t(s),t) : \nabla\mathbf{v} + \mathbf{F}(\mathbf{u}_s+\mathbf{e}_u,t)\mathbf{E}_P(t) : \nabla\mathbf{v}\right]d\Omega - \mathbf{e}_F(\mathbf{v},t)}_{\mathcal{E}(t)}$$
$$\underbrace{- \int_\Omega \mathbf{F}(\mathbf{u}_s,t)\Delta\mathcal{P}(\nabla\mathbf{u}_s^t(s),t) : \nabla\mathbf{v}d\Omega}_{\text{Residuum: } \mathcal{R}(\mathbf{u}_s^t(s);\mathbf{v},t)} = 0. \tag{3.93}$$

with

$$\begin{aligned}
\mathbf{e}_u(t) &= \mathbf{u}_c(t) - \mathbf{u}_s(t), \\
\mathbf{E}_P(t) &= \mathcal{P}_c(\nabla \mathbf{u}_c^t(s), t) - \mathcal{P}_c(\nabla \mathbf{u}_s^t(s), t), \\
\mathbf{e}_F(\mathbf{v}, t) &= F(\mathbf{u}_c(t); \mathbf{v}, t) - F(\mathbf{u}_s(t); \mathbf{v}, t), \\
\Delta\mathcal{P}(\nabla \mathbf{u}_s^t(s), t) &= \mathcal{P}_s(\nabla \mathbf{u}_s^t(s), t) - \mathcal{P}_c(\nabla \mathbf{u}_s^t(s), t).
\end{aligned} \tag{3.94}$$

As indicated in eq. (3.93), the last term of the model difference is defined as residuum. Inherent in this term is the difference between the model definitions. Additionally, it has the advantage, that it can be determined by knowing only the simplified solution $\mathbf{u}_s$. Thus, it is used to steer the adaptive process by indicating when a model change is necessary. An upper error bound for the residuum $\mathcal{R}(\mathbf{u}_s^t(s); \mathbf{v}, t)$ can be found by applying Schwarz's inequality

$$\begin{aligned}
\mathcal{R}(\mathbf{u}_s^t(s); \mathbf{v}, t) \;&\leq\; \eta(t)\, \|\nabla \mathbf{v}\|_{L_2} \\
&\text{with } \eta(t) = \sqrt{\int_\Omega \left[F(\mathbf{u}_s(t); t) \Delta\mathcal{P}(\nabla \mathbf{u}_s^t(s), t)\right]^2 d\Omega}.
\end{aligned} \tag{3.95}$$

Introducing this inequality in (3.93), dividing by $\|\nabla \mathbf{v}\|_{L_2}$ and taking the supremum, results in the global error bound

$$\|\mathcal{E}(t)\|_{V'} \;\leq\; \eta(t), \tag{3.96}$$

where $\|\cdot\|_{V'}$ denotes the norm in the dual space $\mathcal{V}'$ of $\mathcal{V}$. A global error bound is found by calculating $\eta(t)$ element-wise and summing up over the whole domain.

When the derived error bound is applied, it is slightly changed without giving reasons or explanations. The upper error bound, eq. (3.96), is scaled by the norm of the strain energy of the simpler model:

$$\overline{\eta}(t) = \sqrt{\frac{\eta(t)^2}{\eta(t)_{add}^2}} \qquad \text{with } \eta(t)_{add}^2 = \int_\Omega \left[F(\mathbf{u}_s(t); t) \mathcal{P}_s(\nabla \mathbf{u}_s^t(s), t)\right]^2 d\Omega. \tag{3.97}$$

Equation (3.97) is evaluated element-wise and the material model of the elements, where the error bound exceeds a certain tolerance, is upgraded. The proposed procedure gives reasonable results for the example investigated in [49], a plate with a central hole under tension.

Posteriori equilibrium method for dimensional adaptivity

In STEIN ET AL. [67] the posteriori equilibrium method (PEM) is extended towards non-linear problems and goal-oriented error estimates. The derivations are based on the basic assumption, that the error is "small with respect to the associated solution" [67, p. 3602], which is crucial as

it is not fulfilled under all circumstances. Comparable to the approach of HUERTA, see p. 41, the underlying equations are thus linearised, which leads to

$$a_c(\mathcal{P}\mathbf{u}_s + \mathbf{e}_m; \mathbf{v}) \approx a_c(\mathcal{P}\mathbf{u}_s; \mathbf{v}) - a_{T,c}(\mathbf{u}_s; \mathbf{e}_m, \mathbf{v}). \tag{3.98}$$

This allows defining the residual as

$$R(\mathbf{u}_s, \mathbf{v}) = F(\mathbf{v}) - a_c(\mathcal{P}\mathbf{u}_s; \mathbf{v}) \approx a_{T,c}(\mathbf{u}_s; \mathbf{e}_m, \mathbf{v}). \tag{3.99}$$

The norm induced by $a_{T,c}(\mathbf{u}_s; \cdot, \cdot)$ is analogous to the standard energy norm. Applying the Finite Element method, it can be seen that the general structure of $\|\cdot\|_E = a(\mathbf{e}_m, \mathbf{e}_m) = \hat{\mathbf{e}}_m \mathbf{k}_e \hat{\mathbf{e}}_m$ and $a_{T,c}(\mathbf{u}_s; \mathbf{e}_m, \mathbf{e}_m) = \hat{\mathbf{e}}_m \mathbf{k}_T(\hat{\mathbf{u}}_s)\hat{\mathbf{e}}_m$ is equal. Therefore, after linearisation the standard procedure of PEM can be applied, which is:

1. Solution of the simple model $a_s(\mathbf{u}_s; \mathbf{v}) = F(\mathbf{v})$,
2. Elementwise determination of the tractions $\mathbf{t}_e$ according to the procedure given on p. 35 ff.,
3. Solution of local Neumann problems using the previously defined tractions as boundary condition and applying the more sophisticated model a_c elementwise, see p. 49,
4. Determination of the error in the energy norm $\|\mathbf{e}_m\|_E^2 = a_{T,c}(\mathbf{u}_s; \mathbf{e}_m, \mathbf{e}_m)$.

In [36] the authors pursue the same strategy. The residual is first described using the secant form

$$R(\mathbf{u}_s, \mathbf{v}) = \int_0^1 a_{T,c}(\mathbf{u}_s + s\mathbf{e}_m; \mathbf{e}_m, \mathbf{v}), \tag{3.100}$$

and afterwards this expression is simplified using the tangent formulation, see eq. (3.99) . As the best model a_c is often inaccessible in practice, a fine model a_{s+}, which is a hierarchical expansion of the simple one, is used instead. This is comparable to the approach of STEIN ET. AL., who introduces a $2\frac{1}{2}D$ model to estimate the error between a 2D and a 3D model.

3.2.4 Goal-oriented model error estimates for linear problems

In ODEN / VEMAGANTI [45] and ODEN / VEMAGANTI [50] the procedure introduced in 3.2.2 is extended to local model error estimates for elastostatic problems. The goal is to determine the error in the quantity of interest $J(\mathbf{e}_m)$ due to the model error $\mathbf{e}_m = \mathbf{u}_c - \mathbf{u}_s$. According to the procedure introduced in chapter 3.1.4, first the dual problem for the complex model

$$J(\mathbf{v}) = a_c(\mathbf{v}, \mathbf{G}_c) \tag{3.101}$$

and the simplified model

$$J(\mathbf{v}) = a_s(\mathbf{v}, \mathbf{G}_s) \tag{3.102}$$

are introduced. Here $\mathbf{G}_s$ and $\mathbf{G}_c$ are the dual solution or Green's function for the simplified and the complex model, respectively. This leads to the definition of the error in the dual solution as

$$\mathbf{e}_m^* = \mathbf{G}_c - \mathbf{G}_s. \tag{3.103}$$

The error in the goal quantity can be described as

$$\begin{aligned} J(\mathbf{e}_m) &= J(\mathbf{u}_c) - J(\mathbf{u}_s) \\ &= a_c(\mathbf{u}_c, \mathbf{G}_c) - a_c(\mathbf{u}_s, \mathbf{G}_c) = a_c(\mathbf{e}_m, \mathbf{G}_c) \\ &= R_m(\mathbf{u}_s, \mathbf{G}_c). \end{aligned} \tag{3.104}$$

The formulation for the error in the goal quantity (3.104) can be split in two parts

$$J(\mathbf{e}_m) = a_c(\mathbf{e}_m, \mathbf{G}_c) = a_c(\mathbf{e}_m, \mathbf{G}_s + \mathbf{e}_m^*) = a_c(\mathbf{e}_m, \mathbf{G}_s) + a_c(\mathbf{e}_m, \mathbf{e}_m^*). \tag{3.105}$$

The first summand corresponds to the residual function $R_m(\mathbf{u}_s, \mathbf{G}_s)$ and can be calculated according to eq. (3.84). Upper and lower error bounds are defined in eqs. (3.86) and (3.87). For the second term, an approach is used that was already introduced for discretisation errors, see sec. 3.1.4. Introducing a scaling factor s and applying the parallelogram identity results in

$$a_c(\mathbf{e}_m, \mathbf{e}_m^*) = \frac{1}{4}\|s\mathbf{e}_m + \frac{\mathbf{e}_m^*}{s}\|_E - \frac{1}{4}\|s\mathbf{e}_m - \frac{\mathbf{e}_m^*}{s}\|_E. \tag{3.106}$$

Upper estimates $\zeta_{upp}^{\pm}$ for the norm $\|s\mathbf{e}_m \pm \frac{\mathbf{e}_m^*}{s}\|_E$ are found by applying techniques that are known from global model error estimates, see (3.85), (3.86). This leads to

$$\begin{aligned} a_c(s\mathbf{e}_m \pm \frac{\mathbf{e}_m^*}{s}, \mathbf{v}) &= R_m(s\mathbf{u}_s \pm \frac{\mathbf{G}_s}{s}, \mathbf{v}) \\ &= -\int_\Omega \nabla\mathbf{v} : \mathbf{C}\mathcal{I}_0\nabla(s\mathbf{u}_s \pm \frac{\mathbf{G}_s}{s}) d\Omega \end{aligned} \tag{3.107}$$

and with $\mathbf{v} = s\mathbf{e}_m \pm \frac{\mathbf{e}_m^*}{s}$ the upper bound becomes

$$\|s\mathbf{e}_m \pm \frac{\mathbf{e}_m^*}{s}\|_E \leq \sqrt{-\int_\Omega \mathcal{I}_0\nabla(s\mathbf{u}_s \pm \frac{\mathbf{G}_s}{s}) : \mathbf{C}_{fs}\mathcal{I}_0\nabla(s\mathbf{u}_s \pm \frac{\mathbf{G}_s}{s}) d\Omega} = \zeta_{upp}^{\pm}. \tag{3.108}$$

The lower bound $\zeta_{low}^{\pm}$ is defined according to the global error (3.87)

$$\|s\mathbf{e}_m \pm \frac{\mathbf{e}_m^*}{s}\|_E \geq \frac{|R_m(s\mathbf{u}_s \pm \frac{\mathbf{G}_s}{s}, \mathbf{v})|}{\|\mathbf{v}\|_E} = \zeta_{low}^{\pm}. \tag{3.109}$$

The scaling factor s is defined as the square root of $\|\mathbf{e}_m^*\|_E / \|\mathbf{e}_m\|_E$, as it leads to a minimum of $\|s\mathbf{e}_m \pm \frac{\mathbf{e}_m^*}{s}\|_E$. The error in the primal and dual solutions are both unknown and are therefore approximated according to eq. (3.86). This leads to an approximation of the scaling factor

$$s \approx \sqrt{\frac{\eta_{upp}^*}{\eta_{upp}}}. \tag{3.110}$$

Summarising the previously introduced relationships and using (3.48) , the error in the functional becomes

$$\begin{aligned} J(\mathbf{e}_m) \geq \zeta_{low} &= \frac{1}{4}(\zeta_{low}^+)^2 - \frac{1}{4}(\zeta_{upp}^-)^2 + R_m(\mathbf{u}_s, \mathbf{G}_s) \\ \leq \zeta_{upp} &= \frac{1}{4}(\zeta_{upp}^+)^2 - \frac{1}{4}(\zeta_{low}^-)^2 + R_m(\mathbf{u}_s, \mathbf{G}_s). \end{aligned} \tag{3.111}$$

Additionally, an estimate is established, where the second summands in (3.111) are exchanged.

$$\begin{aligned} J(\mathbf{e}_m) \gtrapprox \zeta_{low,est} &= \frac{1}{4}(\zeta_{low}^+)^2 - \frac{1}{4}(\zeta_{low}^-)^2 + R_m(\mathbf{u}_s, \mathbf{G}_s) \\ \lessapprox \zeta_{upp,est} &= \frac{1}{4}(\zeta_{upp}^+)^2 - \frac{1}{4}(\zeta_{upp}^-)^2 + R_m(\mathbf{u}_s, \mathbf{G}_s). \end{aligned} \tag{3.112}$$

For the first and third example mentioned in table 3.1, local error estimates are investigated, see also fig. 3.3. For the heterogenous bar, investigated in [74] and [45], first an investigation of $\zeta_{low}^{\pm}$ and $\zeta_{upp}^{\pm}$ is done. The quantities of interest are the average stress in the interval $0.75 \ldots 0.76$ and the pointwise value of the homogenisation error at $x = 0.75$. For both quantities, the effectivity index of $\zeta_{upp}^{\pm}$ equals one, whereas for $\zeta_{low}^{\pm}$ the values range from 0.57 to 0.98. These errors in the estimation propagate as ζ_{low} and ζ_{upp} are determined. Here the effectivity index reaches values of ± 4.7, which is far away from the optimal value of one. The estimates of the upper and lower bounds for local error $\zeta_{low,est}$ and $\zeta_{upp,est}$ show a better behaviour. From eq. (3.111) it is clear that $\zeta_{upp,est}$ does not use the error-prone quantity $\zeta_{low}^{\pm}$, and in $\zeta_{low,est}$ a cancellation of the error occurs. For the first goal quantity, this leads to $\zeta_{upp,est}$=0.84 and $\zeta_{low,est}$=1.0, for the second one $\zeta_{upp,est}$=0.4 and $\zeta_{low,est}$=0.86. It is conspicuous, that the lower bound is larger than the upper bound.

For the wall structure, see [50], the same behaviour is monitored. Here the goal quantity is the average stress in a small domain. Equ. (3.111) leads to effectivity indices of -163 and 161, respectively. Whereas the estimated bounds, eq. (3.112) , are $\zeta_{upp,est}$=-2.03 and $\zeta_{low,est}$=0.7. "We see that the estimate $\zeta_{low,est}$ alone has a reasonable effectivity index. In our experience, this estimate has performed consistently and can be used to drive the adaptive process." [50, p. 46] Studying VEMAGANTI / ODEN [69] it is conspicuous that this statement is disregarded. Here they take $\zeta_{upp,est}$ as the estimate for the local error and achieve effectivity indices close to one. Summarising these results, the presented methods seems not to be very reliable to the author. Reasons for this are the seemingly arbitrarily chosen estimates for the error and the missing derivations for the error estimates.

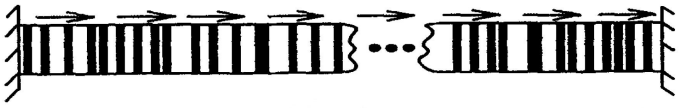

(a) Heterogenous bar, [45]

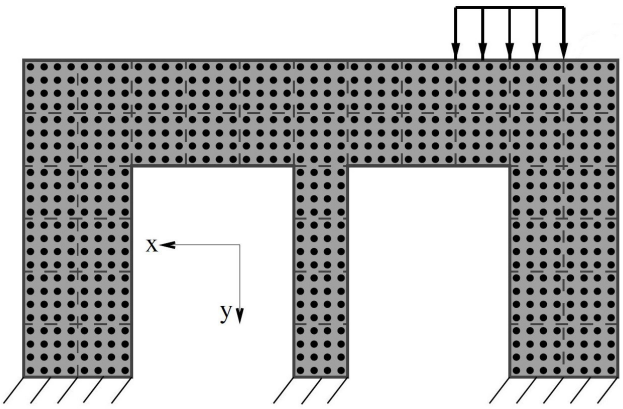

(b) Wall structure with spherical inclusions, [50]

Figure 3.3.: Structures where the goal-oriented model error is determined for linear problems

3.2.5 Goal-oriented model error estimates for non-linear problems

Optimal control approach

Based on the method of BECKER / RANNACHER [12] for discretisation errors, ODEN / PRUDHOMME [48], BRAACK / ERN [14] and KUNOW [33] derive goal-oriented model error estimates for non-linear problems. The variational problems are defined as optimisation problems using Lagrange's multiplier method. For the stationary point $(\mathbf{u}, \mathbf{z})$, with $\mathbf{z}$ as generalised Green's function, it is

- Simple model:

$$\mathcal{L}_s(\mathbf{u}_s, \mathbf{z}_s) = J(\mathbf{u}_s) - [a_s(\mathbf{u}_s; \mathbf{z}_s) - F(\mathbf{z}_s)] \tag{3.113}$$

- Complex model:

$$\begin{aligned} \mathcal{L}(\mathbf{u}_c, \mathbf{z}_c) &= J(\mathbf{u}_c) - [a_c(\mathbf{u}_c; \mathbf{z}_c) - F(\mathbf{z}_c)] \\ &= J(\mathbf{u}_c) - [a_s(\mathbf{u}_c; \mathbf{z}_c) + d(\mathbf{u}_c; \mathbf{z}_c) - F(\mathbf{z}_c)] \\ &= \mathcal{L}_s(\mathbf{u}_c, \mathbf{z}_c) + \underbrace{d\mathcal{L}(\mathbf{u}_c, \mathbf{z}_c)}_{= -d(\mathbf{u}_c; \mathbf{z}_c)} \end{aligned} \tag{3.114}$$

The corresponding primal and dual problems become for the complex model

$$\begin{aligned} a_c(\mathbf{u}_c; \mathbf{v}) - F(\mathbf{v}) &= 0 \\ J'_u(\mathbf{u}_c; \boldsymbol{\rho}) - G'_{c,u}(\mathbf{u}_c; \mathbf{z}_c, \boldsymbol{\rho}) &= 0 \end{aligned} \tag{3.115}$$

and for the simplified model

$$\begin{aligned} a_s(\mathbf{u}_s;\mathbf{v}) - F(\mathbf{v}) &= 0 \\ J'_u(\mathbf{u}_s;\boldsymbol{\rho}) - G'_{s,u}(\mathbf{u}_s;\mathbf{z}_s,\boldsymbol{\rho}) &= 0. \end{aligned} \tag{3.116}$$

The error in the goal quantity becomes

$$\begin{aligned} J(\mathbf{e}_m) = J(\mathbf{u}_c) - J(\mathbf{u}_s) &= \mathcal{L}(\mathbf{u}_c,\mathbf{z}_c) - \mathcal{L}_s(\mathbf{u}_s,\mathbf{z}_s) \\ &= \mathcal{L}(\mathbf{u}_c,\mathbf{z}_c) - \mathcal{L}(\mathbf{u}_s,\mathbf{z}_s) + \underbrace{d\mathcal{L}(\mathbf{u}_s,\mathbf{z}_s).}_{=-d(\mathbf{u}_s;\mathbf{z}_s)} \end{aligned} \tag{3.117}$$

The term $\mathcal{L}(\mathbf{u}_c,\mathbf{z}_c)$ is expanded in a Taylor series, and after some rearrangements this results in

$$\begin{aligned} \mathcal{L}(\mathbf{u}_c,\mathbf{z}_c) - \mathcal{L}(\mathbf{u}_s,\mathbf{z}_s) &= \frac{1}{2}\mathcal{L}'(\mathbf{u}_s,\mathbf{z}_s)(\mathbf{e}_m,\mathbf{e}_m^*) + \frac{1}{2}\mathcal{L}'(\mathbf{u}_c,\mathbf{z}_c)(\mathbf{e}_m,\mathbf{e}_m^*) \\ &+ \underbrace{\frac{1}{2}\int_0^1 \mathcal{L}'''(\mathbf{u}_s + s\mathbf{e}_m, \mathbf{z}_s + s\mathbf{e}_m^*)(\mathbf{e}_m,\mathbf{e}_m^*)(\mathbf{e}_m,\mathbf{e}_m^*)(\mathbf{e}_m,\mathbf{e}_m^*)\epsilon(\epsilon-1)\,d\epsilon.}_{Res^{(3)}} \end{aligned} \tag{3.118}$$

In the stationary point $(\mathbf{u}_c,\mathbf{z}_c)$, the derivative of the Lagrangian $\mathcal{L}$ is zero, which leads to the fact, that the term $\mathcal{L}'(\mathbf{u}_c,\mathbf{z}_c)(\mathbf{e}_m,\mathbf{e}_m^*)$ vanishes in eq. (3.118) . The summand $\mathcal{L}'(\mathbf{u}_s,\mathbf{z}_s)(\mathbf{e}_m,\mathbf{e}_m^*)$ can be split according to eq. (3.114) . In the stationary point $(\mathbf{u}_s,\mathbf{z}_s)$ for the simplified Lagrangian $\mathcal{L}_s$, the same regularity holds as used before

$$\begin{aligned} \mathcal{L}'(\mathbf{u}_s,\mathbf{z}_s)(\mathbf{e}_m,\mathbf{e}_m^*) &= \mathcal{L}'_s(\mathbf{u}_s,\mathbf{z}_s)(\mathbf{e}_m,\mathbf{e}_m^*) + d\mathcal{L}'(\mathbf{u}_s,\mathbf{z}_s)(\mathbf{e}_m,\mathbf{e}_m^*) \\ &= -\underbrace{d(\mathbf{u}_s;\mathbf{e}_m^*)}_{d'_z(\mathbf{u}_s,\mathbf{z}_s)} - \underbrace{d'_u(\mathbf{u}_s;\mathbf{e}_m,\mathbf{z}_s).}_{d'_u(\mathbf{u}_s,\mathbf{z}_s)} \end{aligned} \tag{3.119}$$

Summarizing these derivations results in the representation of the goal-oriented error as

$$J(\mathbf{e}_m) = -d(\mathbf{u}_s;\mathbf{z}_s) - \frac{1}{2}\left[d(\mathbf{u}_s;\mathbf{e}_m^*) + d'_u(\mathbf{u}_s;\mathbf{e}_m,\mathbf{z}_s) - Res^{(3)}\right]. \tag{3.120}$$

It can be seen that except the first summand, all terms depend on the solution of the complex model. For their determination the solution of the complex model and/or the knowledge of the error term is necessary. In case the error is small, all terms in squared brackets are negligible, as they are quadratic or cubic in $(\mathbf{e}_m,\mathbf{e}_m^*)$. Thus BRAACK / ERN [14] defines the approximated estimator as

$$J(\mathbf{e}_m) \approx -d(\mathbf{u}_s;\mathbf{z}_s). \tag{3.121}$$

This formulation is similar to the goal-oriented error representation for linear problems, see eq. (3.81) . Alternatively eq. (3.120) can be written as

$$J(\mathbf{e}_m) = -d(\mathbf{u}_s; \mathbf{z}_c) - \frac{1}{2}\left[\Delta R - Res^{(3)}\right], \tag{3.122}$$

because the equality $d'_u(\mathbf{u}_s; \mathbf{e}_m, \mathbf{z}_s) = d(\mathbf{u}_s; \mathbf{e}^*_m) + \Delta R$ holds; for details see [48].

In KUNOW [33] the error estimator eq. (3.121) is applied to non-linear material models. The comparison of the estimated and the real error shows the problems inherent in the proposed simplification. The approximated error estimator is not able to capture non-linearities. As long as the error increases linearly, the estimator equals the real error. If the relation between the local error, here the displacement error, and the change in the material model, here change in the modulus of elasticity, becomes non-linear, the estimator fails in predicting the behaviour correctly.

Estimates based on linearisation of the primal and dual problems

In LARSSON / RUNESSON [36] and STEIN ET AL. [67] the error in the goal quantity is determined by linearisation of the underlying variational equation. The procedure continues the work on global error estimates, which is described on p. 51 f. In [36] the dual problem is defined as

$$\int_0^1 a_T(\mathbf{u}_s + \epsilon\mathbf{e}_m; \mathbf{z}_c, \mathbf{v})d\epsilon = \int_0^1 J_T(\mathbf{u}_s + \epsilon\mathbf{e}_m, \mathbf{v})d\epsilon. \tag{3.123}$$

After linearisation it can be formulated in tangent form as

$$a_T(\mathbf{u}_s; \mathbf{z}_c, \mathbf{v}) = J_T(\mathbf{u}_s, \mathbf{v}). \tag{3.124}$$

The model chosen for the linearisation is in the optimal case the complex one. If this model is not available or its evaluation is too complicated, then the use of an enhanced simplified model a_{s+} is recommended to determine the dual solution $\mathbf{z}_c$. The same result can be achieved following the approach of [67].

Due to the introduced linearisations for the simple and the complex non-linear model, the definition of the error in the goal quantity is simplified. For linear or linearised problems, Green's identity can be applied, see sec. 3.1.4 or eq. (3.104) . In [36] a slightly different definition of the residual is chosen, which leads to an error definition as follows

$$J(\mathbf{e}_m) = J(\mathbf{u}_s) - J(\mathbf{u}_c) = a_s(\mathbf{u}_s; \mathbf{z}_c) - a_c(\mathbf{u}_s; \mathbf{z}_c). \tag{3.125}$$

Again, if the evaluation of a_c is not possible, an enhanced simplified model a_{s+} can be used. This kind of error formulations provides the possibility to use the difference term, see eq. (3.73) , to determine the error

$$J(\mathbf{e}_m) = -d(\mathbf{u}_s; \mathbf{z}_c). \tag{3.126}$$

Thus the error in the goal quantity can be determined by knowing the difference in the formulation of both models, the solution of the simple model $\mathbf{u}_s$ and the dual solution $\mathbf{z}_c$, which can be found easily due to linearisation.

In [67] a slightly different approach is presented. Also, based on Green's identity, they define the error directly as

$$J(\mathbf{e}_m) = a_T(\mathbf{u}_s; \mathbf{e}_m, \mathbf{z}_c). \tag{3.127}$$

Thus, the same strategy already introduced for global errors, the posteriori equilibrium method (PEM), see p. 51, can be used.

3.3 Selection of methods applied on kinematical models

On the previous pages, methods for estimating the discretisation and model errors in structural mechanics have been introduced. The main focus is placed on the complete representation of techniques regarding non-linear model problems and goal-oriented model error estimators. To the knowledge of the author, other approaches have not been published. Within the scope of this thesis, the presented methods should be applied to kinematical models to answer the question of whether a geometrical non-linear calculation is necessary or not.

Model error estimations techniques developed for linear models cannot be used, as at least the complex model describing the displacement-strain relationship is non-linear. For the determination of the global model error, both methods for non-linear problems that are presented will be implemented. The estimation technique based on the differences between the complex and the simplified models is adapted to the kinematical models and tested. The second approach, based on linearisation of the differential equations, is applied with some changes. The general idea of linearisation is maintained, but finally the error is not found using PEM. Here the problem arises whereby local Neumann problems are introduced, which have the drawback, that rigid body modes need to be eliminated before they can be solved. Therefore, an enhanced global problem is defined to test the applicability of the basic idea. These investigations show the general effects of linearisation, so this method is not tested a second time for goal-oriented errors.

No attempt is made to adopt the idea of ODEN / VEMAGANTI [45], [50] for estimating the local errors based on parallelogram identity to non-linear problems, as the derivation of the applied equations is not clearly documented and the efficiency indices achieved were not very promising. The goal-oriented model error estimator derived from an optimisation problem is tested. For this method, practical experience is only available to a minor degree. It is investigated whether the limitation of the exact error equation to terms that can be determined based on the solution of the simplyfied model, leads to meaningful results and to which extent the different terms contribute to the final result.

4 Applicability of different model error estimation strategies to geometrical non-linear problems

The application of the various error estimation strategies to kinematical models is the content of this chapter. First, different error norms are studied to determine the most significant one with respect to the total scalar value and the error distribution, and to provide knowledge regarding the exact error. For estimation of the global error, three methods are studied: a strategy based on the direct evaluation of the difference term between the various models, the determination of the upper bound of the residuum using Schwarz' inequality and an estimate based on linearisation. Goal-oriented error estimates can be found based on the model difference and in a round-about way via the definition of an optimisation problem.

4.1 Summary kinematical models

Different error estimation techniques will be studied regarding their ability to estimate the model error when using different kinematical descriptions. Before the different strategies introduced in the previous chapter are applied to assess different kinematic descriptions, the underlying variational formulations are summarised based on chapter 2.1. The linear model is represented by

$$a_l(\mathbf{u}_l, \mathbf{v}) = \int_\Omega \boldsymbol{\sigma}(\mathbf{u}_l)\, \boldsymbol{\varepsilon}(\mathbf{v}) d\Omega = F(\mathbf{v}), \quad \text{with } \boldsymbol{\varepsilon}(\mathbf{v}) = \frac{1}{2}\left(\nabla \mathbf{v} + \nabla \mathbf{v}^T\right), \tag{4.1}$$

and the non-linear model by

$$\begin{aligned} a_{nl}(\mathbf{u}_{nl}; \mathbf{v}) &= \int_\Omega \mathbf{S}_{nl}(\mathbf{u}_{nl})\, \mathbf{E}_u(\mathbf{v}) d\Omega = F(\mathbf{v}) \\ \text{with } \mathbf{E}_u(\mathbf{v}) &= \frac{1}{2}\left(\nabla \mathbf{v} + \nabla \mathbf{v}^T + \nabla \mathbf{u}_{nl}^T \nabla \mathbf{v} + \nabla \mathbf{v}^T \nabla \mathbf{u}_{nl}\right). \end{aligned} \tag{4.2}$$

From the non-linear strain and stress tensors, the linear part can be separated:

$$\mathbf{E}_u(\mathbf{v}) = \boldsymbol{\varepsilon}(\mathbf{v}) + \Delta \mathbf{E}(\mathbf{v}, \mathbf{u}_{nl}), \qquad \mathbf{S}_{nl}(\mathbf{u}_{nl}) = \boldsymbol{\sigma}(\mathbf{u}_{nl}) + \Delta \mathbf{S}(\mathbf{u}_{nl}). \tag{4.3}$$

The difference d between both models (4.1) and (4.2) is defined as

$$d(\mathbf{u}_{nl}, \mathbf{v}) = \int_{\Omega} \boldsymbol{\sigma}(\mathbf{u}_{nl}) \cdot \Delta\mathbf{E}(\mathbf{u}_{nl}, \mathbf{v}) + \Delta\mathbf{S}(\mathbf{u}_{nl}) \cdot \boldsymbol{\varepsilon}(\mathbf{v}) + \Delta\mathbf{S}(\mathbf{u}_{nl}) \cdot \Delta\mathbf{E}(\mathbf{u}_{nl}, \mathbf{v}) d\Omega. \qquad (4.4)$$

For all the examples discussed later, sufficiently small discretisation errors are assumed. Thus the investigations can be limited to model errors.

After the error estimation techniques are adapted for the problem under investigation, they will be applied for the model assessment of different structural systems. The same structural systems will be used for this purpose, which makes it meaningful to introduce them once. The idea is to test structures that are modelled using different element types with respect to their dimensions. In addition, the examples can be distinguished by their sensitivity to being modelled using different kinematical assumptions. Some structures are insensitive regarding geometrical non-linear effects; for other systems, the choice of the appropriate kinematical model is crucial.

4.2 Investigated structural systems

Truss structures Two structural systems composed of truss elements are introduced for the following investigations: the Mises truss and a cantilever composed of truss elements. For the Mises truss, fig. 4.1, only half of the system is modelled due to symmetry conditions. For the truss can-

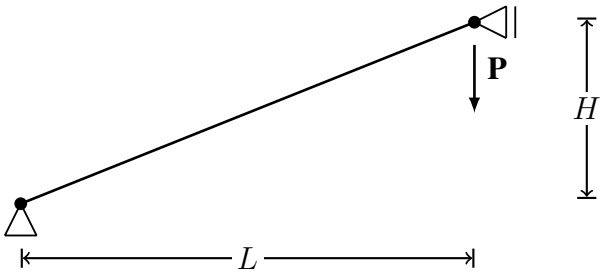

Figure 4.1.: Geometry Mises truss: H=50 cm, L=100 cm, Modulus of elasticity E=21000 kN/cm^2, Cross section A=10 cm^2, Load P=1500 kN

tilever, the structural system is shown in fig. 4.2. The deformation of the system considering a linear and non-linear kinematic description is shown in fig. 4.3

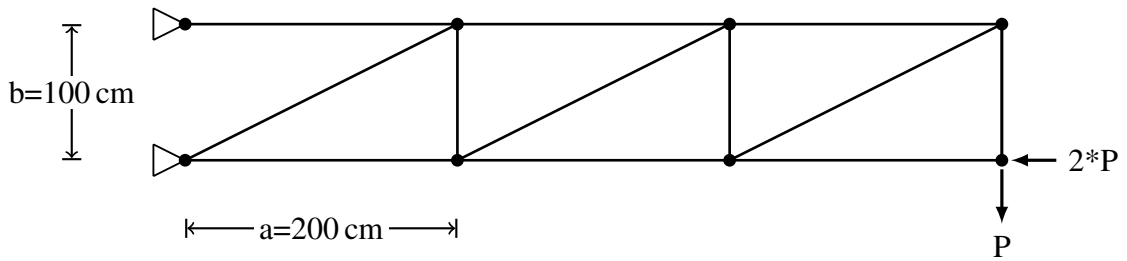

Figure 4.2.: Geometry truss cantilever: Modulus of elasticity E=21000 kN/cm^2, Cross section A=10 cm^2, Load P=500 kN

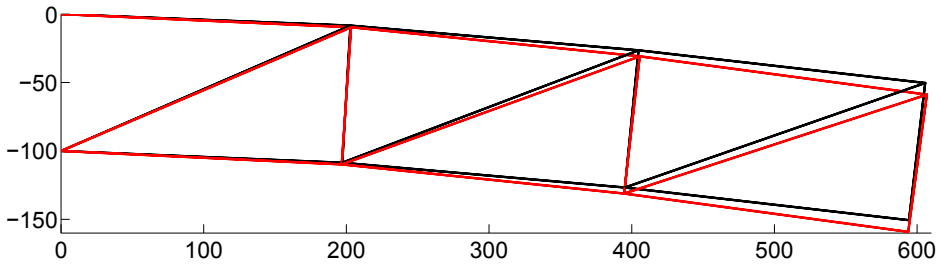

Figure 4.3.: Displacement truss cantilever: geometrical linear (black) and non-linear (red) solution

Simple supported beam Basically the same structural system is investigated using different loading conditions. A simple supported beam is first loaded in the mid-span perpendicular to its longitudinal axis with P=3000 kN, see fig. 4.4 in green colour. Under this loading condition, the structural response is quite insensitive to the kinematical description, see fig. 4.5. In contrast, in the second example the structure is loaded in a way that makes a non-linear kinematic description necessary, see fig. 4.6 in red colour. The applied load can be characterised as compression force and it has to be mentioned, that the shape of the beam is slightly changed. To prevent the structure from becoming a classic Euler beam, it has a sinusoidal curvature, indicated by the dashed line in the figure, with an imperfection in the middle of the beam of $L/400$. Bernoulli beam elements are used to model both structures. Here the non-linearity is only incorporated in the axial deformation, thus the formulation of the model error is identical to the truss, see sec. A.2.2.

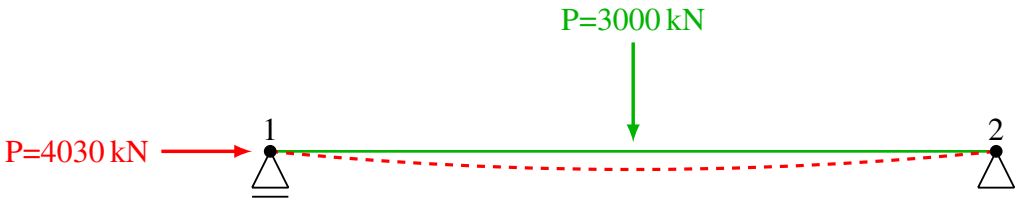

Figure 4.4.: Geometry of the simple supported beam: Length L=2 m, Cross section A=0.1x0.1 m, Modulus of elasticity E=$2*10^8$ kN/m^2

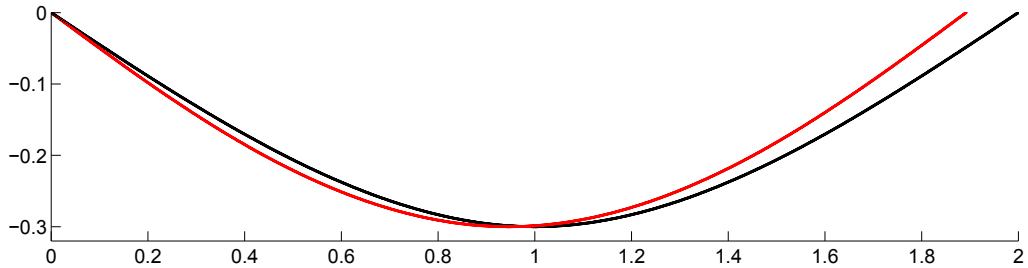

Figure 4.5.: Displacement bending beam: geometrical linear (black) and non-linear (red) solution

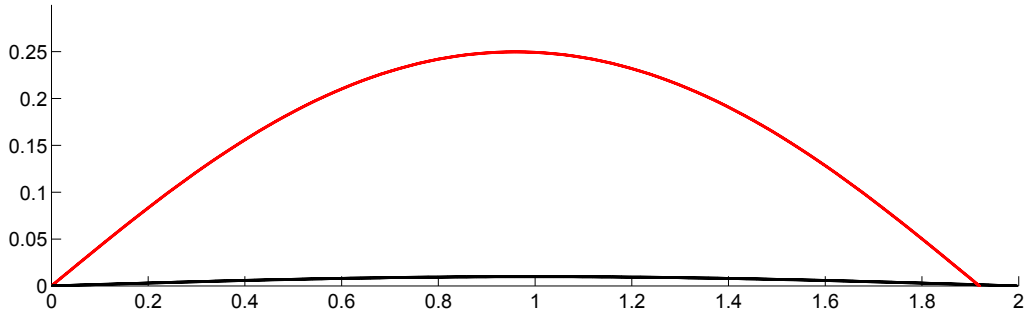

Figure 4.6.: Displacement Euler beam: geometrical linear (black) and non-linear (red) solution

Structures composed of plane elements Both structures, see fig. 4.7 and 4.8, are modelled with bilinear plane elements for plain strain conditions. This element type is quite sensitive regarding locking effects and element distortion; a fine discretisation is used to prevent these effects. Convergence studies have proven that the mesh is sufficiently fine. With the continuously loaded wall structure, a system that is insensitive to geometrical non-linearities is introduced. In contrast the cantilever response is substaintially influenced by this phenomena, as loading effects increase significantly due to deformation, see fig. 4.9(b).

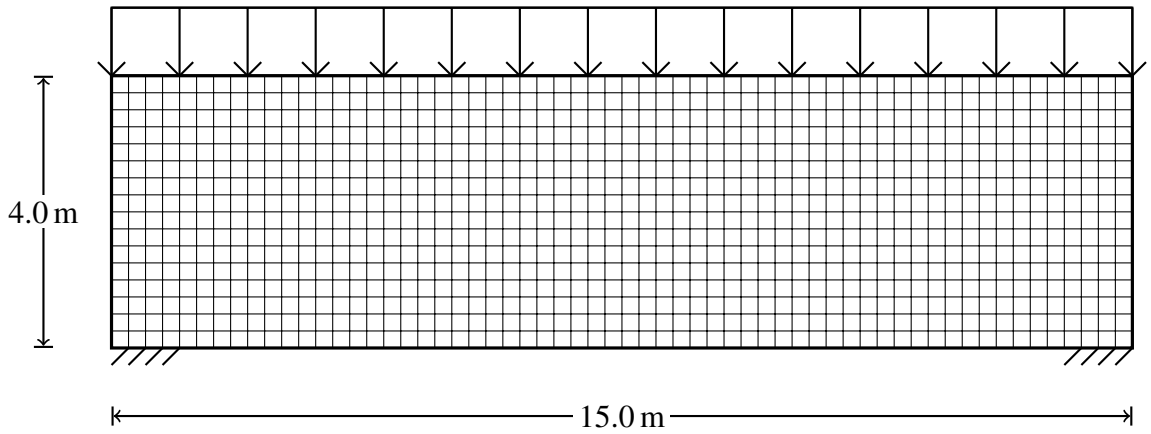

Figure 4.7.: Wall structure: Element size=0.25x0.25 m, Thickness t=0.1 m, Modulus of elasticity E=3*10^7 kN/m^2, Poisson's ratio η=0.2

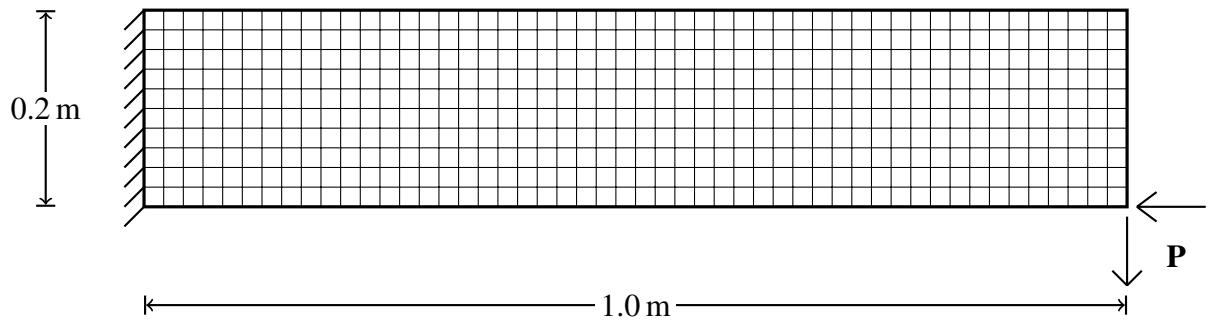

Figure 4.8.: Cantilever: Element size=0.02x0.02 m, Thickness t=0.1 m, Modulus of elasticity E=4.4*10^7 kN/m^2, Poisson's ratio η=0.2, Force P=2000 kN

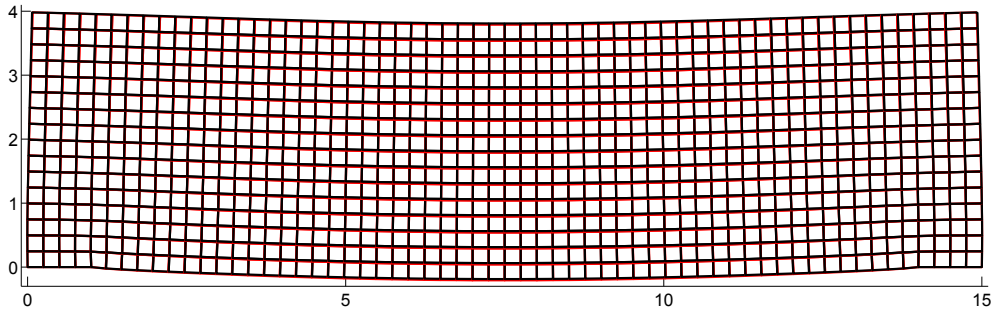

(a) Wall structure

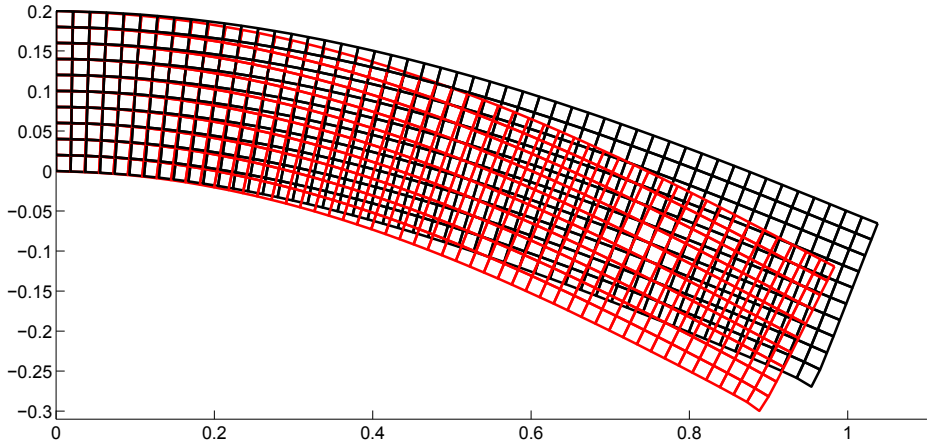

(b) Cantilever

Figure 4.9.: Displacement 2D-structures for the geometrical linear (black) and non-linear (red) solution

4.3 Investigation of possible error norms

All structural systems presented in the previous section, are chosen in a way that linear as well as the non-linear variational formulations, and therewith the simple and complex kinematical models, can be evaluated within a reasonable time span. So the actual model error is known and can be used to judge the quality of the different error estimation techniques. Possible error measures are, see e.g. [64]:

$$\begin{aligned} &\text{Energy norm based on } \mathbf{u} && \eta^2_{E,u} &&= \|\mathbf{u}_c - \mathbf{u}_s\|^2_E \\ &\text{Energy norm based on } \boldsymbol{\sigma} && \eta^2_{E,\sigma} &&= \|\boldsymbol{\sigma}_c - \boldsymbol{\sigma}_s\|^2_E \\ &\text{Displacement error in } \mathrm{L}_2\text{-norm} && \eta_{L_2} &&= \|\mathbf{u}_c - \mathbf{u}_s\|_{L_2} \end{aligned} \tag{4.5}$$

The goal of this preliminary study is to investigate the informative value of the different error measures. Besides this, additional questions should be answered:

- Is it meaningful to standardise the error norms? The displacement error in the L_2-norm might be scaled by $\|\mathbf{u}_s\|_{L_2}$, and the error in the energy norm based on the linear displacements $\|\mathbf{u}_s\|_E$.
- For the calculation of the error in the energy norm, either the linear variational a_l or the non-linear variational form a_{nl} could be used. Does the result differ significantly?
- What informative value does the element-wise distribution of the error provide?

For the different structural systems, the various error formulations are presented in table 4.1. One needs to be aware that all error terms are dependent on the discretisation. They converge with an increasing element number to the exact value, see [9, p. 285].

Table 4.1.: Exact error representations - different structural systems

	Mises truss	Truss cantilever	Bending beam	Euler beam	Wall	Cantilever
η_L	0.47	13.1	0.59	3.21	0.47	0.83
$\eta_L/\|\mathbf{u}_s\|_{L_2}$	0.12	0.16	0.15	46.4	0.11	0.27
$\eta^2_{E,u}(a_l)$	81.5	$1.8{*}10^4$	$1.7{*}10^7$	$8.8{*}10^6$	$2.8{*}10^5$	$1.1{*}10^7$
$\eta^2_{E,u}(a_l)/\|\mathbf{u}_s\|^2_E$	0.01	0.57	18.5	534.9	0.015	17.5
$\eta^2_{E,u}(a_{nl})$	80.6	$1.7{*}10^4$	$1.7{*}10^7$	$2.9{*}10^5$	$2.7{*}10^5$	$9.0{*}10^6$
$\eta^2_{E,u}(a_{nl})/\|\mathbf{u}_s\|^2_E$	0.01	0.54	18.5	17.3	0.015	14.3
$\eta^2_{E,\sigma}$	17	2664	$1.3{*}10^{-6}$	$5.9{*}10^5$	$1.0{*}10^5$	$1.4{*}10^5$
$\eta^2_{E,\sigma}/\|\mathbf{u}_s\|^2_E$	0.003	0.09	0	35.5	0.006	0.08

The following observations can be made:

- There is no significant influence whether a_l or a_{nl} is used to determine $\eta_{E,u}$. Hence the classical energy norm, eq. (A.6) , is used.
- The interpretation of the different norms is better when they are standardised.
- For the beam elements, only the energy norm based on the stresses, $\eta^2_{E,\sigma}$, and its standardised value provide meaningful information. The energy norm based on the displacement difference does not lead to a small error for the bending beam, as expected.

General advice as to which norm to choose can hardly be given. For the structures composed of beam and plane elements, there is always one candidate insensitive to the kinematic description and one that is sensitive. These effects are well captured by $\eta_L/\|\mathbf{u}_s\|_{L_2}$. Concerning the energy norm, differences can be monitored. For the plane elements, the energy norm based on the displacement difference captures the error quite well, whereas the interpretation of $\eta^2_{E,\sigma}$ is difficult. The contrary behaviour can be observed for the beam structures. In this context, it needs to be mentioned that the representation based on the standardised value might be confusing. A value of 0.08 for $\eta^2_{E,\sigma}/\|\mathbf{u}_s\|^2_E$

of the cantilever means that the error equals 8% of the linear energy. Whether this is considered as a large value depends on the definition of the tolerance value for model adaptivity.

To get more insight into the problem, the error distribution for the different norms and problems are studied, see figures 4.10 to 4.13. As a reference, the differences in the energy based on the linear and non-linear variational formulations are chosen. It can be seen that for all examples the error in the energy norm based on stress $\eta^2_{E,\sigma}$ leads to a more reasonable distribution than the error in the energy norm based on displacements $\eta^2_{E,u}$. The only exception is the bending beam. An explanation for the un-symmetric distribution might be the fact, that the element-wise values are approximately zero and numerical errors occur.

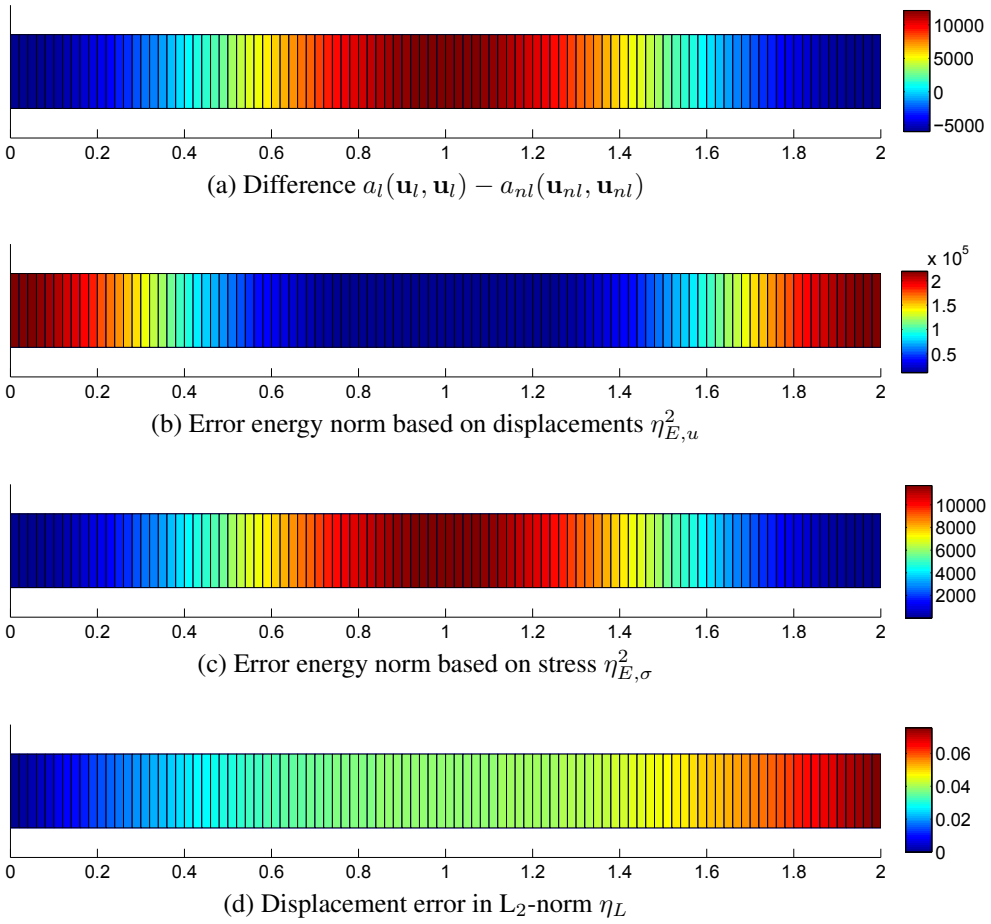

(a) Difference $a_l(\mathbf{u}_l, \mathbf{u}_l) - a_{nl}(\mathbf{u}_{nl}, \mathbf{u}_{nl})$

(b) Error energy norm based on displacements $\eta^2_{E,u}$

(c) Error energy norm based on stress $\eta^2_{E,\sigma}$

(d) Displacement error in L_2-norm η_L

Figure 4.10.: Euler beam: Distribution of global error for different norms

The conclusions that can be drawn from this investigation are:

- For the case where the serviceability of a structure is investigated, the L_2-norm error in the displacements might be preferred.

- The error in the energy norm based on stresses leads to the most meaningful results. This conclusion is assured by the analysis of STEIN / OHNIMUS [64]. It can be used to judge the ability of a model to reproduce the correct stress and strain distribution and is therefore

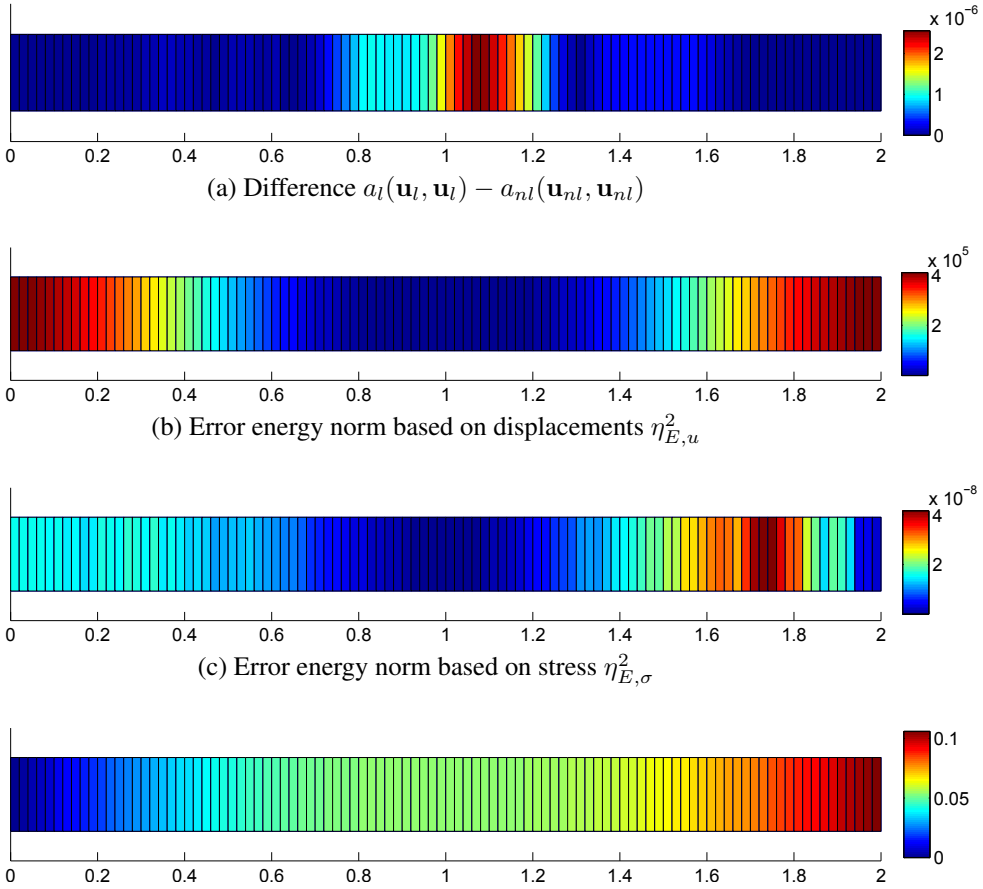

(a) Difference $a_l(\mathbf{u}_l, \mathbf{u}_l) - a_{nl}(\mathbf{u}_{nl}, \mathbf{u}_{nl})$

(b) Error energy norm based on displacements $\eta^2_{E,u}$

(c) Error energy norm based on stress $\eta^2_{E,\sigma}$

(d) Displacement error in L_2-norm η_L

Figure 4.11.: Bending beam: Distribution of global error for different norms

the preferred method when the ultimate limit state of a structure is investigated. An explanation for this observation can be found in the underlying mechanical formulation. The energy norm based on stresses considers, besides the different displacement solutions, also the different stress and strain definitions inherent in the geometrical linear and non-linear formulations. Thus, more meaningful results are achieved.

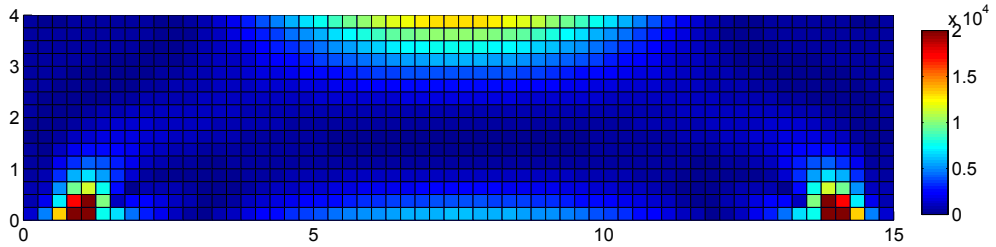

(a) Difference $a_l(\mathbf{u}_l, \mathbf{u}_l) - a_{nl}(\mathbf{u}_{nl}, \mathbf{u}_{nl})$

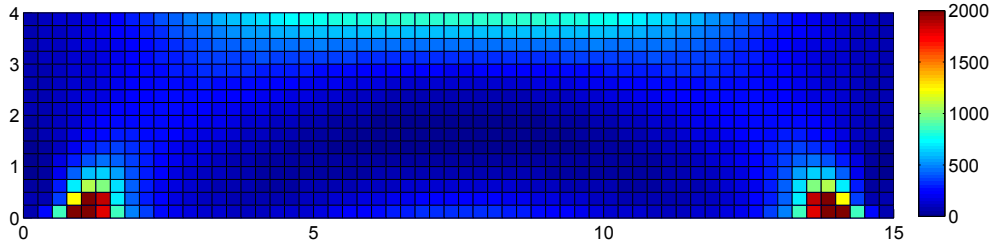

(b) Error energy norm based on displacements $\eta^2_{E,u}$

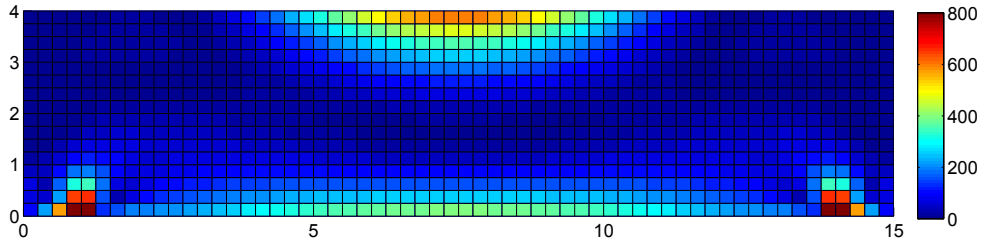

(c) Error energy norm based on stress $\eta^2_{E,\sigma}$

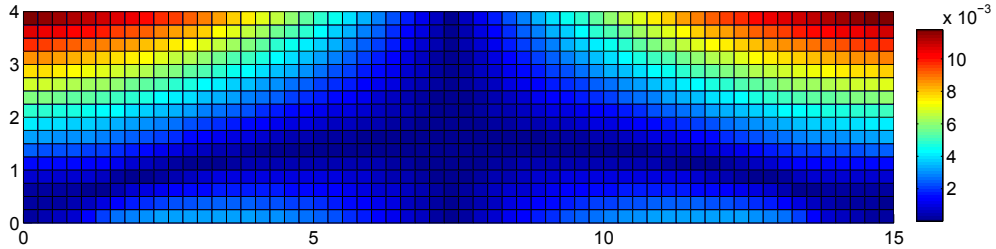

(d) Displacement error in L_2-norm η_L

Figure 4.12.: Wall structure: Distribution of global error for different norms

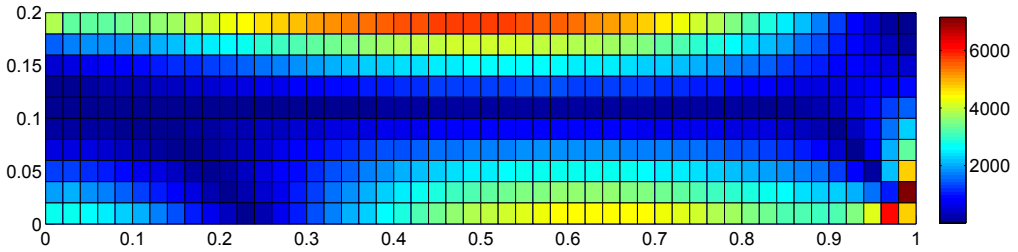

(a) Difference $a_l(\mathbf{u}_l, \mathbf{u}_l) - a_{nl}(\mathbf{u}_{nl}, \mathbf{u}_{nl})$

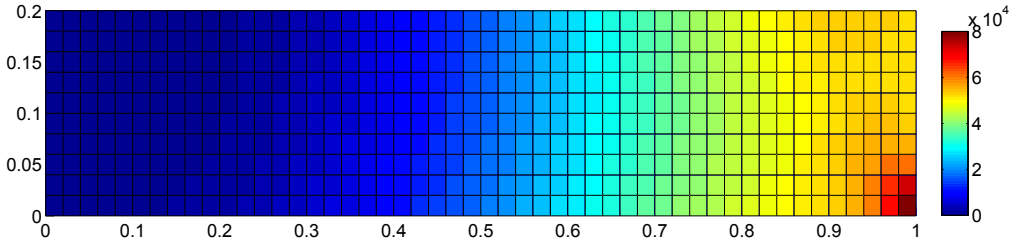

(b) Error energy norm based on displacements $\eta^2_{E,u}$

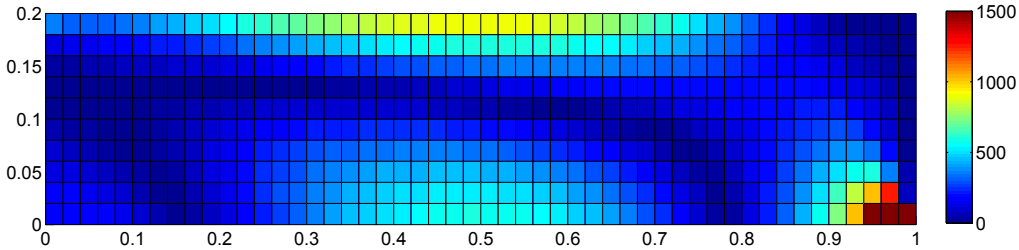

(c) Error energy norm based on stress $\eta^2_{E,\sigma}$

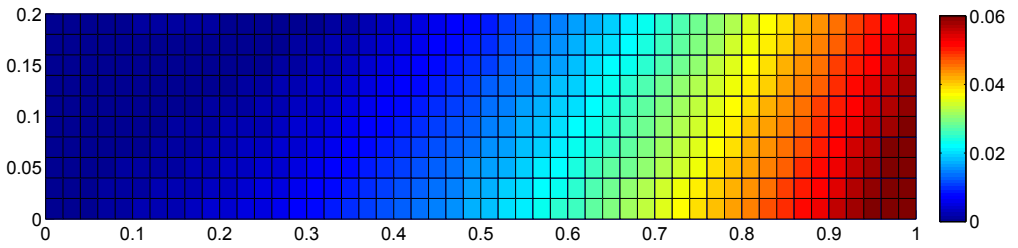

(d) Displacement error in L_2-norm η_L

Figure 4.13.: Cantilever: Distribution of global error for different norms

4.4 Global model error

4.4.1 Direct evaluation of the difference term *d*

General idea

Studying the descriptions of the variational formulations based on the different kinematical model, the question arises whether a direct evaluation of the difference term $d(\mathbf{u}_{nl}, \mathbf{v})$, eq. (4.4) would lead to sufficiently exact information concerning the model error and its distribution. In this context the following questions should be answered:

- Can the error term $d(\mathbf{u}, \mathbf{v})$ be interpreted easily? Which values can be used as reference values to compare the error term with?
- Does the approximation of the model error based on the linear solution give reliable results?
- Are there differences between the application to different structural elements?

Concerning the first question, it seems to be reasonable to choose a_l and the term $a_{nl} - a_l$ as reference values for the global error. Is the error large compared to these values? This should indicate, that a non-linear calculation is necessary.

Truss structures

The results for both truss structures introduced in sec. 4.2 are summarised in tables 4.2 and 4.3.

Table 4.2.: Results of global model error determined using difference term *d* for the Mises truss

Error measure	$d(\mathbf{u}_{nl}, \mathbf{u}_{nl})$	-780 kNcm
	$d(\mathbf{u}_l, \mathbf{u}_l)$	-562 kNcm
Energy	a_{lin}	5990 kNcm
	a_{nl}	6688 kNcm

Table 4.3.: Results of global model error determined using difference term *d* for the truss cantilever

		load P=500 kN	load P=150 kN
Error measure	$d(\mathbf{u}_{nl}, \mathbf{u}_{nl})$	$-2.5 * 10^4$ kNcm	-284 kNcm
	$d(\mathbf{u}_l, \mathbf{u}_l)$	$1.32 * 10^4$ kNcm	-17.5 kNcm
Energy	a_{lin}	$3.1 * 10^4$ kNcm	2792 kNcm
	a_{nl}	$3.83 * 10^4$ kNcm	2976 kNcm

For the Mises truss, the difference term $d(\mathbf{u}_{nl}, \mathbf{u}_{nl})$ is a suitable measure for non-linearity of the system. It equals 13 % of a_{lin}, which is quite close to the value of $a_{nl} - a_l$ =12 % of a_{lin}. Its

approximation deviates about 25 %, which is an acceptable range. Based on this information, one can decide on the necessity of a geometrical non-linear calculation.

For the truss cantilever loaded with P=500 kN, it is noted that the $d(\mathbf{u}_{nl}, \mathbf{u}_{nl})$ equals 80 % of a_{lin}. Compared to the difference $a_{nl} - a_l$ =23 % of a_{lin}, this is much larger. An estimation based on the linear displacements gives a wrong value with respect to magnitude and algebraic sign. For a reduced load level, the informative value of the difference term improves. Its approximation has at least the same algebraic sign, but still the magnitude is not correct.

Simple supported beams

Studying table 4.4 it becomes obvious that for both loading conditions an approximation of the difference term using u_{lin} does not lead to satisfying results. Additionally, it is difficult to assess the measure $d(\mathbf{u}_{nl}, \mathbf{u}_{nl})$. Its value is one or two orders of magnitude larger than the linear and non-linear energy terms. So it is hard to find a value for comparison that leads to a meaningful interpretation of the calculated term. Especially for the example with the vertical load in the mid-span, it is not reasonable that such a high d-value, indicating a large errors, occurs. As the example is a pure bending problem, where geometrical non-linearities are of minor influence, one would expect that a chosen error measure would indicate this with a scalar value close to one.

Table 4.4.: Results of global model error determined using difference term d for the simple supported beam with compression force and single load in mid-span

		Compression force	Bending force
Error measure	$d(\mathbf{u}_{nl}, \mathbf{u}_{nl})$	$-9.1 * 10^6$ Nm	$-1.7 * 10^7$ Nm
	$d(\mathbf{u}_l, \mathbf{u}_l)$	-355 Nm	$3.3 * 10^7$ Nm
Energy	a_{lin}	$1.6 * 10^4$ Nm	$9 * 10^5$ Nm
	a_{nl}	$3.3 * 10^5$ Nm	$9 * 10^5$ Nm

Structures composed of plane elements

The calculation of the difference term d and its approximation gives meaningful results for the wall structure, see table 4.5. The maximum difference between the exact and the approximated value is 32 % and the element-wise distribution is equal, see fig. 4.14. The total value equals 12.3 % of a_{lin}, which is also a reasonable compared to the difference $a_{nl}(\mathbf{u}_{nl}, \mathbf{v}) - a_{lin}(\mathbf{u}_l, \mathbf{v})$ =11.9 % of a_{lin}.

Table 4.5.: Results of global model error determined using difference term d for the wall structure with continuous loading and the cantilever

		Wall structure	Cantilever	Cantilever, pure bending
Error measure	$d(\mathbf{u}_{nl}, \mathbf{u}_{nl})$	$-2.2 * 10^6$ Nm	$-1.1 * 10^7$ Nm	$-2.1 * 10^6$ Nm
	$d(\mathbf{u}_{l}, \mathbf{u}_{l})$	$-1.5 * 10^6$ Nm	$1.1 * 10^7$ Nm	$6.3 * 10^6$ Nm
Energy	a_{lin}	$1.8 * 10^7$ Nm	$6.3 * 10^5$ Nm	$4.7 * 10^5$ Nm
	a_{nl}	$2.0 * 10^7$ Nm	$8.2 * 10^5$ Nm	$4.2 * 10^5$ Nm

Applied on the cantilever, the simplified approach using the linear deformations is not successful. When compared with the exact values, the difference is far too great. This holds for the sum of all elements as well as the element-wise distribution, see fig. 4.15. Even if it is expected that a global model measure reaches a large value due to the non-linear effects incorporated in that example, a value two orders of magnitude larger than the deformation energy can hardly be interpreted. In order to ensure that the bad quality of the results for the cantilever was not due to singularities caused by using the point loading, the structure was loaded using distributed forces, too. The evaluation of the exact and approximated difference terms did not show any improvement.

Additionally, the cantilever was investigated as a pure bending problem, which means without any horizontal force. The displacements as well as the deformation energy differ only slightly between linear and non-linear solutions. The same problems can be studied as with the beam loaded in its mid-span, see tab. 4.5 last column. Even if the phenomenon of geometrical non-linearity does not affect the solution, the introduced error measure in terms of $d(\mathbf{u}_{nl}, \mathbf{u}_{nl})$ indicates a large error, if the problem is solved linearly.

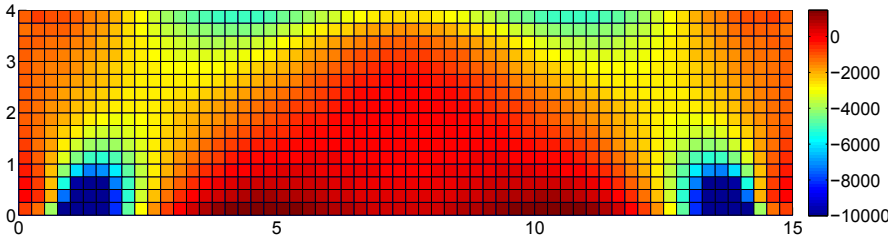

(a) Exact calculation $d(\mathbf{u}_{nl}, \mathbf{v})$

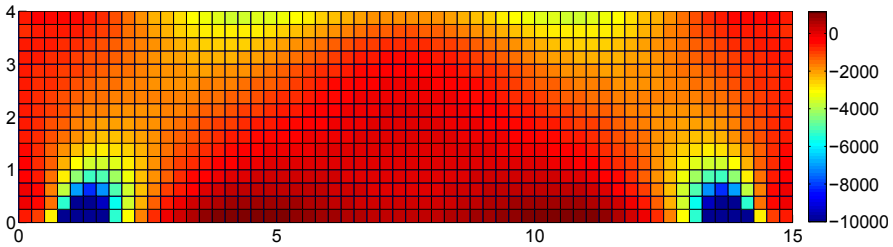

(b) Approximated calculation $d(\mathbf{u}_{l}, \mathbf{v})$

Figure 4.14.: Distribution global error based on difference term d of the wall structure

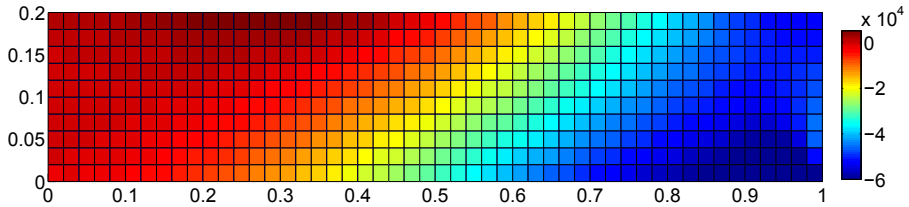

(a) Exact calculation $d(\mathbf{u}_{nl}, \mathbf{v})$

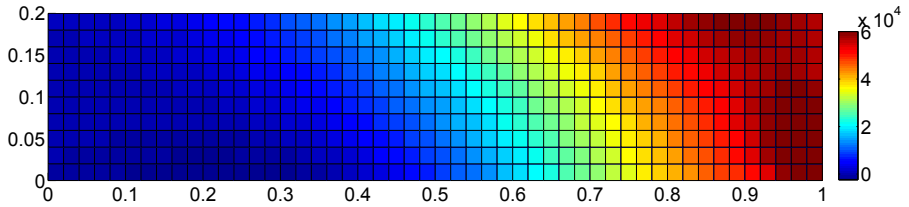

(b) Approximated calculation $d(\mathbf{u}_l, \mathbf{v})$

Figure 4.15.: Distribution global error based on difference term *d* of the Cantilever

Problems of the proposed method and possible extensions

The examples discussed in the previous sections show, that a direct evaluation of the d-term, eq. (4.4) , does not provide a meaningful error estimate. A suitable reference value that the d-term can be related to, could not be identified. Possible values like $a_l(\mathbf{u}_l, \mathbf{u}_l)$ or the difference $a_{nl}(\mathbf{u}_{nl}, \mathbf{u}_{nl}) - a_l(\mathbf{u}_l, \mathbf{u}_l)$ have not proven to be suitable for all cases, as for most examples the term $d(\mathbf{u}_{nl}, \mathbf{u}_{nl})$ differs one or even more orders of magnitude. An approximation of the difference term d using the linear solution $\mathbf{u}_l$ is not reliable.

Table 4.6.: Decomposition: virtual deformation energy

	$a_l(\mathbf{u}_{nl}, \mathbf{u}_{nl})$	$d(\mathbf{u}_{nl}, \mathbf{u}_{nl})$	$a_{nl}(\mathbf{u}_{nl}, \mathbf{u}_{nl})$
Mises truss	7468 kNcm	−780 kNcm	6688 kNcm
Truss cantilever	63168 kNcm	−25000 kNcm	38300 kNcm
Simple supported beam			
compression force	$9.46 * 10^6$ Nm	$-9.1 * 10^6$ Nm	$3.3 * 10^5$ Nm
bending force	$1.75 * 10^7$ Nm	$-1.67 * 10^7$ Nm	$9 * 10^5$ Nm
Wall structure	$2.2 * 10^7$ Nm	$-2.2 * 10^6$ Nm	$2 * 10^7$ Nm
Cantilever	$1.2 * 10^7$ Nm	$-1,1 * 10^7$ Nm	$8.2 * 10^5$ Nm

The term $d(\mathbf{u}_{nl}, \mathbf{v})$, (4.4), is a only a part of the virtual deformation energy. That a more or less arbitrarily chosen term out of the total equilibrium formulation is extracted, might be the reason for the problems concerning the interpretation. The total non-linear virtual energy consists of two parts $a_{nl}(\mathbf{u}_{nl}, \mathbf{u}_{nl}) = a_l(\mathbf{u}_{nl}, \mathbf{u}_{nl}) + d(\mathbf{u}_{nl}, \mathbf{u}_{nl})$ following the definition above. In table 4.6 the results for the decomposed virtual energy are shown explicitly. It becomes clear that only $a_{nl}(\mathbf{u}_{nl}, \mathbf{u}_{nl})$ has a physical meaning. An assessment of the influence of geometrical non-linear effects based on $d(\mathbf{u}_{nl}, \mathbf{u}_{nl})$ is thus not reasonable.

The term $d(\mathbf{u}_{nl}, \mathbf{u}_{nl})$ itself does not provide the information needed. It can be shown, that the difference between the linear and non-linear virtual energy consists of two parts. There is on one hand the term d, but additionally there is a difference between $a_l(\mathbf{u}_{nl}, \mathbf{u}_{nl})$ and $a_l(\mathbf{u}_l, \mathbf{u}_l)$. It is possible to split the linear part of the energy due to the non-linear displacements as follows

$$\begin{aligned} a_{lin}(\mathbf{u}_{nl}, \mathbf{u}_{nl}) &= \int_\Omega \mathbf{S}_l(\mathbf{u}_{nl})\, \mathbf{E}_l(\mathbf{u}_{nl}) d\Omega \\ &= \int_\Omega \left(\mathbf{S}_l(\mathbf{u}_l) + \mathbf{S}_l(\mathbf{e}_m)\right) \left(\mathbf{E}_l(\mathbf{u}_l) + \mathbf{E}_l(\mathbf{e}_m)\right) d\Omega \\ &= \int_\Omega \underbrace{\mathbf{S}_l(\mathbf{u}_l)\mathbf{E}_l(\mathbf{u}_l)}_{a_l(\mathbf{u}_l, \mathbf{u}_l)} + \underbrace{\left(\mathbf{S}_l(\mathbf{u}_l)\mathbf{E}_l(\mathbf{e}_m) + \mathbf{S}_l(\mathbf{e}_m)\mathbf{E}_l(\mathbf{u}_l) + \mathbf{S}_l(\mathbf{e}_m)\mathbf{E}_l(\mathbf{e}_m)\right)}_{\Delta a_l(\mathbf{u}_l, \mathbf{e}_m)} d\Omega. \end{aligned} \tag{4.6}$$

If $d(\mathbf{u}_{nl}, \mathbf{u}_{nl})$ would be extended by the term $\Delta a_l(\mathbf{u}_l, \mathbf{e}_m)$, the result would be much more interpretable, as it equals the difference between the linear and non-linear virtual deformation energy,

$$a_{nl}(\mathbf{u}_{nl}, \mathbf{u}_{nl}) - a_l(\mathbf{u}_l, \mathbf{u}_l) = d(\mathbf{u}_{nl}, \mathbf{u}_{nl}) + \Delta a_l(\mathbf{u}_l, \mathbf{e}_m). \tag{4.7}$$

It is obvious that this procedure has a disadvantage. The initial goal of the introduction of the concept of model errors was to approximate the error based on the linear solution. Looking at eq. (4.6) it is obvious that $\Delta a_l(\mathbf{u}_l, \mathbf{e}_m)$ cannot be calculated if $\mathbf{u}_{nl}$ is unknown. So besides the difference of $d(\mathbf{u}_{nl}, \mathbf{u}_{nl})$ and $d(\mathbf{u}_l, \mathbf{u}_l)$, which could be recognised for the various structural systems, an additional source for the unreliability of the prognosis comes into play. From table 4.7 and fig. 4.16 it becomes clear that already the neglect of $\Delta a_l(\mathbf{u}_l, \mathbf{e}_m)$ has a strong influence.

Table 4.7.: Decomposition: virtual deformation energy II

	$d(\mathbf{u}_{nl}, \mathbf{u}_{nl})$	$\Delta a_l(\mathbf{u}_l, \mathbf{e}_m)$	$a_{nl}(\mathbf{u}_{nl}, \mathbf{u}_{nl}) - a_l(\mathbf{u}_l, \mathbf{u}_l)$
Simple supported beam			
compression force	$-9.1 * 10^6$ Nm	$9.44 * 10^6$ Nm	$3.14 * 10^5$ Nm
bending force	$-1.67 * 10^7$ Nm	$1.67 * 10^7$ Nm	0.0 Nm
Wall structure	$-2.2 * 10^6$ Nm	$4.2 * 10^6$ Nm	$2 * 10^6$ Nm
Cantilever	$-1.12 * 10^7$ Nm	$1.14 * 10^7$ Nm	$1.92 * 10^5$ Nm

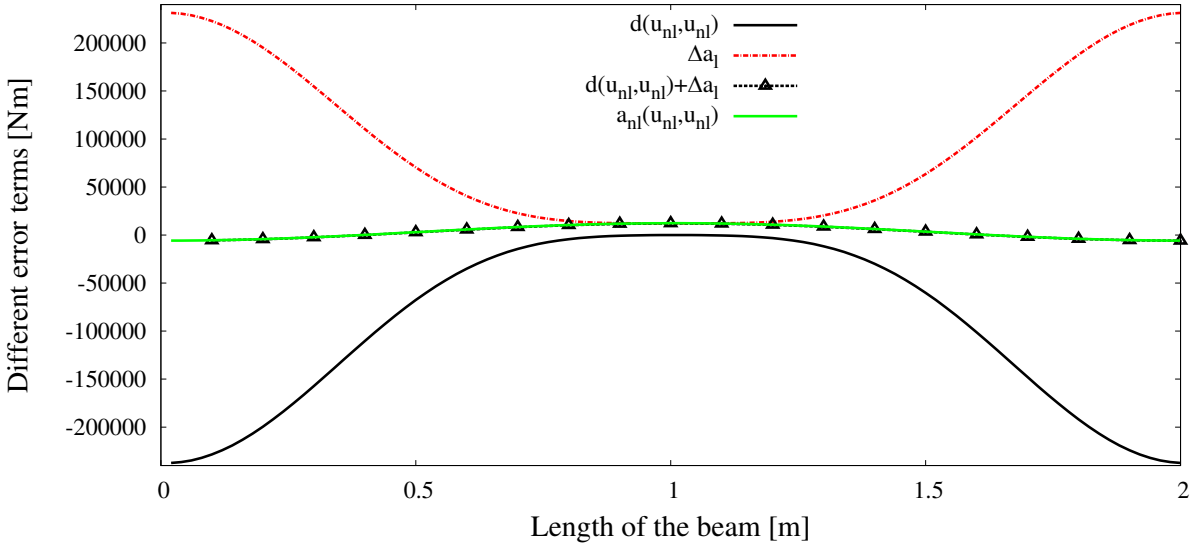

Figure 4.16.: Extension for model error formulation based on difference term d, Example: Simple supported beam with compression force

4.4.2 Error estimation using a residuum-based on model difference

The method introduced by ODEN ET AL. [49], see also chapter 3.2.3, is applied to kinematical models. Before the procedure can be tested regarding its applicability, the residuum $\mathcal{R}$ needs to be determined according to eqs. (3.93) and (3.95). The difference between a model with linear kinematic description and a model considering geometrical non-linear effects is

$$\begin{aligned} & a_{nl}(\mathbf{u}_{nl};\mathbf{v}) - a_l(\mathbf{u}_l,\mathbf{v}) \\ =& \int_\Omega \mathbf{S}_{nl}(\mathbf{u}_{nl})\mathbf{E}_u(\mathbf{v})d\Omega - \int_\Omega \boldsymbol{\sigma}(\mathbf{u}_l)\boldsymbol{\varepsilon}(\mathbf{v})d\Omega \\ =& \int_\Omega \boldsymbol{\sigma}(\mathbf{u}_{nl})\boldsymbol{\varepsilon}(\mathbf{v}) + \boldsymbol{\sigma}(\mathbf{u}_{nl})\Delta\mathbf{E}(\mathbf{u}_{nl},\mathbf{v}) + \Delta\mathbf{S}(\mathbf{u}_{nl})\boldsymbol{\varepsilon}(\mathbf{v}) \\ & \qquad + \Delta\mathbf{S}(\mathbf{u}_{nl})\Delta\mathbf{E}(\mathbf{u}_{nl},\mathbf{v})d\Omega - \int_\Omega \boldsymbol{\sigma}(\mathbf{u}_l)\boldsymbol{\varepsilon}(\mathbf{v})d\Omega. \end{aligned} \tag{4.8}$$

Additionally, the displacement solution of the non-linear formulations $\mathbf{u}_{nl}$ is partitioned into the linear solution $\mathbf{u}_l$ and an error term $\mathbf{e}_m$. Introducing a partition in the first term of eq. (4.8) yields to

$$\int_\Omega \boldsymbol{\sigma}(\mathbf{u}_{nl})\boldsymbol{\varepsilon}(\mathbf{v})d\Omega = \int_\Omega \boldsymbol{\sigma}(\mathbf{u}_l)\boldsymbol{\varepsilon}(\mathbf{v})d\Omega + \int_\Omega \boldsymbol{\sigma}(\mathbf{e}_m)\boldsymbol{\varepsilon}(\mathbf{v})d\Omega. \tag{4.9}$$

The term marked in blue cancels out with the last integral in eq. (4.8). The other terms of the first integral in eq. (4.8) can be split into:

$$\begin{aligned}
&\int_\Omega \boldsymbol{\sigma}(\mathbf{u}_{nl})\Delta\mathbf{E}(\mathbf{u}_{nl},\mathbf{v})d\Omega \\
&\quad= \int_\Omega \left[\boldsymbol{\sigma}(\mathbf{u}_l)+\boldsymbol{\sigma}(\mathbf{e}_m)\right]\left[\nabla(\mathbf{u}_l+\mathbf{e}_m)^T\nabla\mathbf{v}+\nabla\mathbf{v}^T\nabla(\mathbf{u}_l+\mathbf{e}_m)\right]d\Omega \\
&\quad= \int_\Omega \left[\boldsymbol{\sigma}(\mathbf{u}_l)+\boldsymbol{\sigma}(\mathbf{e}_m)\right]\left[\nabla\mathbf{u}_l^T\nabla\mathbf{v}+\nabla\mathbf{e}_m^T\nabla\mathbf{v}+\nabla\mathbf{v}^T\nabla\mathbf{u}_l+\nabla\mathbf{v}^T\nabla\mathbf{e}_m\right]d\Omega \\
&\quad= \int_\Omega \boldsymbol{\sigma}(\mathbf{u}_l)\Delta\mathbf{E}(\mathbf{u}_l,\mathbf{v})d\Omega + \int_\Omega \boldsymbol{\sigma}(\mathbf{u}_l)\Delta\mathbf{E}(\mathbf{e}_m,\mathbf{v})+\boldsymbol{\sigma}(\mathbf{e}_m)\Delta\mathbf{E}(\mathbf{u}_{nl},\mathbf{v})d\Omega
\end{aligned} \tag{4.10}$$

$$\begin{aligned}
\int_\Omega \Delta\mathbf{S}(\mathbf{u}_{nl})\boldsymbol{\varepsilon}(\mathbf{v})d\Omega &= \int_\Omega \mathbf{C}\left[\nabla\mathbf{u}_{nl}^T\nabla\mathbf{u}_{nl}\right]\boldsymbol{\varepsilon}(\mathbf{v})d\Omega \\
&= \int_\Omega \mathbf{C}\left[\nabla(\mathbf{u}_l+\mathbf{e}_m)^T\nabla(\mathbf{u}_l+\mathbf{e}_m)\right]\boldsymbol{\varepsilon}(\mathbf{v})d\Omega \\
&= \int_\Omega \Delta\mathbf{S}(\mathbf{u}_l)\boldsymbol{\varepsilon}(\mathbf{v})d\Omega + \int_\Omega \mathbf{C}\left[\nabla\mathbf{e}_m^T\nabla\mathbf{u}_l+\nabla\mathbf{u}_l^T\nabla\mathbf{e}_m+\nabla\mathbf{e}_m^T\nabla\mathbf{e}_m\right]\boldsymbol{\varepsilon}(\mathbf{v})d\Omega
\end{aligned} \tag{4.11}$$

$$\begin{aligned}
\int_\Omega \Delta\mathbf{S}(\mathbf{u}_{nl})\Delta\mathbf{E}(\mathbf{u}_{nl},\mathbf{v})d\Omega &= \int_\Omega \mathbf{C}(\nabla\mathbf{u}_l^T\nabla\mathbf{u}_l+\nabla\mathbf{e}_m^T\nabla\mathbf{u}_l+\nabla\mathbf{u}_l^T\nabla\mathbf{e}_m+\nabla\mathbf{e}_m^T\nabla\mathbf{e}_m) \\
&\quad\cdot\left[\nabla\mathbf{u}_l^T\nabla\mathbf{v}+\nabla\mathbf{e}_m^T\nabla\mathbf{v}+\nabla\mathbf{v}^T\nabla\mathbf{u}_l+\nabla\mathbf{v}^T\nabla\mathbf{e}_m\right]d\Omega \\
&= \int_\Omega \Delta\mathbf{S}(\mathbf{u}_l)\Delta\mathbf{E}(\mathbf{u}_l,\mathbf{v})d\Omega + \dots\ .
\end{aligned} \tag{4.12}$$

All terms marked in grey in the previous equations can be summarised as

$$R(\mathbf{u}_l,\mathbf{v}) = d(\mathbf{u}_l,\mathbf{v}) = \int_\Omega \boldsymbol{\sigma}(\mathbf{u}_l)\Delta\mathbf{E}(\mathbf{u}_l,\mathbf{v}) + \Delta\mathbf{S}(\mathbf{u}_l)\boldsymbol{\varepsilon}(\mathbf{v}) + \Delta\mathbf{S}(\mathbf{u}_l)\Delta\mathbf{E}(\mathbf{u}_l,\mathbf{v})d\Omega. \tag{4.13}$$

This is the only part of the difference defined in eq. (4.8) that can be determined without knowing the solution of the non-linear calculation or the error $\mathbf{e}_m$. Following the idea of ODEN ET AL. [49], this term is defined as residuum and interpreted as an estimate of the error caused by using the linear model.

Applying Schwarz's inequality results in

$$R(\mathbf{u}_l, \mathbf{v}) \leq \sqrt{\int_\Omega |\boldsymbol{\sigma}(\mathbf{u}_l)\nabla\mathbf{u}_l^T|^2 d\Omega}\, \|\nabla\mathbf{v}\|_{L_2} + \sqrt{\int_\Omega |\Delta\mathbf{S}(\mathbf{u}_l)|^2 d\Omega}\, \|\nabla\mathbf{v}\|_{L_2} + \sqrt{\int_\Omega |\Delta\mathbf{S}(\mathbf{u}_l)\nabla\mathbf{u}_l^T|^2 d\Omega}\, \|\nabla\mathbf{v}\|_{L_2}. \quad (4.14)$$

Dividing by $\|\nabla\mathbf{v}\|_{L_2}$ leads to an upper bound for the error η_{Oden} caused by using a linear kinematical model instead of a geometrical non-linear formulation.

$$\|\mathcal{E}\|_{V'} \leq \eta = \sqrt{\int_\Omega |\boldsymbol{\sigma}(\mathbf{u}_l)\nabla\mathbf{u}_l^T|^2 d\Omega} + \sqrt{\int_\Omega |\Delta\mathbf{S}(\mathbf{u}_l)|^2 d\Omega} + \sqrt{\int_\Omega |\Delta\mathbf{S}(\mathbf{u}_l)\nabla\mathbf{u}_l^T|^2 d\Omega} \quad (4.15)$$

The term $\|\mathcal{E}\|_{V'}$ describes, according to eq. (3.93) , the norm in the dual space $\mathcal{V}'$ of all summands of eqs. (4.10) to (4.12) , which incorporate the error $\mathbf{e}_m$. Additionally, a normed upper error bound is defined according to eq. (3.97),

$$\overline{\eta} = \frac{\eta}{\eta_{add}} \qquad \text{with } \eta_{add} = \sqrt{\int_\Omega |\mathbf{C}\,\nabla\mathbf{u}_l|^2 d\Omega}. \quad (4.16)$$

The applicability of the proposed method is first tested on the beam structures. For the bending beam, the error distribution is shown in fig. 4.17. It is comparable to the distribution of $\eta_{E,u}^2$, shown in fig. 4.11(b). It can be seen that the error is overestimated, which is confirmed by the scaled error bound with $\overline{\eta} = 0.81$. Compared to the bending beam, the global error of the Euler beam seems to

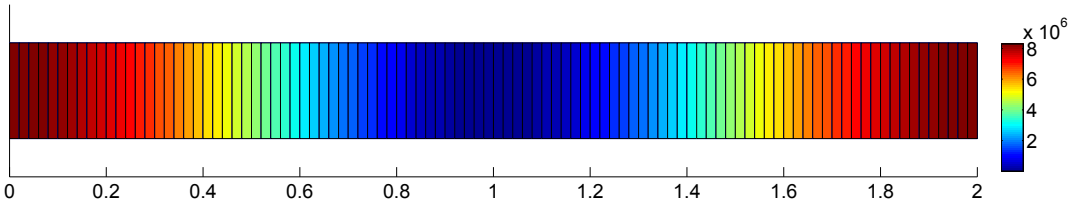

Figure 4.17.: Global error η for the bending beam, $\Sigma\eta = 4.2 * 10^8$

be underestimated; see fig. 4.18 and consider the scaled measure $\overline{\eta} = 0.002$. As shown in sec. 4.3, one would expect the error to be larger, as this kind of structural system is quite sensitive to the kinematical formulation.

For the structures composed of plane elements, the results are summarised in fig. 4.19 and 4.20. The scaled error bound $\overline{\eta}$ is 0.08 for the wall structure and 3.6 for the cantilever. Here the relation of the real relation of the errors of these structures is well captured. The values that have been achieved are comparable to the scaled energy norm based on the exact error $\eta_{E,u}^2/\|\mathbf{u}_s\|_E^2$ summarised in tab. 4.1. On the other hand, it can be seen in comparison to fig. 4.12 that the error

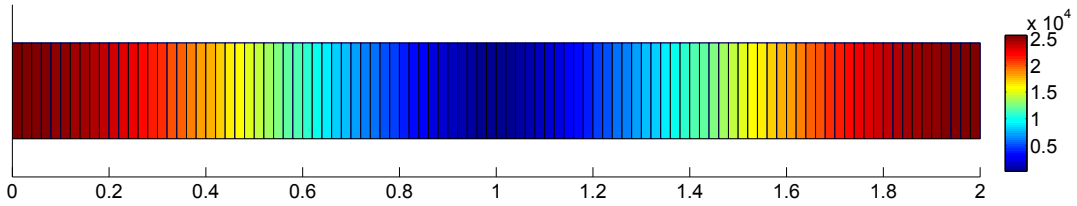

Figure 4.18.: Global error η for the Euler beam, $\Sigma\eta = 1.4 * 10^6$

distribution for the wall is not well represented. The distribution of the error for the cantilever equals fig. 4.13(b).

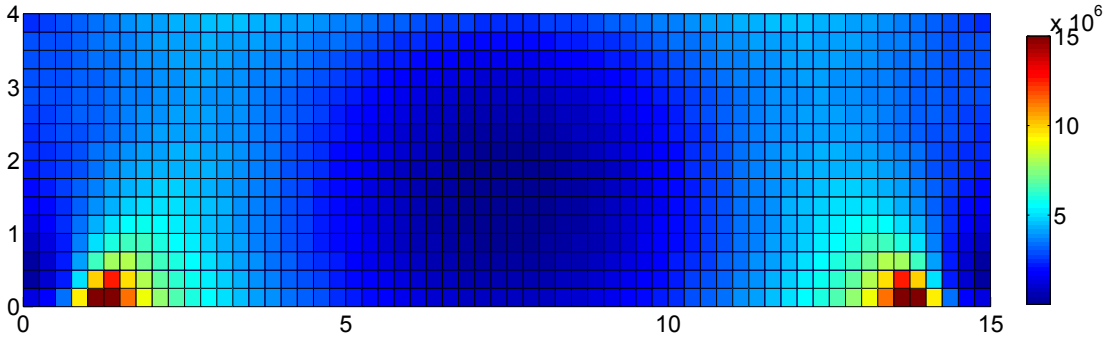

Figure 4.19.: Global error η for the wall structure, $\Sigma\eta = 2.9 * 10^9$

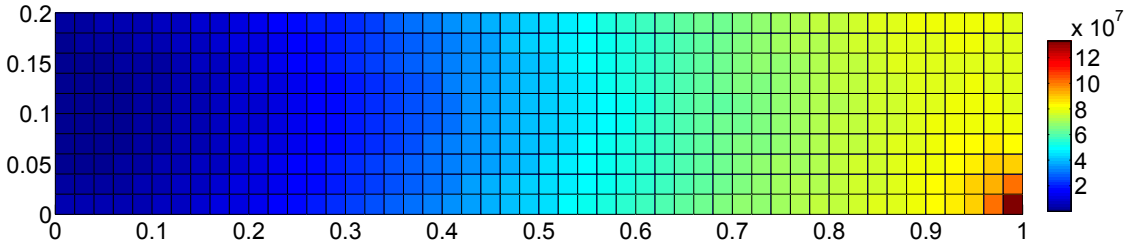

Figure 4.20.: Global error η for the cantilever, $\Sigma\eta = 2.1 * 10^{10}$

Summarising this investigation, the following conclusions can be drawn:

- The estimation technique for global errors of non-linear problems proposed in [47], does not provide reliable information concerning the error when investigating different kinematical descriptions. The distribution as well as scalar value corresponds only for some problems to the expected behaviour.
- Scaling the error according to eq. (4.16) leads to results that can be interpreted better.
- Considering the results of sec. 4.4.1, it was to some extent expected that this procedure does not lead to useful results. The more or less arbitrary choice of the residuum $R(\mathbf{u}_l, \mathbf{v})$ from the total difference of the linear and non-linear variational formulation eq. (4.8) neglects significant parts of the exact error.

4.4.3 Error estimation based on linearisation

Following the approach of STEIN ET AL. [67] and HUERTA ET AL. [24], it is investigated whether a reliable error estimate can be found linearising the non-linear kinematic equation. According to eq. (3.99) the residuum can be defined as

$$R(\mathbf{u}_l, \mathbf{v}) = F(\mathbf{v}) - a_{nl}(\mathbf{u}_l; \mathbf{v}) \approx a_{T,nl}(\mathbf{u}_l; \mathbf{e}_m, \mathbf{v}). \tag{4.17}$$

Applying the Finite Element method, this equals

$$R(\mathbf{u}_l, \mathbf{v}) = \sum_{e=1}^{n_e} \hat{\mathbf{e}}_m \mathbf{k}_T(\hat{\mathbf{u}}_l)\hat{\mathbf{v}}. \tag{4.18}$$

Thus, an energy norm equivalent can be defined as

$$\|\mathbf{e}_m\|_{E,e}^2 = \sum_{e=1}^{n_e} \hat{\mathbf{e}}_m \mathbf{k}_T(\hat{\mathbf{u}}_l)\hat{\mathbf{e}}_m. \tag{4.19}$$

The error $\mathbf{e}_m$ or the solution of the geometrical non-linear problem $\mathbf{u}_{nl}$ needs to be estimated to evaluate eq. (4.19) . STEIN ET AL. [67] applies for this purpose the posteriori equilibrium method, which involves the analyses of local Neumann problems. Here the problem arise, that rigid body modes need to be eliminated before these local problems can be solved. This is prevented by solving an auxiliary global problem based on the linearised form of the complex model. An approximation of the non-linear displacement is found by solving

$$\mathbf{K}_T(\hat{\mathbf{u}}_l)\, \hat{\mathbf{u}}_{nl,app} = \hat{\mathbf{p}}. \tag{4.20}$$

Thus, the error $\mathbf{e}_m$ and the associated energy norm (4.19) can be approximated. The interpretation of the norm is optimised by scaling it with the energy norm based on the linear displacements. The results for the different structural systems are summarised in tab. 4.8 and the error distribution is shown in figs. 4.21. This error formulation is comparable to the definition of the error norm

Table 4.8.: Global error estimates based on linearisation - different structural systems

	Bending beam	Euler beam	Wall	Cantilever
$\|\mathbf{e}_m\|_{E,e}^2$	9.9*10^7	1.1*10^5	7.9*10^5	3.3*10^7
$\|\mathbf{e}_m\|_{E,e}^2/\|\mathbf{u}_l\|_E^2$	110	6.6	0.04	53

based on the displacements $\eta_{E,u}$ and therefore the results are compared to the related exact error representation in tab. 4.1. For the plane elements, a good agreement can be monitored. For the bending beam, the error estimate is even higher than the exact value of $\eta_{E,u}$ and thus the real behaviour of this structure is not captured. Comparing the error distribution with exact figures 4.10 to 4.13, it is monitored that it equals $\eta_{E,u}$ for all structures except the Euler beam.

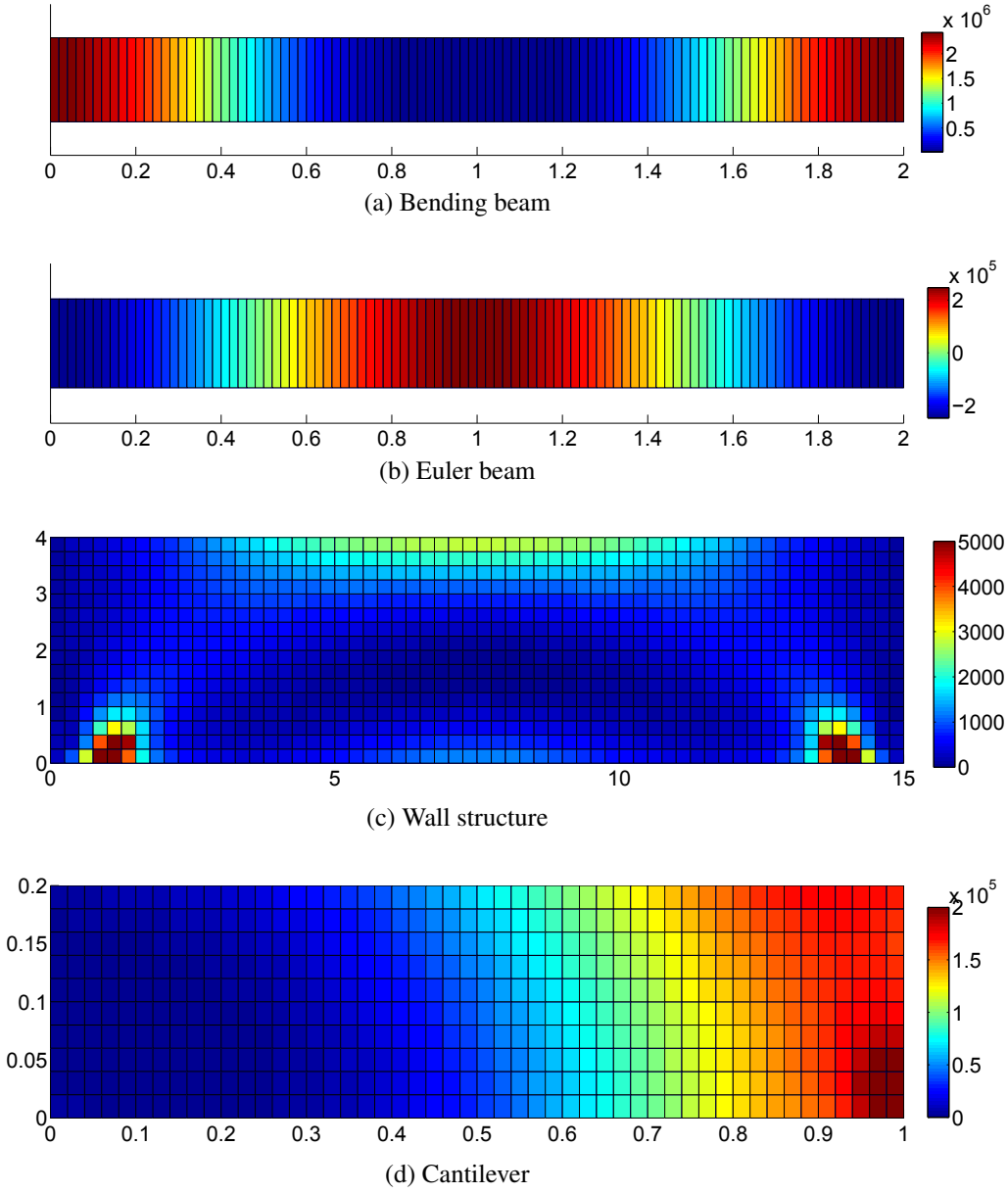

(a) Bending beam

(b) Euler beam

(c) Wall structure

(d) Cantilever

Figure 4.21.: Distribution global model error estimate based on linearisation of geometrical non-linear model

It can be summarised that the exact values for the error in the energy norm are partially well captured. Based on the observations in chap. 4.3, it is known that the representation of the error in the energy norm based on stresses leads to more meaningful results. Therefore, $\eta_{E,\sigma}$ is approximated based on the results achieved using eq. (4.20) . The results are summarised in tab. 4.9 and it can be seen that for most of the structures the error is overestimated. It attracts positive attention that for structures that are rather insensitive regarding the kinematical model the error estimates are lower compared to deformation sensitive examples. Nevertheless, also the plot of the error distribution, fig. 4.22, confirms that the error estimate does not capture the real behaviour very well. Only for the wall structure do the calculations lead to reasonable results. Here the difference in displace-

ments between both models is small.[1] This proves that the prerequisite of small errors, formulated in [67] and [24], is crucial for the applicability of this method. Unfortunately, this can never be known in advance.

Table 4.9.: Estimate of $\eta_{E,\sigma}$ based on linearisation - different structural systems

	Bending beam	Euler beam	Wall	Cantilever
$\|\mathbf{e}_m\|^2_{E,\sigma,app}$	8.8*10^5	6.9*10^9	1.3*10^5	1.2*10^7
$\|\mathbf{e}_m\|^2_{E,\sigma,app}/\|\mathbf{u}_l\|^2_E$	0.98	4.2*10^5	0.01	18.2

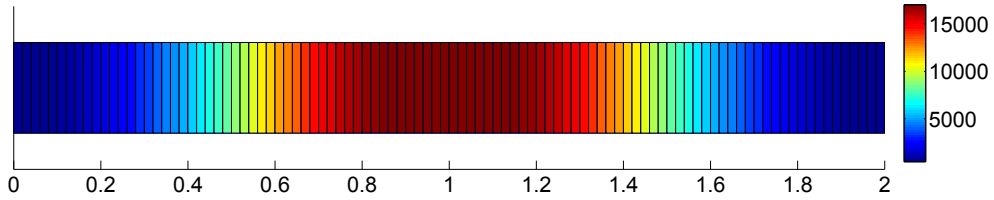

(a) Bending beam

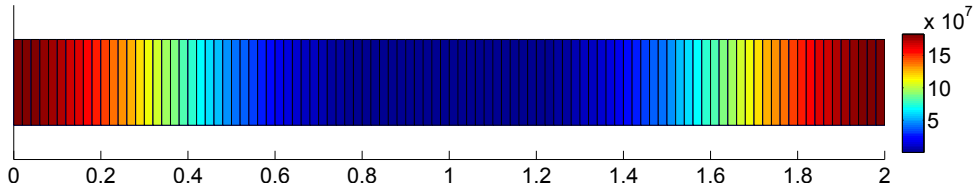

(b) Euler beam

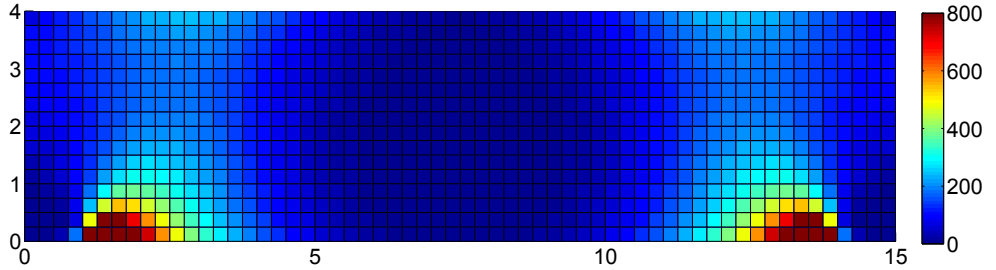

(c) Wall structure

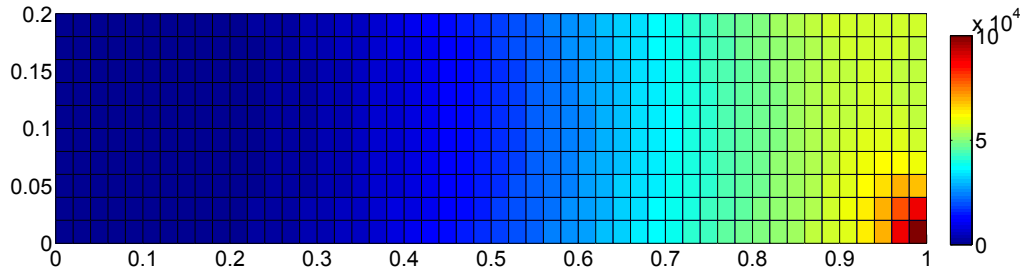

(d) Cantilever

Figure 4.22.: Distribution global model error estimate based on estimated stress difference

[1] At first sight, the bending beam fulfils the requirement of small displacement differences, too. But if the horizontal displacements are studied, it is obvious that in the linear case they are zero, and in the non-linear case there are movements that are infinitely large related to the linear one.

4.5 Goal-oriented error estimates

4.5.1 Direct evaluation of the difference term *d*

In BRAACK / ERN [14] it is shown that for linear models, eq. (3.76) is valid. For the specific case of the comparison of geometrical linear and non-linear models, this relationship can be applied, as the simple model is a linear one

$$a_l(\mathbf{u}_{nl}, \mathbf{v}) - a_l(\mathbf{u}_l, \mathbf{v}) = a_l(\mathbf{e}_m, \mathbf{v}) = -d(\mathbf{u}_{nl}; \mathbf{v}). \tag{4.21}$$

This relationship allows for the definition of an estimator for the error in the goal quantity. The test function $\mathbf{v}$ can be chosen arbitrarily and is set to $\mathbf{G}_l$.

$$a_l(\mathbf{e}_m, \mathbf{G}_l) = -d(\mathbf{u}_{nl}; \mathbf{G}_l) \tag{4.22}$$

In section 3.1.4 it is shown, eq. (3.40) , that for linear models, the dual problem is defined as

$$a(\mathbf{G}, \mathbf{v}) = J(\mathbf{v}).$$

Using $\mathbf{e}_m$ as a test function and shifting the components due to symmetry conditions leads to

$$J(\mathbf{e}_m) = a_l(\mathbf{G}_l, \mathbf{e}_m) = a_l(\mathbf{e}_m, \mathbf{G}_l). \tag{4.23}$$

The final definition of the goal-oriented error becomes

$$J(\mathbf{e}_m) = -d(\mathbf{u}_{nl}, \mathbf{G}_l). \tag{4.24}$$

To get a solution without knowing the exact solution $\mathbf{u}_{nl}$, the error is approximated as

$$J(\mathbf{e}_m) \approx -d(\mathbf{u}_l, \mathbf{G}_l). \tag{4.25}$$

To what extent this simplification leads to reasonable results will be investigated for the structural systems introduced in chapter 4.2. Table 4.10 shows the result for the exact and approximated errors in the goal quantity. The application of the simplified approach, eq. (4.25) , only leads to reasonable results for the Mises truss and the wall structure. Here the exact and the approximated errors deviate 20 %. For all other structural systems, the predictions based on the displacement solution $\mathbf{u}_l$ are of poor quality. The approximated error is not reliable at all. It can be seen that no general rule can be established concerning the question about which condition eq. (4.25) is applicable. The failure of the approximated error is neither related to a certain type of structural element nor to the sensitivity of the structure regarding the kinematic formulation.

Table 4.10.: Goal-oriented error estimate

	$u_{Goal,l}$	$u_{Goal,nl}$	$-d(\mathbf{u}_{nl}, \mathbf{G}_l)$	$-d(\mathbf{u}_l, \mathbf{G}_l)$	Difference
Mises truss vertical displacement in the loaded point	4.0 cm	4.5 cm	0.47	0.37	20 %
Truss cantilever vertical displacement in the loaded point, P=500 kN	50.6 cm	57.8 cm	7.2	-26	460 %
Truss cantilever P=150 kN	15.2 cm	15.8 cm	0.7	-0.2	130 %
Bending beam vertical displacement at $L/2$	3.0 cm	3.0 cm	0.0	11.1	∞
Euler beam vertical displacement at $L/2$	0.5 cm	24.5 cm	24.0	0.5	98 %
Wall structure horizontal displacement upper corner	-7.0 cm	-8.2 cm	-1.2	-0.9	17 %
Cantilever vertical displacement of loaded point	27 cm	30 cm	3.0	-490	∞

4.5.2 Strategy derived from an optimisation problem

Finally, the method introduced in sec. 3.2.5, p. 55 is applied to the geometrical non-linear problem. First the equations for the primal and dual problems are adapted. For the complex model, this yields

$$\begin{aligned} a_{nl}(\mathbf{u}_{nl}; \mathbf{v}) - F(\mathbf{v}) &= 0 \\ J'_u(\mathbf{u}_{nl}; \boldsymbol{\rho}) - G'_{nl,u}(\mathbf{u}_{nl}; \mathbf{z}_{nl}, \boldsymbol{\rho}) &= 0, \end{aligned} \tag{4.26}$$

and for the simplified model

$$\begin{aligned} a_l(\mathbf{u}_l; \mathbf{v}) - F(\mathbf{v}) &= 0 \\ J'_u(\mathbf{u}_l; \boldsymbol{\rho}) - G'_{l,u}(\mathbf{u}_l, \mathbf{z}_l, \boldsymbol{\rho}) &= 0. \end{aligned} \tag{4.27}$$

The simple model, assuming a linear kinematic description, allows for a simplified description of the dual problem. As we are dealing here with a linear variational formulation, the concepts

introduced in sec. 3.1.4 are valid; *Betti's theorem* can be applied. It leads to the same formulations as the Gâteaux derivative of the linear variational formulation,[2] which is

$$a_l(\mathbf{z}_l, \boldsymbol{\rho}) - F(\boldsymbol{\rho}) = 0. \tag{4.28}$$

For the complex model, such simplification cannot be found, which makes it necessary to calculate the derivatives. The derivative of the non-linear variational formulation G_{nl} is already introduced in eq. (2.42) . Therefore, for the discretisation case we can write

$$G'_{nl,u}(\mathbf{u}_{nl}; \mathbf{z}_{nl}, \boldsymbol{\rho}) = \hat{\boldsymbol{\rho}}\, \mathbf{k}_T(\hat{\mathbf{u}}_{nl})\, \hat{\mathbf{z}}_{nl}. \tag{4.29}$$

Adapting eq. (3.120) , which describes the error in the goal quantity, to the problem of geometrical non-linearity, it becomes

$$J(\mathbf{e}_m) = -d(\mathbf{u}_l; \mathbf{z}_l) - \frac{1}{2}\left[d(\mathbf{u}_l; \mathbf{e}^*_m) + d'_u(\mathbf{u}_l; \mathbf{e}_m, \mathbf{z}_l) - Res^{(3)}\right]. \tag{4.30}$$

In [48] as well [14] it is assumed that certain terms in the error definition can be neglected if the error is small, which leads to the simplification

$$J(\mathbf{e}_m) \approx -d(\mathbf{u}_l; \mathbf{z}_l). \tag{4.31}$$

It is shown in sec. 4.5.1, that this assumption is not valid for the problem under investigation. Therefore, the different structural system, the different terms in eq. (4.30) are evaluated. Initially point-wise displacements as goal quantities are studied, which leads to the simplification $J'_u(\mathbf{u}; \boldsymbol{\rho}) = 1$.

The evaluation of the first two terms of eq. (4.30) is straightforward an found by using (4.4) . To determine the third term, some derivations are necessary. Based on the known partition of the difference term d

$$d(\mathbf{u}_l; \mathbf{z}_l) = a_{nl}(\mathbf{u}_l; \mathbf{z}_l) - a_l(\mathbf{u}_l, \mathbf{z}_l), \tag{4.32}$$

the calculation of the Gâteaux derivative in the direction of $\mathbf{e}_m$ leads to

$$d'(\mathbf{u}_l; \mathbf{e}_m, \mathbf{z}_l) = G'_{nl,u} - a_l(\mathbf{e}_m, \mathbf{z}_l). \tag{4.33}$$

Approximating this expression using Finite Elements leads to the following matrix equation

$$d'_u(\mathbf{u}_l; \mathbf{e}_m, \mathbf{z}_l) = \sum_{e=1}^{n_e} \hat{\mathbf{z}}_l \, \left[\mathbf{k}_T(\hat{\mathbf{u}}_l) - \mathbf{k}_e\right] \, \hat{\mathbf{e}}_m. \tag{4.34}$$

[2] $G'_{l,u}(\mathbf{u}_l; \mathbf{z}_l, \boldsymbol{\rho}) = a'_l(\mathbf{u}_l, \boldsymbol{\rho}) = \lim_{\epsilon \to 0} \frac{1}{\epsilon}\left[a'_l(\mathbf{u}_l + \epsilon \mathbf{z}_l, \boldsymbol{\rho}) - a'_l(\mathbf{u}_l, \boldsymbol{\rho})\right] = a_l(\mathbf{z}_l, \boldsymbol{\rho})$

The last term of eq. (4.30) is not considered, as its evaluation is quite tedious and it does not provide any further information. In tab. 4.11 the results are summarised. In comparison to the previous section, where only the term $d(\mathbf{u}_l, \mathbf{G}_l)$ was considered as an error estimate, a significant improvement of the estimate can be monitored if eq. (4.31) is extended

$$J(\mathbf{e}_m)_{app} = -d(\mathbf{u}_l; \mathbf{z}_l) - \frac{1}{2}\left[d(\mathbf{u}_l; \mathbf{e}^*_m) + d'_u(\mathbf{u}_l; \mathbf{e}_m, \mathbf{z}_l)\right]. \tag{4.35}$$

The term ΔJ represents the difference $J(\mathbf{e}_m) - J(\mathbf{e}_m)_{app}$.

Table 4.11.: Goal-oriented error estimate derived using an optimisation problem; Influence of the different terms of the error definition

	$d(\mathbf{u}_l, \mathbf{z}_l)$	$d(\mathbf{u}_l, \mathbf{e}^*_m)$	$d'_u(\mathbf{u}_l; \mathbf{e}_m, \mathbf{z}_l)$	$J(\mathbf{e}_m)_{app}$	ΔJ
Mises truss vertical displacement in the loaded point	-0.37	-0.096	-0.086	0.47	0 %
Truss cantilever vertical displacement in the loaded point, P=500 kN	26	-38.4	29.1	7.8	8 %
Truss cantilever P=150 kN	0.24	-0.95	-0.87	0.67	4 %
Bending beam vertical displacement at $L/2$	-11.1	11.1	11.1	0.0	0 %
Euler beam vertical displacement at $L/2$	-0.5	-36.0	-35.8	36.4	52 %
Wall structure horizontal displacement upper corner	0.9	0.3	0.26	-1.18	2 %
Cantilever vertical displacement of loaded point	-490	601	461	-41	1470 %

Concluding this investigation, it becomes clear that any simplification of the formulation of the goal-oriented error eq. (4.30) does not lead to correct information concerning the error. Just for the Mises truss and the wall structures, the limitation to the first term of this equation results in a good approximation. It is never known in advance, how a structural system will behave. Therefore, it is discouraged from using eq. (4.31) or any other simplification of eq. (4.30) . Unfortunately, any estimation of the goal-oriented error that is more accurate requires $\mathbf{u}_{nl}$ or information concerning

the primal and dual error. As this information is generally not known in advance or can only be approximated by introducing more uncertainties, this approach is abandoned.

4.6 Summary: Model error estimation for kinematical models

For a variety of structural system that differ with respect to dimension and sensitivity regarding deformations, different model error estimation techniques have been tested concerning their ability to reproduce the error caused by using a simple kinematical model instead of full geometrical non-linear description. To find an appropriate reference value, the error estimates can be compared with different error norms that have been investigated using the exact solutions of the geometrical linear and non-linear models. It was found that the error in the energy norm based on the stress differences lead to the most meaningful results with respect to the total scalar value and the error distribution.

The investigated global error estimators did not provide reliable information concerning the model error. One reason might be that most of them are based on other norms than the preferred one. The only method that measured the error in the energy norm $\eta_{E,\sigma}$ is based on linearisation of the complex model. At least for small displacement differences, the estimate was close to the real error, but for larger errors meaningful results could not be achieved. As the magnitude of the model error is never known in advance, this method is unfortunately not applicable. Global error estimates based on a direct evaluation of difference tern $d(.;.)$ were not successful, as important information is neglected. If the missing parts were included, the results would be better interpretable, but information about the error itself has to be available. The third approach, a residuum described based on the linear solution and bounded from above by applying the Cauchy-Schwarz inequality, also showed severe problems in predicting the error correctly. To sum up, none of the investigated global error estimation techniques led to reliable estimates for all the structural systems under investigation.

For goal-oriented error estimates, it was possible to derive a procedure that directly refers to the difference term d due to the linear structure of the simple model. Unfortunately, the definition requires knowledge regarding the solution of the complex model. Using the simplified solution instead leads to severe inaccuracies. The derivation of an estimator in a round-about way by defining an optimisation problem, results in a formula containing several terms. In contrast to recommendations made in former publication, it could be shown that none of these terms can be neglected without introducing significant errors.

A prediction of the model error for non-linear models, either global or local, seems not to be possible as long as only the solution of the simpler model is known. Only for some rare cases where the model error is small can the applied estimator lead to meaningful results. Unfortunately the magnitude of the error is hardly known in advance. It is assumed that the difficulty when dealing with non-linear problems lies in prediction of the non-linear load-deflection path. Information regarding its evolution can hardly be captured within an estimator. This assumption is supported

by the preliminary studies, see p. 8, where it was shown that a prediction of the structural behaviour under high loads cannot be predicted by informations gathered from lower load level if the difference of the loading is large.

5 Conclusions

"Was man mit Fehlerkontrolle nicht berechnen kann, darüber muss man schweigen."

(cf. WITTGENSTEIN [70]*)*

The goal of this thesis was the introduction of a method for model quality assessment for kinematical models. Within the scope of this research, the problem was limited to the question of whether a geometrical linear or non-linear calculation is necessary. The underlying models are assigned to the class of white box models, where the model hierarchy is known. The goal was to steer the model choice using an adaptive process. The control parameter is the model error, which is determined based on the results of the simpler model. For this purpose, first the theory of discretisation and model error estimators is studied. Methods for the determination of model errors for non-linear problems are adapted to the problem of kinematic models, and their applicability and accuracy are studied, respectively.

The strategy that can be used to judge the model quality strongly depends on the kind of model under investigation. Kinematical models are white box models, which means that they are derived analytically, based on physical laws. In this context, simple and more complex models deviate with respect to certain phenomena, which are either included or neglected. Thus, a clear model hierarchy can be established. In this context, the question does not arise about which model is best. In fact, it needs to be investigated whether or not the additional effort of evaluating a complex model leads to a significant improvement in the solution quality.

Generally, the decision about which model to use is made based on engineering experience. To prevent incorrect decisions, an adaptive process steered by suitable error measures should be established. Preliminary investigations were carried out to investigate the problem more deeply. In a first approach, it was tested whether it is possible to approximate the deformation energy of the non-linear model based on the linear solution. The second method applied the load in several portions and tried to predict the final deformation based on an extrapolation of the results of the first load steps. Both attempts did not lead to reliable results. An alternative had to be found. Within the theory of model error estimation, which attracted notice in the beginning of the 1990s, this question is addressed. The necessary condition for the application of this theory has to be mentioned: "... a sequence of hierarchically reduced, i.e. simplified, mathematical models derived from an appropriate master model is required for [...] model [...] adaptivity, controlled by the model error [...]." [66, p. 105], is fulfilled.

Model error estimators are derived from the well-established theories for determination of discretisation errors. These techniques started to develop with the introduction of the Finite Element

method. The goal is to estimate the error due to meshing and determine the optimal mesh for a certain problem with respect to accuracy and computational effort. *A priori* estimates study the convergence behaviour for a certain problem. *A posteriori* techniques provides estimates or upper and lower error bounds. For linear problems, differences can be distinguished between residual-based estimates, averaging-type estimates, and implicit/absolute error bounds, where auxiliary problems are solved. For non-linear problems these techniques are adopted. After linearisation of the underlying equations, the standard techniques can be used.

In engineering practise, the focus is often shifted towards errors in quantities of interest. Goal-oriented error estimators are derived for such problems. If linear models are investigated, *Betti's theorem* can be used to determine a dual problem related to the local quantity. The error in the dual problem is then used to scale the primal error. For non-linear models, an optimisation problem needs to be introduced that provides a basis for the definition of the primal and dual problems.

Methods to estimate the model error are derived with the goal to steer an adaptive process within a class of white box models. Of course, the most complex model would lead to the most accurate result, at least as long as the stochastic character of the input parameters is neglected, but the computational effort is much too large. This thesis provides a summary of the most important publications in this field. Following the classification already introduced for discretisation errors, one can distinguish between global and goal-oriented estimates for linear and non-linear problems.

For linear material models, the error due to homogenisation can be determined in the energy norm based on the difference between both models under investigation. For dimensional adaptivity, the posteriori equilibrium method (PEM) is introduced, which is an extension of implicit methods. Here local *Neumann problems* are solved to find the error in the energy norm. For non-linear problems, this approach can be applied without significant changes. The underlying equations are linearised and an energy norm equivalent is defined. For non-linear material models, a residuum based on the model difference is defined, which only depends on the solution of the simpler model. Applying *Cauchy-Schwarz inequality* yields an upper error bound.

In the case of linear models, *Betti's theorem* can again be applied to formulate a dual problem in accordance with the goal quantity. The local error is assembled using a residual, determined in a comparable manner to the global model error, and a second term, where the error of the primal problem is weighted by the one of the dual problem. This additional term is estimated using parallelogram identity, an approach already known from discretisation error estimates. For non-linear problems, the approach of introducing a, optimisation problem is adapted. The error in the goal quantity is assembled from several terms, which partially contain the unknown errors of the primal and dual problems. Based on the assumption of small errors, these terms are often neglected.

The applicability of various model error estimation techniques is investigated for the problem of geometrical non-linearity. Various test structures are introduced for this purpose. They differ with respect to dimension and their sensitivity regarding the chosen kinematical formulation. Before

the error estimation strategies are tested, suitable error measures are investigated. The goal was to identify suitable errors norms and reference values for the error estimates. The energy norm based on displacement and stress differences as well as the L_2-norm of the displacements are investigated with respect to their total scalar value and their distribution. As a reference value, the difference of the linear and non-linear deformation energy is chosen. Finally, the normalised value of the energy norm based on stresses proved to be the most suitable measure.

First, the techniques for calculating the estimate for the global error are tested. Many of the proposed methods are based on the term d defining the difference between the simple and complex models. It is investigated whether the direct evaluation of this term leads to meaningful results. In comparison with the previously determined exact error, an agreement could be monitored only for some examples. In most of the cases, this approach failed to predict the scalar value and the error distribution correctly. The reason for this failure is that the term d does not capture the total energy difference between the linear and non-linear solutions. A possible extension is not meaningful, as it requires knowledge about the error in the displacement itself.

The second approach tested to determine the global model error was first introduced for material models and comprises the definition of a residual based on the model difference. It is important to note that the residual is limited to terms that can be determined knowing only the solution of the linear model. The upper error bound, found by applying *Cauchy-Schwarz inequality*, becomes more interpretable after scaling. The information provided by this estimate is not reliable. Even if the total scalar value is meaningful for some examples, the error distribution is misleading. Finally, a method is applied that is based on the linearisation of the geometrical non-linear model. Here, meaningful results could only be achieved in the case of small model errors; a prerequisite, whose compliance cannot be guaranteed in advance.

For the determination of the goal-oriented model error, a significant simplification can be introduced. The simple model for describing the kinematics is a linear one and Betti's theorem can be applied. Thus, the error in the goal quantity can be determined directly through an evaluation of the difference term d using the non-linear solution of the primal problem and the linear solution of the dual problem. An investigation of whether the primal solution of the linear model can be used instead of the non-linear one did not lead to reliable results. Therefore the method based on the formulation of an optimisation problem for defining the primal and the dual problems is tested. It leads to an error definition based on several summands that partly depend on the unknown error of the primal and dual solutions. It is shown that none of these terms can be neglected. Any simplification based on the assumption of small errors provides erroneous information. As any estimation of the unknown primal and dual errors would cause additional inaccuracies, this method is not applicable.

The application of different error estimation techniques to judge the accuracy of a simplified kinematical model does not prove successful. Without knowing the solution of the more complex model and therewith the error in the displacement solution, a reliable prediction of the model

error is hardly possible. Based on these results, the author assumes that this problem might also occur for other non-linear models in case of larger errors. In contrast to linear models, non-linear problems are mostly solved using an iterative procedure to find the equilibrium point. Therefore, an approximation of the non-linear solution that is equitable to error estimation and based on the results of the simplified model does not seem to be successful, as the neglected iterative solution procedure can hardly be compensated. Any approximations of the exact error representation that are made assuming small errors seem to be unreliable, as the magnitude of the error is unknown in advance. Thus, for practical applications no methodology can be provided that allows an automatic model adaption. The engineer needs to rely on his experience when choosing the kinematical model or study the results of all available models to judge the system's behaviour.

A Appendix

A.1 Mathematical background

Sobolev spaces and norms

The *$L_2(\Omega)$-space* is the most general space that can be defined in a functional analysis. It contains all functions that can be *Lebesgue* integrated. The norm of a function in this space is defined as

$$\|u(x)\|_{L_2} = \left(\int_{\Omega} u(x)^2 \, d\Omega \right)^{1/2} . \tag{A.1}$$

If, in addition, a scalar product and a corresponding norm exist, the functional space $\mathrm{L}_2(\Omega)$ becomes a *Hilbert space* $\mathcal{H}^m(\Omega)$. Here $m \geq 0$ defines the number of weak derivatives that can be determined. According to the order of m, the Hilbert-norms can be defined:

$$\left(\|\mathbf{v}\|_{\mathcal{H}^0}\right)^2 = \int_{\Omega} \left(\sum_{i=1}^{3} v_i^2 \right) d\Omega, \qquad m = 0, \tag{A.2}$$

$$\left(\|\mathbf{v}\|_{\mathcal{H}^1}\right)^2 = \left(\|\mathbf{v}\|_{\mathcal{H}^0}\right)^2 + \int_{\Omega} \left(\sum_{i=1,j=1}^{3} \left(\frac{\partial v_i}{\partial x_j} \right)^2 \right) d\Omega, \qquad m = 1. \tag{A.3}$$

The Hilbert seminorm $|.|_{\mathcal{H}^m}$ only considers the integration over the m*th* derivative and skips the summation over all *m*. For more details see e.g. BRAESS [15].

In error estimation, also the control of the error in the displacements is of interest. The L_2 norm of the displacement vector is defined as

$$\|\mathbf{u}\|_{L_2} = \sqrt{(\mathbf{u}, \mathbf{u})} = \left(\int_{\Omega} \mathbf{u} \cdot \mathbf{u} \, d\Omega \right)^{1/2} . \tag{A.4}$$

It can be shown, see e.g. [15, p. 87], that:

$$\|\mathbf{u}\|_{\mathcal{H}^0} = \|\mathbf{u}\|_{L_2}. \tag{A.5}$$

Another important norm for error estimation in structural mechanics is the *energy norm*

$$\|\mathbf{v}\|_E = \sqrt{a(\mathbf{v},\mathbf{v})} = \left(\int_\Omega \boldsymbol{\sigma}(\mathbf{v}) \cdot \boldsymbol{\varepsilon}(\mathbf{v})\, d\Omega \right)^{1/2} . \tag{A.6}$$

For a discretised domain, the energy norm can be evaluated elementwise and summed up.

Galerkin orthogonality

The Finite Element method involves the projection of the exact solution $\mathbf{u}$ from the space $\mathcal{V}$ to the space of ansatz functions $\mathcal{V}_h$. The Galerkin orthogonality

$$a(\mathbf{e}_h, \mathbf{v}_h) = 0 \tag{A.7}$$

states that the discretisation error $\mathbf{e}_h$ is energy-orthogonal to the space of ansatz functions. From this, the following properties can be deduced, see also figure A.1:

- The projected solution $\mathbf{u}_h$ is shorter than the exact solution $\mathbf{u}$. Therefore, the deformation energy of the Finite Element solution is always smaller compared to the exact one, which means the discretised system behaves more stiffly.

- The Finite Element solution for a specific mesh is always the best possible solution within this mesh, because the error $\mathbf{e}_h$ is the shortest connection between $\mathcal{V}$ and $\mathcal{V}_h$.

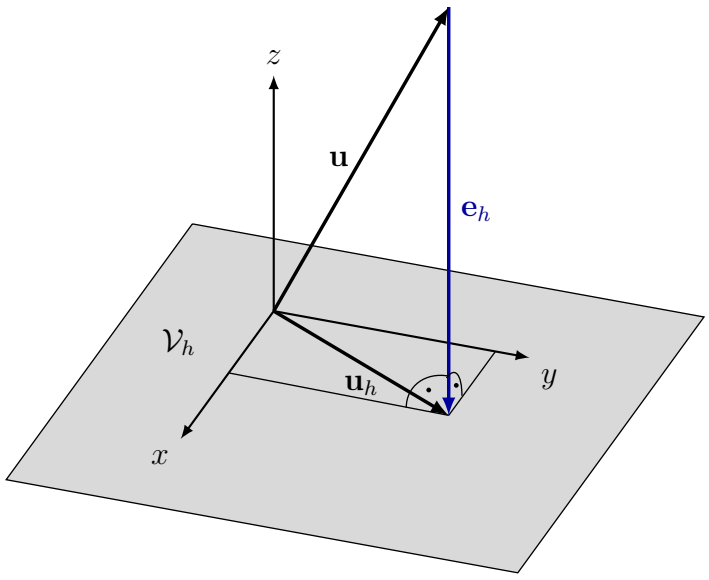

Figure A.1.: Galerkin orthogonality

Cauchy-Schwarz inequality

For vectors, the Cauchy-Schwarz inequality states:

$$(\mathbf{x}, \mathbf{y}) \leq (\mathbf{x}, \mathbf{x}) \cdot (\mathbf{y}, \mathbf{y}) = \|\mathbf{x}\|^2 \|\mathbf{y}\|^2, \tag{A.8}$$

where $\mathbf{x}$ and $\mathbf{y}$ are defined in a real vectorial space with the inner product $(\mathbf{x}, \mathbf{y})$.
The upper bound for an integral over two functions can be defined using Cauchy-Schwarz inequality as:

$$\left(\int_{\Omega} f(x)\, g(x)\, d\Omega \right)^2 \leq \int_{\Omega} f(x)^2\, d\Omega \int_{\Omega} g(x)^2\, d\Omega. \tag{A.9}$$

A.2 Mechanical background

A.2.1 Derivation of 2. Piola-Kirchhoff stress tensor

The basis for the derivation of the relationship between the *Cauchy stress tensor* and the *2nd Piola-Kirchhoff stress tensor* is the *Nanson formula*:

$$\mathbf{n}\, da = det\mathbf{F}\, (\mathbf{F}^{-1})^T\, \mathbf{N}\, dA. \tag{A.10}$$

It relates the area of a surface element in the initial configuration dA and the area of a surface elemente in the actual configuration da. The vectors $\mathbf{N}$ and $\mathbf{n}$ denote the unit normal through the surface in initial and actual configuration, respectively.[1] The relationship of the stresses on a surface and the forces $d\mathbf{p}_s$ acting on that surface are:

- in deformed/actual configuration: $d\mathbf{p}_s = \boldsymbol{\sigma}\, \mathbf{n}\, da$,
- related to the initial/undeformed configuration it becomes: $d\mathbf{p}_s = \mathbf{P}\, \mathbf{N}\, dA$, with the *1st Piola-Kirchhoff stress tensor* $\mathbf{P}$.

Using *Nanson formula* the *1st Piola-Kirchhoff stress tensor* can be written in terms of *Cauchy stresses* as

$$\mathbf{P} = det\mathbf{F}\, \boldsymbol{\sigma}\, (\mathbf{F}^{-1})^T \tag{A.11}$$

To get a symetric tensor, eq. (A.11) is multiplied by $\mathbf{F}^{-1}$ and the *2nd Piola Kirchhoff stress tensor* $\mathbf{S}$ is defined as:

$$\mathbf{S} = \mathbf{F}^{-1}\, \mathbf{P} = \mathbf{F}^{-1}\, J\, \boldsymbol{\sigma}\, (\mathbf{F}^{-1})^T \tag{A.12}$$

[1] All quantities in the initial position are described using capital letters, whereas for the state after deformation lowercase letters are used.

A.2.2 Kinematic description truss and beam elements

Plane truss systems

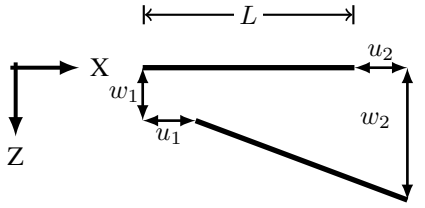

$$u' = \frac{u_2 - u_1}{L}$$
$$w' = \frac{w_2 - w_1}{L}$$
$$\varepsilon = u'$$
$$E = u' + \frac{1}{2}w'^2$$
$$\delta E = \delta u' + \frac{1}{2}(w'\,\delta w' + \delta w'\,w')$$

Figure A.2.: Deformation of a truss elememt, Definition of strain measures

Based on strain definitions in fig. A.2, the formulas for the direct evaluation of the difference term d becomes for the global error

$$d(\mathbf{u}_{nl}, \mathbf{u}_{nl}) = (u'_{nl} \cdot E \cdot w'_{nl} w'_{nl} + \frac{1}{2} w'^2_{nl} \cdot E \cdot u'_{nl} + \frac{1}{2} w'^2_{nl} \cdot E \cdot w'_{nl} w'_{nl}) * A * L, \tag{A.13}$$

and for the goal-oriented error it can be specified as

$$d(\mathbf{u}_{nl}, \mathbf{G}_l) = (u'_{nl} \cdot E \cdot w'_{nl} w'_{dual} + \frac{1}{2} w'^2_{nl} \cdot E \cdot u'_{dual} + \frac{1}{2} w'^2_{nl} \cdot E \cdot w'_{nl} w'_{dual}) * A * L. \tag{A.14}$$

Beam elements

For two-dimensional Bernoulli beam elements, the linear and non-linear internal energy can be calculated as follows, whereas the same notation as in fig. A.2 is used.

$$a_{lin} = \sum_{e=1}^{no_{elem}} (\varepsilon * EA * \delta\varepsilon + \kappa * EI * \delta\kappa) * L \tag{A.15}$$

$$\begin{aligned} a_{nl} &= \sum_{e=1}^{no_{elem}} (\varepsilon_{nl} * EA * \delta\varepsilon_{nl} + \kappa * EI * \delta\kappa) * L \\ &= \sum_{e=1}^{no_{elem}} (u' + \frac{1}{2}w'^2) * EA * (\delta u' + \frac{1}{2}(w'\,\delta w' + \delta w'\,w')) + \kappa * EI * \delta\kappa) * L \end{aligned} \tag{A.16}$$

The term κ describes the curvature of the beam and is unembodied in fig. A.2. It is obvious that the non-linearity is captured in the longitudinal strain and therefore the difference term d is defined identically to eqs. (A.13) and (A.14) .

Bibliography

[1] AIAA: Guide for the verification and validation of computational fluid dynamics simulations / American institute of aeronautics and astronautics. 1998 (AIAA-G-077-1998). – Tech. report 3

[2] AINSWORTH, Mark ; ODEN, J. T.: A posteriori error estimation in Finite Element analysis. In: *Comp. Methods Appl. Mech. Engrg.* 142 (1997), 1–88 11, 30

[3] BABUSKA, I. ; MILLER, A.: A feedback Finite Element method with a posteriori error estimation: Part I. The Finite Element method and some basic properties of the a posteriori error estimator. In: *Comp. Methods Appl. Mech. Engrg.* 61 (1987), 1–40 33

[4] BABUSKA, I. ; ODEN, J. T.: Verification and validation in computational engineering and science: Basic concepts. In: *Comput. Methods Appl. Mech. Engrg.* 193 (2004), 4057–4066 3

[5] BABUSKA, I. ; RHEINBOLDT, W.C.: A-posteriori error estimates for the Finite Element method. In: *Int J Numer Meth Engng* 12 (1978), 1597–1615 12, 33, 49

[6] BABUSKA, I. ; STROUBOULIS, T. ; COPPS, K. ; GANGARAJ, S.K. ; UPADHYAY, C.S.: A posteriori error estimation for Finite Element and generalized Finite Element method / University of Texas. 1998 (98-01). – TICAM Report 40

[7] BANGERTH, W. ; RANNACHER, R.: *Adaptive Finite Element methods for differential equations*. Birkhäuser, 2003 42

[8] BANK, R. E. ; WEISER, A.: Some a posteriori error estimators for elliptic partial differential equations. In: *Mathematics of Computation* 44 (1985), 303–320 35

[9] BATHE, K.-J.: *Finite Element procedures*. Springer, 1996 29, 31, 64

[10] BAUNETZ: *"Knick-Ei" zum Dritten - Halstenbeker Sporthalle wird weitergebaut*. 08 2003. – URL `http://www.baunetz.de/meldungen/Meldungen_Halstenbeker_Sporthalle_wird_weitergebaut_14463.html` 7

[11] BECKER, R. ; RANNACHER, R.: A feed-back approach to error control in Finite Element methods: Basic analysis and examples. In: *East-West J. Numer. Math.* 4 (1996), 237–264 12, 38, 40, 41

[12] BECKER, R. ; RANNACHER, R.: An optimal control approach to a posteriori error estimation in Finite Element methods. In: *Acta Numerica* 10 (2001), 1–102 12, 42, 43, 45, 55

[13] BONET, J. ; WOOD, R. D.: *Nonlinear continuum mechanics for Finite Element analysis*. Cambridge University Press, 1997 24

[14] BRAACK, M. ; ERN, A.: A posteriori control of modeling errors and discretization errors. In: *Multisale Model. Simul.* 1 (2003), 221–238 13, 45, 46, 55, 56, 81, 83

[15] BRAESS, D.: *Finite Elemente: Theorie, schnelle Löser und Anwendungen in der Elastizitätstheorie*. Springer, 2007 91

[16] CIRAK, F.: *Adaptive Finite-Element-Methoden bei der nichtlineare Analyse von Flächentragwerken*, Universität Stuttgart, PhD thesis, 1998 39, 41

[17] CIRAK, F. ; RAMM, E.: A posteriori error estimation and adaptivity for elastoplasticity using the reciprocal theorem. In: *Int J Numer Meth Engng* 47 (2000), 379–393 13, 44

[18] CRISFIELD, M. A.: *Non-linear Finite Element analysis of solids and structures*. Vol. 2 Advanced Topics. Wiley, 1997 15, 27

[19] EPA: Guidance on the Development, Evaluation, and Application of Environmental Models / Council for Regulatory Environmental Modeling; U.S. Environmental Protection Agency. 2009. – Tech. report 2, 3

[20] ERIKSSON, A.: On improved predictions for structural equilibrium path evaluations. In: *Int J Numer Meth Engng* 36 (1993), 201–220 11

[21] GRÄTSCH, T. ; BATHE, J.: A posteriori error estimation techniques in practical Finite Element analysis. In: *Computers and Structures* 83 (2005), 235–265 11, 30, 31, 33, 35, 40

[22] HAUGEN, B. ; FELIPPA, C.A.: A unified formulation of co-rotational Finite Elements: I. Theory. In: *Comp. Methods Appl. Mech. Engrg.* 194 (2005), 2285–2335 15

[23] HOLZAPFEL, G. A.: *Nonlinear solid mechanics*. Wiley, 2000 24

[24] HUERTA, A. ; RODRÍGUEZ-FERRAN, A. ; DÍEZ, P.: Error estimation and adaptivity for nonlinear FE analysis. In: *Int. J. Appl. Math. Comput. Sci.* 12 (2002), 59–70 41, 78, 80

[25] IRGENS, F.: *Continuum Mechanics*. Springer, 2008 15, 19

[26] JELENIC, G. ; CRISFIELD, M.A.: Geometrically exact 3D beam theory: Implementation of a strain-invariant Finite Element for statics and dynamics. In: *Comp. Methods Appl. Mech. Engrg.* 171 (1999), 141–171 15

[27] JIRÁSEK, Milan: *Modeling of Localized Inelastic Deformation, Lecture Notes*. – Course at the Czech Technical University in Prague, 13-17 September 2010 18

[28] KEITEL, H.: *Bewertungsmethoden für die Prognosequalität von Kriechmodelle des Betons*, Bauhaus Universität Weimar, PhD thesis, 2011 4

[29] KIM, Jong H. ; KIM, Yong H.: A predictor-corrector method for structural non-linear analysis. In: *Comp. Methods Appl. Mech. Engrg.* 191 (2001), 959–974 11

[30] KNABE, T.: *Assessment of constitutive approaches for soil in civil engineering applications*, Bauhaus Universität Weimar, PhD thesis, 2011 4

[31] KOK, Lübbert: *Das Knickei von Halstenbek*. 01 2009. – URL `http://www.knickei.de/ursachen2.php` 6

[32] KUHL, D.: Finite Elemente I+II / Universität Kassel, Institut für Baustatik und Baudynamik. 2007. – Tech. report 24

[33] KUNOW, T.: *Modellfehler und Greensche Funktionen in der Statik*, Universität Kassel, PhD thesis, 2008 55, 57

[34] LADEVEZE, P. ; LEGUILLON, D.: Error estimate procedure in the Finite Element method and applications. In: *SIAM Journal on Numerical Analysis* 20 (1983), 485–509 35

[35] LARSSON, F. ; HANSBO, P. ; RUNESSON, K.: Strategies for computing goal-oriented a posteriori error measures in non-linear elasticity. In: *Int J Numer Meth Engng* 55 (2002), 879–894 38

[36] LARSSON, F. ; RUNESSON, K.: Modeling and discretization errors in hyperelasto-(visco-) plasticity with a view to hierachical modeling. In: *Comp. Methods Appl. Mech. Engrg.* 193 (2004), 5283–5300 52, 57

[37] LARSSON, F. ; RUNESSON, K.: Adaptive computational meso-macro-scale modeling of elastic composites. In: *Comp. Methods Appl. Mech. Engrg.* 195 (2006), 324–338 13, 45

[38] LEMAITRE, Jean: *A course on Damage Mechanics*. Springer-Verlag Berlin, 1996 18

[39] MANG, H. ; HOFSTETTER, G.: *Festigkeitslehre*. Springer, 2000 15, 19

[40] MATERNA, D.: *Goal-oriented recovery bei nichtlinearen Scheibenproblemen*, Universität Kassel, Master's thesis, 2004 42

[41] MEEK, J.L. ; TAN, H.S.: A stiffness matrix extrapolation strategy for nonlinear analysis. In: *Comp. Methods Appl. Mech. Engrg.* 43 (1984), 181–194 10

[42] MERDON, C.: *A posteriori Fehlerschätzer für elliptische partielle Differentialgleichungen*, Humboldt-Universität Berlin, Master's thesis, 2009 31

[43] MINSKY, M. L.: Matter, minds and models. In: *Proc. International Federation of Information Processing Congress* Vol. 1, 1965, 45–49 1

[44] OBERKAMPF, W. L. ; TRUCANO, T. G. ; HIRSCH, C.: Verification, validation, and predictive cabability in computational engineering and physics. In: *Foundations for verification and validation in the 21st century workshop*, 2002 3

[45] ODEN, J. T. ; VEMAGANTI, K.: Adaptive modeling of composite structures: Modeling error estimation. In: *Texas Institute for Computational and Applied Mathematics* 1 (1999), 1–16 45, 48, 52, 54, 55, 58

[46] ODEN, J. T. ; PRUDHOMME, S.: On goal-oriented error estimation for local elliptic problems: Application to the control of pointwise errors. In: *Comp. Methods Appl. Mech. Engrg.* 176 (1999), 313–331 12, 40, 45

[47] ODEN, J. T. ; PRUDHOMME, S.: Goal-oriented error estimation and adaptivity for the Finite Element method. In: *Computers and mathematics with application* 41 (2001), 735–756 12, 40, 77

[48] ODEN, J. T. ; PRUDHOMME, S.: Estimation of modeling error in computational mechanics. In: *Journal of Computational Physics* 182 (2002), 496–515 13, 45, 55, 57, 83

[49] ODEN, J. T. ; PRUDHOMME, S. ; HAMMERAND, D.l ; KUCZMA, M.: Modeling error and adaptivity in non-linear continuum mechanics. In: *Comp. Methods Appl. Mech. Engrg.* 190 (2001), 6663–6684 45, 50, 51, 74, 75

[50] ODEN, J. T. ; VEMAGANTI, K.: Estimation of local modeling error and goal-oriented adaptive modeling of heterogeneous materials; Part I : Error estimates and adaptive algorithms. In: *J. Comp. Physics.* 164 (2000), 22–47 13, 45, 48, 52, 54, 55, 58

[51] ODEN, J.T. ; ZOHDI, T. J.: Analysis and adaptive modeling of highly heterogeneous elastic structures. In: *Comp. Methods Appl. Mech. Engrg.* 148 (1997), 367–391 13, 45, 46, 48

[52] OHNIMUS, S.: *Theorie und Numerik dimensions- und modelladaptiver Finite-Elemente-Methoden von Flächentragwerken*, Universität Hannover, PhD thesis, 1996. – Forschungs- und Seminarbericht aus dem Bereich der Mechanik der Universität Hannover; Bericht Nr. F96/6 45, 48, 49

[53] OHNIMUS, S. ; STEIN, E. ; WALHORN, E.: Local error estimates of FEM for displacements and stresses in linear elasticity by solving local Neumann problems. In: *Int J Numer Meth Engng* 52 (2001), 727–746 13, 36

[54] ORESKES, N. ; SHRADER-FRECHETTE, K. ; BELITZ, K.: Verifivation, validation, and confirmation of numerical models in the earth science. In: *Science* 263 (1994), 641–645 2

[55] PETERSEN, C.: *Stahlbau: Grundlagen der Berechnung und baulichen Ausbildung von Stahlbauten*. Vieweg, 1993 8

[56] PROSKE, D.: Zur Zukunft der Sicherheitskonzepte im Bauwesen. In: *Bautechnik* 88 (2011), 217–224 4

[57] RANKIN, C. C. ; BROGAN, F. A.: An element independent procedure for the treatment of large rotations. In: *J. Pressure Vessel Technol.* 108 (1986), 165–174 15

[58] RANNACHER, R. ; SUTTMEIER, F.-T.: A feed-back approach to error control in Finite Element methods: Application to linear elasticity. In: *Computational Mechanics* 19 (1997), 434–446 40, 41

[59] RANNACHER, R. ; SUTTMEIER, F.-T.: A posteriori error control in Finite Element methods via duality techniques: Application to perfect plasticity. In: *Computational Mechanics* 21 (1998), 123–133 43

[60] RUBIN, H.: Das Q_Δ-Verfahren zur vereinfachten Berechnung verschieblicher Rahmensysteme nach dem Traglastverfahren der Theorie II. Ordnung. In: *Der Bauingenieur* 48 (1973), 275–285 8

[61] SCHEER, J.: *Versagen von Bauwerken - Band 2: Hochbauten und Sonderbauwerke*. Ernst und Sohn, 2001 6, 7

[62] STEEB, H.: *Fehlerschätzer für FE-Berechnungen bei entfestigenden Materialien*, Universität Stuttgart, PhD thesis, 2002 33, 37, 101

[63] STEIN, E. ; OHNIMUS, S.: Dimensional adaptivity in linear elasticity with hierachical testspaces for h- and p-refinement processes. In: *Engineering with Computers* 12 (1996), 107–119 45, 48

[64] STEIN, E. ; OHNIMUS, S.: Coupled model- and solution adaptivity in the Finite Element method. In: *Comp. Methods Appl. Mech. Engrg.* 150 (1997), 327–350 13, 36, 37, 45, 48, 49, 63, 65

[65] STEIN, E. ; OHNIMUS, S.: Anisotropic discretization- and model-error estimation in solid mechanics by local Neumann problems. In: *Comp. Methods Appl. Mech. Engrg.* 176 (1999), 363–385 37

[66] STEIN, E. ; RÜTER, M. ; OHNIMUS, S.: Adaptive Finite Element analysis and modelling of solids and structures. Findings, problems and trends. In: *Int J Numer Meth Engng* 60 (2004), 103–138 1, 13, 30, 87

[67] STEIN, E. ; RÜTER, M. ; OHNIMUS, S.: Error-controlled adaptive goal-oriented modeling and Finite Element approximations in elasticity. In: *Comp. Methods Appl. Mech. Engrg.* 196 (2007), 3598–3616 45, 51, 57, 58, 78, 80

[68] STEIN, E. ; RÜTER, M. ; OHNIMUS, S.: Implicit upper bound error estimates for combined expansive model and discretization adaptivity. In: *Comp. Methods Appl. Mech. Engrg.* 200 (2011), 2626–2638 45

[69] VEMAGANTI, K. ; ODEN, J. T.: Estimation of local modeling error and goal-oriented adaptive modeling of heterogenous materials, Part II: A computational environment for adaptive modeling of heterogenous elastic solids. In: *Comp. Methods Appl. Mech. Engrg.* 190 (2001), 6089–6124 54

[70] WITTGENSTEIN, L.: *Logisch-philosophische Abhandlung*. Suhrkamp, 1963 87

[71] WUNDERLICH, W. ; KIENER, G.: *Statik der Stabtragwerke*. B. G. Teubner Verlag, 2004 4, 7

[72] ZIENKIEWICZ, O. C. ; ZHU, J. Z.: A simple error estimator and adaptive procedure for practical engineering analysis. In: *Int J Numer Meth Engng* 24 (1987), 337–357 12, 34

[73] ZIENKIEWICZ, O. C. ; ZHU, J. Z.: The superconvergent patch recovery and a posteriori error estimates. Part I: The recovery technique. In: *Int J Numer Meth Engng* 33 (1992), 1331–1364 34

[74] ZOHDI, T. I. ; ODEN, J.T. ; RODIN, G. J.: Hierarchical modeling of heterogeneous bodies. In: *Comp. Methods Appl. Mech. Engrg.* 138 (1996), 273–298 45, 47, 48, 54

List of Figures

List of Tables